

ADVERTIMENT. La consulta d'aquesta tesi queda condicionada a l'acceptació de les següents condicions d'ús: La difusió d'aquesta tesi per mitjà del servei TDX (www.tesisenxarxa.net) ha estat autoritzada pels titulars dels drets de propietat intel·lectual únicament per a usos privats emmarcats en activitats d'investigació i docència. No s'autoritza la seva reproducció amb finalitats de lucre ni la seva difusió i posada a disposició des d'un lloc aliè al servei TDX. No s'autoritza la presentació del seu contingut en una finestra o marc aliè a TDX (framing). Aquesta reserva de drets afecta tant al resum de presentació de la tesi com als seus continguts. En la utilització o cita de parts de la tesi és obligat indicar el nom de la persona autora.

ADVERTENCIA. La consulta de esta tesis queda condicionada a la aceptación de las siguientes condiciones de uso: La difusión de esta tesis por medio del servicio TDR (www.tesisenred.net) ha sido autorizada por los titulares de los derechos de propiedad intelectual únicamente para usos privados enmarcados en actividades de investigación y docencia. No se autoriza su reproducción con finalidades de lucro ni su difusión y puesta a disposición desde un sitio ajeno al servicio TDR. No se autoriza la presentación de su contenido en una ventana o marco ajeno a TDR (framing). Esta reserva de derechos afecta tanto al resumen de presentación de la tesis como a sus contenidos. En la utilización o cita de partes de la tesis es obligado indicar el nombre de la persona autora.

WARNING. On having consulted this thesis you're accepting the following use conditions: Spreading this thesis by the TDX (www.tesisenxarxa.net) service has been authorized by the titular of the intellectual property rights only for private uses placed in investigation and teaching activities. Reproduction with lucrative aims is not authorized neither its spreading and availability from a site foreign to the TDX service. Introducing its content in a window or frame foreign to the TDX service is not authorized (framing). This rights affect to the presentation summary of the thesis as well as to its contents. In the using or citation of parts of the thesis it's obliged to indicate the name of the author

PhD thesis

A hydrogeological approach in urban underground infrastructures

by Alejandro Serrano Juan

Advisors

Enric Vazquez Suñé
Estanislao Pujades Garnes

Institute of Environmental Assessment and Water Research (IDAEA), CSIC
Department of Geotechnical Engineering and Geosciences, Universitat Politècnica de Catalunya (UPC)
Associated Unit: Hydrogeology Group (UPC-CSIC)



*« Per fer les coses bé cal: primer, l'amor,
segon, la tècnica. »*

Antoni Gaudí i Cornet (1852-1926)

Summary

The competition for space in urban areas due to an exponential growth of population makes underground engineering plays a crucial role in the development of cities. New urban planning concepts, technology advances and innovative construction capabilities condition the implementation of larger and more highly efficient infrastructures. These urban underground infrastructures deal with variables such as cost, duration, safety, and management; faces political, social, economic and environmental issues; and guarantees future sustainability, maintenance, and energy efficiency. To do so, all these concepts and variables must be kept in mind during the whole construction process: (I) project design, (II) project construction and (III) project exploitation. **This thesis aims to demonstrate how the construction cycle deals with the various impacts produced by the interaction of underground constructions with groundwater at each stage of the process, with a view to providing improved processes.**

During the project design (stage I) previous data is collected, new data is generated, created (boreholes, field tests, chemical samples...) and processed, helping to understand the context and to design the infrastructure. There are very advanced tools to store and process geological, hydrochemical and hydrogeological data, but most of these tools are not common in infrastructure projects. Often most of the constructions only perform

the minimum legal requirement to characterize the ground: a pumping test. Therefore, there is a need to provide the constructors with a set of methods and tools to allow them to increase the quality of their hydrogeological analysis, which will allow early detection problems associated with the groundwater.

The interaction of underground constructions with groundwater generates impacts. These impacts can usually be minimized by using mitigation measures. The most common impacts caused by underground constructions are the groundwater barrier effect (impact on the groundwater) and the groundwater pressure distribution and limitation under the bottom slab (impact in the underground construction). In the literature there are many examples and designs to mitigate both groundwater barrier effect and groundwater pressure distribution and limitation under the bottom slab. However, to the author's knowledge, there is no design that integrates both solutions. Since it is illogical to design a solution without considering all the factors involved in the problem, all mitigation measures depending on or affecting the groundwater head should consider the groundwater head variation caused by the affection of other mitigation measures. This thesis presents an innovative groundwater by-pass design that enables the groundwater to flow through the structure and provide a homogenous distribution of the water pressure under the bottom slab. The new integrated design was applied to the largest underground infrastructure of Barcelona: La Sagrera railway station. A hydrogeological model was implemented to test the original and the integrated designs in three different scenarios. This new solution mitigates the groundwater barrier effect and optimizes the bottom slab, considerably reducing the costs and increasing safety during the construction phase.

During the construction (stage II) a great amount of new data is generated. Monitoring is required when dewatering underground constructions in order to anticipate unexpected events and preserve nearby existing structures and/or buildings. The most accurate and spread monitoring method to measure displacements is levelling, a point-like surveying technique that typically allows for tens of discrete in-situ sub-millimetric measurements per squared kilometer. Another emerging technique for mapping soil deformation is the Interferometric Synthetic Aperture Radar (InSAR), which is based on SAR images acquired from orbiting satellites or by ground-based stations (GB-SAR). This remote sensing technique can provide better spatial point density than levelling, more extensive spatial coverage and cheaper acquisitions. Both satellite and ground-based SAR systems have been used and tested in a variety of analyses. However, nobody has applied this technology as a monitoring tool during construction works yet.

This thesis contributes to data storing and data analysis software that implies new and significant method developments for increasing the quality of the hydrogeological analysis; it provides new approaches to address the groundwater corrective measures definition during the design stage, and it develops and applies new methods of infrastructure monitoring using ground-based and satellite SAR sensors during the construction stage.

Resum

Degut al creixement exponencial de la població i tenint en compte que l'espai dins les àrees urbanes és finit és necessari la construcció d'infraestructures subterrànies. L'execució d'infraestructures més grans i eficients és possible gràcies als nous conceptes en planificació urbana i a l'avenç tecnològic en la construcció. No obstant això, variables com el cost, la durada, la seguretat i la gestió; els problemes polítics, socials, econòmics i ambientals; garantir la sostenibilitat futura, el manteniment i l'eficiència energètica, fan d'aquesta execució un problema complex. Per això, totes aquestes variables han d'estar presents durant totes les fases del procés constructiu: (I) fase de disseny, (II) fase de construcció, i (III) fase d'exploració. Les construccions subterrànies interactuen amb el medi subterrani, el resultat de la interacció són uns impactes en la construcció i en el medi ambient. Tots aquests impactes són avaluats al llarg del procés constructiu per tal de ser corregits o minimitzats. **L'objectiu principal d'aquesta tesi és conèixer com s'avaluen els diferents impactes a cadascuna de les fases del procés constructiu per poder així proposar millores.**

Durant el disseny del projecte (fase I) i per tal d'entendre el context i el disseny de la infraestructura es recullen dades històriques i es generen noves dades (pous, proves de camp, mostres químiques ...). Tot i que actualment hi ha eines molt avançades que permeten emmagatzemar i processar informació geològica, hidroquímica i hidrogeològica, l'ús de la majoria d'aquestes eines no és habitual en els projectes

d'infraestructures subterrànies ja que la majoria de les construccions caracteritzen el terreny únicament amb una prova de bombament. Per tant, és necessari proporcionar als constructors un conjunt de mètodes i d'eines que permetin augmentar la qualitat dels seus anàlisis (com per exemple les proves de bombament), per augmentar així la detecció primerenca de problemes associats a les aigües subterrànies.

La interacció de les construccions subterrànies amb les aigües subterrànies genera impactes. Aquests impactes es poden minimitzar mitjançant l'ús de mesures de mitigació. Els impactes més comuns causats per construccions subterrànies són l'efecte barrera (impacte en les aigües subterrànies) i la distribució i limitació de subpressions sota la llosa de fons (impacte en la construcció subterrània). A la literatura hi ha molts dissenys que permeten mitigar l'efecte barrera i millorar la distribució de les subpressions sota la llosa de fons. No obstant això, no hi ha cap disseny que integri les dues solucions. És il·lògic dissenyar una mesura correctora sense tenir en compte tots els factors que intervenen en el problema. Aquesta tesi presenta un disseny innovador per bypassar les aigües subterrànies a través de l'estructura proporcionant una distribució homogènia de les subpressions sota la llosa de fons. El nou disseny s'ha aplicat en la infraestructura subterrània més gran de Barcelona: la futura estació de tren de la Sagrera. S'ha realitzat un model hidrogeològic per provar els nous dissenys en tres escenaris diferents. Aquesta nova solució minimitza l'efecte barrera de les aigües subterrànies i optimitza la llosa de fons, reduint considerablement els costos i augmentant la seguretat durant la fase de construcció.

Durant la construcció de les infraestructures (fase II) es generen una gran quantitat de dades. Quan una construcció rebaixa el nivell freàtic cal auscultar els nivells i la deformació del terreny per tal d'anticipar esdeveniments inesperats i preservar les estructures i / o edificis propers existents. El mètode actual més utilitzat per mesurar desplaçaments en el terreny és l'anivellament, una tècnica que permet avaluar in situ desenes de punts discrets amb una precisió submil·limètrica. Una tècnica emergent per mesurar la deformació del sòl és el Radar d'Obertura Sintètica Interferomètrica (InSAR), que es basa en imatges SAR adquirides des de satèl·lits en òrbita o bé des d'estacions al terra (GB-SAR). Aquesta tècnica de detecció remota proporciona una major cobertura espacial i més econòmica que els mètodes d'auscultació tradicionals. Tot i que la tecnologia SAR s'ha utilitzat i validat en una gran varietat d'anàlisis, ningú ha aplicat encara aquesta tecnologia com a eina d'auscultació durant la construcció d'infraestructures.

Aquesta tesi contribueix a: (I) millorar l'emmagatzematge i processament de dades a través de nous desenvolupaments i mètodes que permeten augmentar la qualitat de l'anàlisi hidrogeològic; (II) oferir noves formes d'anàlisi per al disseny de mesures correctores durant l'etapa de disseny; i (III) desenvolupar i aplicar nous mètodes d'auscultació d'infraestructura a través de sensors SAR (terrestres i satèl·lit) durant la fase constructiva.

Resumen

La limitación de espacio en áreas urbanas junto al crecimiento exponencial de la población, hace necesaria la construcción de infraestructuras subterráneas. Nuevos conceptos en planificación urbana junto con los avances tecnológicos en la construcción hacen posible la ejecución de infraestructuras más grandes y de más eficiencia. No obstante, variables tales como el coste, la duración, la seguridad y la gestión; los problemas políticos, sociales, económicos y ambientales; y garantizar la sostenibilidad futura, el mantenimiento y la eficiencia energética, hacen de esta ejecución un problema complejo. Por ello, todas estas variables deben estar presentes durante todo el proceso constructivo: (I) diseño del proyecto, (II) construcción del proyecto y (III) explotación del proyecto. Esta tesis tiene como objetivo principal **saber cómo el ciclo constructivo (diseño del proyecto, construcción y explotación de proyectos) procesa las problemáticas inducidas por la interacción de las nuevas infraestructuras subterráneas urbanas con las aguas subterráneas para luego mejorarlo.**

Durante el diseño del proyecto (fase I) se recogen los datos históricos, se generan nuevos datos (pozos, pruebas de campo, muestras químicas ...) y se procesa conjuntamente, lo que ayuda a entender el contexto y el diseño de la infraestructura. Existen herramientas muy avanzadas para almacenar y procesar información geológica, hidroquímica e hidrogeológica, aunque la mayoría de estas herramientas no son comunes en los

proyectos de infraestructuras subterráneas ya que es común que la mayoría de las construcciones sólo se realice una prueba de bombeo para caracterizar el subsuelo. Por lo tanto, hay una necesidad de proporcionar un conjunto de métodos y de herramientas a los constructores para que puedan aumentar la calidad de su análisis (como pruebas de bombeo), para aumentar así la detección temprana de problemas asociados a las aguas subterráneas.

La interacción de las construcciones subterráneas con las aguas subterráneas genera impactos. Estos impactos generalmente pueden minimizarse mediante el uso de medidas correctoras. Los impactos más comunes causados por las construcciones subterráneas son el efecto barrera (impacto en las aguas subterráneas) y la distribución y limitación de subpresiones bajo la losa de fondo (impacto en la construcción subterránea). En la literatura hay muchos ejemplos de diseños para mitigar tanto el efecto barrera y como para mejorar la distribución de las subpresiones bajo la losa de fondo. Sin embargo, no hay ningún diseño que integre ambas soluciones. Es ilógico diseñar una medida correctora sin tener en cuenta todos los factores que intervienen en el problema. Esta tesis presenta un diseño innovador de by-pass para las aguas subterráneas que permite el flujo de agua subterránea a través de la estructura a la vez que proporciona una distribución homogénea de las subpresiones bajo la losa de fondo. El nuevo diseño se ha aplicado en la infraestructura subterránea más grande de Barcelona: la futura estación de tren de La Sagrera. Se ha realizado un modelo hidrogeológico para probar los nuevos diseños en tres escenarios diferentes. Esta nueva solución mitiga el efecto barrera de las aguas subterráneas y optimiza la losa de fondo, lo que reduce considerablemente los costes y aumenta la seguridad durante la fase de construcción.

Durante la construcción (fase II) se genera una gran cantidad de nuevos datos. Es necesario auscultar los niveles y la deformación del terreno cuando una construcción rebaja el freático con el fin de anticiparse a acontecimientos inesperados y a preservar las estructuras y / o edificios cercanos existentes. El método actual más usado para medir desplazamientos en el terreno es la nivelación, una técnica que permite evaluar in situ decenas de puntos discretos con una precisión sub-milimétrica. Una técnica emergente para medir la deformación del suelo es el Radar de Apertura Sintética Interferométrica (InSAR), que se basa en imágenes SAR adquiridas o bien desde satélites en órbita o bien desde estaciones en tierra (GB-SAR). Esta técnica de detección remota proporciona una mayor cobertura espacial y más barata que los métodos de auscultación tradicionales. Aunque la tecnología SAR se ha utilizado y validado en una gran variedad de análisis, nadie ha aplicado esta tecnología como una herramienta de auscultación durante la construcción de infraestructuras.

Esta tesis contribuye a mejorar el almacenamiento y tratamiento de datos a través de nuevos desarrollos y métodos que permiten aumentar la calidad del análisis hidrogeológico; ofrece nuevas formas de análisis para el diseño de medidas correctoras durante la etapa de diseño; y desarrolla y aplica nuevos métodos de auscultación de infraestructura a través de sensores SAR (terrestres y satélite) durante la fase constructiva.

Acknowledgements

First and foremost, I want to thank my advisors, **Enric Vázquez and Estanislao Pujades** for their continuous support, for their guidance, their patience, for responding fast when I needed them, for pushing me to become better, for all that they have taught me. Thanks for bringing me the opportunity to enjoy my PhD.

Half of my thesis is the results of the collaboration with the Centre Tecnològic de Telecomunicacions de Catalunya (CTTC). Special thanks to **Michele Crosetto and Oriol Monserrat**, who had the patience to teach me all I know about SAR. Thank you time and your trust. Working with you has been a pleasure.

I must also acknowledge **all of the colleagues of the hydrogeology group**. Both those who finished and those who still have part of the way in front of them. I loved coming to an office where I felt like home. Thanks for making that possible. Special thanks to **Rotman Criollo**; working next to him made the task much more enjoyable thanks to all for becoming friends.

I would also acknowledge ADIF (Administration), INECO (Construction Management), AudingIntraesa-Ayesa-Cicsa (technical assistance) and Dragados-Acciona-Comsa-Acsa (construction companies) for their support throughout this thesis. Special thanks to **Alejandro Lopez, Ingrid Pujol and Carlos Puig**.

A mi familia...

*Con un afecto especial quiero dar las gracias a **mis padres y a mi hermana**. Vuestro apoyo incondicional ha sido, y aún es, un faro que me muestra que puedo ser mejor cada día, tanto en lo profesional como en lo personal. Gracias!*

*Aquest temps no he caminat sol. He anat de la mà de la meva preciosa dona Anna, a qui estimo incondicionalment. Ella m'ha donat l'estabilitat emocional i l'amor necessari per fer d'aquests últims anys els millors de la meva vida. Gràcies bonica per ser com ets. **Anna, aquesta tesi te la dedico a tu, perquè, a l'igual que en la nostra relació, això és el resultat de treballar bé cada dia.***

List of Contents

SUMMARY	III
RESUM	V
RESUMEN	VII
ACKNOWLEDGEMENTS	IX
LIST OF CONTENTS	XI
LIST OF FIGURES	XV
LIST OF TABLES	XIX
CHAPTER 1. INTRODUCTION.....	1
1.1. MOTIVATION AND OBJECTIVES	1
1.2. THESIS OUTLINE	6
CHAPTER 2. HOW TO IMPROVE AND CUSTOMIZE HYDROGEOLOGICAL SOFTWARE.....	9
2.1. INTRODUCTION	9
2.2. METHODOLOGY	11
2.2.1. <i>General systems development</i>	11

2.2.2.	<i>The Updating Approach</i>	12
2.3.	APPLICATION EXAMPLES	15
2.3.1.	<i>MIX 2.0</i>	15
2.3.2.	<i>Other examples</i>	18
2.3.3.	<i>Reused software validation</i>	20
2.4.	SYSTEM REQUIREMENTS AND PROGRAM AVAILABILITY	21
2.5.	SUMMARY AND CONCLUSIONS	21

CHAPTER 3.	INTEGRATION OF GROUNDWATER BY-PASS FACILITIES IN THE BOTTOM SLAB DESIGN FOR LARGE UNDERGROUND STRUCTURES.	23
3.1.	INTRODUCTION	23
3.2.	MATERIALS AND METHODS	28
3.2.1.	<i>Geographical, geological, and hydrogeological description</i>	28
3.2.2.	<i>Basic concepts: Groundwater barrier effect</i>	30
3.2.3.	<i>Problem statement</i>	31
3.2.3.1.	Groundwater By-pass	31
3.3.	NEW INTEGRATED DESIGN	33
3.3.1.	<i>Integrated Design description</i>	33
3.3.1.1.	Design 1: Artesian wells drilled inside the retaining walls	33
3.3.1.1.	Design 2: Artesian wells drilled outside the retaining walls	33
3.3.2.	<i>Numerical model</i>	35
3.3.1.	<i>Scenario simulation</i>	36
3.4.	RESULTS	38
3.1.	DISCUSSION AND CONCLUSIONS	41

CHAPTER 4.	GB-SAR INTERFEROMETRY DISPLACEMENT MEASUREMENTS DURING DEWATERING IN CONSTRUCTION WORKS.	45
4.1.	INTRODUCTION	45
4.2.	PROBLEM STATEMENT AND GB-SAR EXPERIMENT DESIGN	47
4.2.1.	<i>GB-SAR BASICS</i>	47
4.2.2.	<i>LA SAGRERA STATION EXCAVATION AREA</i>	49
4.2.2.1.	General situation	49
4.2.2.2.	Geological and hydrogeological settings	50
4.2.2.3.	Construction characteristics	53
4.2.3.	<i>EXPERIMENT SETUP</i>	53
4.2.3.1.	Pumping test	54
4.2.3.2.	GB-SAR location	54
4.2.3.1.	GB-SAR measurements	55
4.2.3.2.	Other measurements	56
4.2.3.3.	Hydrogeological and hydromechanical numerical models	56
4.3.	RESULTS AND DISCUSSION	56
4.4.	CONCLUSIONS	61

CHAPTER 5. LEVELLING VS. INSAR IN AN URBAN UNDERGROUND CONSTRUCTION MONITORING: PROS AND CONS.	63
5.1. INTRODUCTION	63
5.2. MATERIALS AND METHODS	65
5.2.1. <i>Geographical, geological and hydrogeological description</i>	65
5.2.2. <i>Construction characteristics</i>	67
5.2.3. <i>Levelling</i>	67
5.2.4. <i>InSAR</i>	68
5.2.5. <i>Calculation of the pumping settlements (numerical model and analytical equations)</i>	68
5.3. RESULTS AND DISCUSSION	70
5.3.1. <i>Levelling</i>	70
5.3.2. <i>InSAR</i>	72
5.3.1. <i>Levelling vs. InSAR</i>	73
5.4. CONCLUSIONS	76
CHAPTER 6. GENERAL CONCLUSIONS.	77
APPENDIX	79
6.1. SUPPLEMENTARY MATERIAL CHAPTER 2	81
6.2. SUPPLEMENTARY MATERIAL CHAPTER 3	84
6.3. SUPPLEMENTARY MATERIAL CHAPTER 4	87
REFERENCES	91
LIST OF PUBLICATIONS	105
6.4. SCIENTIFIC ARTICLES	107
6.5. BOOK CHAPTERS	110
6.6. PROCEEDINGS	111
6.7. SOFTWARE REGISTRATION	112
6.8. PROJECTS DEVELOPED AND RELATED WITH THE THESIS	114
6.8.1. <i>Public Research Projects</i>	114
6.8.2. <i>Private Research Projects</i>	115
ABOUT THE AUTHOR	121

List of Figures

FIGURE 1. MODIFICATION OF THE “MACLEAMY CURVE” WHICH ILLUSTRATES THE CONCEPT OF MAKING DESIGN DECISIONS EARLIER IN THE PROJECT WHEN OPPORTUNITY TO INFLUENCE POSITIVE OUTCOMES IS MAXIMIZED AND THE COST OF CHANGES MINIMIZED, ESPECIALLY AS REGARDS THE DESIGNER AND DESIGN CONSULTANT ROLES.....	5
FIGURE 2. DECISION FLOW DIAGRAM: PROGRAMMING STEPS.	14
FIGURE 3. COMPARISON BETWEEN THE OLD MIX INPUT FILE (TOP) AND THE NEW MIX v2013 INPUT DYNAMIC TABLE (DOWN)...	17
FIGURE 4. COMPARISON BETWEEN THE OLD MIX OUTPUT FILE (WITH MORE THAN 6.000 LINES) (LEFT) AND THE NEW MIX v2013 OUTPUT GUI (PIE PLOTS, DATA REARRANGEMENT AND SCATTER PLOTS) (RIGHT).....	18
FIGURE 5. FLOW DIAGRAM PATHS FOLLOWED BY EACH OF THE PRESENTED CASE STUDIES: EASYQUIM, EASYBAL, MIX AND BRINEMIX.	20
FIGURE 6. BOTTOM SLAB WATER PRESSURE DISTRIBUTION SCHEME. (1) STATES THE PROBLEM, (2) SHOWS A POSSIBLE SOLUTION.	24
FIGURE 7. GROUNDWATER BARRIER EFFECT SCHEME. (1) STATES THE PROBLEM, (2) SHOWS A POSSIBLE SOLUTION.	25
FIGURE 8 GROUNDWATER BY-PASS DESIGNS. (1) REMOVAL OF CUT-OFF WALL, (2) INTAKE AND RECHARGE PIPES INSTALLED IN DRILLED HOLE, (3) INTAKE AND RECHARGE THROUGH PERMEABLE CUT-OFF WALLS, AND (4) INTAKE AND RECHARGE WELLS. MODIFIED FIGURE FROM AKAGI, 2004. NOT TO SCALE.	26
FIGURE 9. THIS FIGURE SHOWS HOW THE BOTTOM SLAB WATER PRESSURE DISTRIBUTION AND THE GROUNDWATER BARRIER EFFECT PROBLEMS MIGHT BE CONSIDERED.	27

FIGURE 10. GEOGRAPHICAL LOCATION OF THE STUDY SITE.	28
FIGURE 11. DETAILED GEOLOGICAL PROFILE OF THE SITE. (1) PLAN VIEW OF THE GEOLOGICAL BASEMENT, (2) CROSS SECTION A-B, (3) CROSS SECTION C-D. EXCAVATION AREA, LIMITED BY DIAPHRAGM WALLS, IS SHOWN IN LIGHT BROWN COLOR. BOTH CROSS SECTIONS SHOW THE MAXIMUM EXCAVATION AND THE REQUIRED DEWATERING SYSTEM.	29
FIGURE 12. CROSS SECTION OF A THEORETICAL AQUIFER WITH A STRUCTURE REDUCING ITS NATURAL TRANSMISSIVITY. GROUNDWATER BARRIER EFFECT SCHEME. MODIFIED FROM PUJADES, 2012.	30
FIGURE 13. ORIGINAL DESIGN SCHEME. (1) PLAN VIEW. (2) CROSS SECTION. BOTTOM SLAB	32
FIGURE 14. INTEGRATED DESIGNS SCHEME. (1) PLAN VIEW. (2) CROSS SECTION.	34
FIGURE 15. NUMERICAL MODEL MESH AND BOUNDARY CONDITIONS.	37
FIGURE 16. (1) DETAILED WATER TABLE LOCATION FOR EACH SCENARIO. (2) DESIGNS AND SCENARIO EVALUATION.	37
FIGURE 17. SIMULATION RESULTS: WATER HEADS (IN M.A.S.L.) FOR EACH SCENARIO AND DESIGN.	39
FIGURE 18. SIMULATION RESULTS: WATER PRESSURE (IN M.W.P.) FOR EACH SCENARIO AND DESIGN.	40
FIGURE 19. ILLUSTRATION OF HANS MELLER TO EMPHASIZE DIVERGENCE IN INTERPRETATIONS.	46
FIGURE 20. GROUND-BASED SAR IMAGES TREATMENT. THE PHYSICS AND THE MATHEMATICS.	48
FIGURE 21. GEOGRAPHICAL LOCATION OF THE STUDY SITE. THE YELLOW WELLS ARE THE ONES ACTIVATED DURING THE PUMPING TEST.	49
FIGURE 22. SOIL AND EXCAVATION PROFILE CORRESPONDING TO THE TRANSVERSE SECTION A6 (SEE FIGURE 25 TO LOCATE THE SECTION) AT THE TIME OF THE EXPERIMENT. A6 IS ALSO THE TRANSVERSE SECTION OF THE HYDROMECHANICAL MODEL ©PLAXIS.	51
FIGURE 23. DETAILED GEOLOGICAL PROFILE OF THE SITE. (1) PLAN VIEW OF THE GEOLOGICAL BASEMENT, (2) CROSS SECTION A-B, (3) CROSS SECTION C-D. EXCAVATION AREA, LIMITED BY DIAPHRAGM WALLS, IS SHOWN IN LIGHT BROWN COLOR. BOTH CROSS SECTIONS SHOW THE MAXIMUM EXCAVATION AND THE REQUIRED DEWATERING SYSTEM.	52
FIGURE 24. SCHEME OF THE EXPERIMENT AND THE EXPECTED WALL DEFORMATION.	54
FIGURE 25. RADAR POSITION, GB-SAR ANALYSIS AREA, MANUAL ACQUISITION DATA TARGETS (BLUE CIRCLES, MON) AND INCLINOMETERS (YELLOW SQUARES), PUMPING WELL POSITIONS (RED CIRCLES) AND GB-SAR (BLACK DASHED LINES) AND ©PLAXIS (RED DASHED LINE) SECTION ANALYSIS.	55
FIGURE 26. SUMMARY OF THE EXPERIMENT DATES. INCREASES INSIDE THE ENCLOSURE, PUSHING THE WALL IN FRONT OF THE ...	57
FIGURE 27. HYDROMECHANICAL MODEL (©PLAXIS) RESULTS. CROSS SECTION: HORIZONTAL DISPLACEMENT INDUCED BY DEWATERING CALCULATED IN THE MODEL FOR SECTION A6. (1) SCHEME, (2) MODEL RESULTS.	58
FIGURE 28. RADAR OUTPUT: DISPLACEMENTS ESTIMATED BY THE GB-SAR. ALL PIXELS WITH DISCARDED DATA DUE TO THE LACK OF COHERENCE ARE SHOWN IN BLACK. THE RED DASHED LINE REPRESENTS THE MEASURED DIAPHRAGM WALL. NEGATIVE VALUES REPRESENT MOVEMENTS TOWARDS THE SENSOR.	59
FIGURE 29. PLAN VIEW: COMPUTED (GRAY BAND) AND MEASURED (RED ARROWS) HORIZONTAL DISPLACEMENTS FOR THE MOUNTAIN SIDE RETAINING WALL IN ALL SECTIONS CONSIDERED. (3) CROSS SECTION: LOCATIONS OF THE ANCHORS.	60
FIGURE 30. MULTI-PARAMETER CORRELATION: PUMPING RATES, DRAWDOWNS AND GB-SAR WALL HORIZONTAL DISPLACEMENTS. THE MEASUREMENTS ARE SHOWN IN CIRCLES. THE DASHED LINE REPRESENTS A DATA GAP. THE REST OF THE CROSS-SECTIONS ARE INCLUDED IN THE APPENDIX.	60
FIGURE 31. GEOGRAPHICAL LOCATION OF THE STUDY SITE AND DETAILED GEOLOGICAL PROFILE OF THE SITE. (1) PLAN VIEW OF THE GEOLOGICAL BASEMENT, (2) CROSS SECTION A-B, (3) CROSS SECTION C-D. EXCAVATION AREA, LIMITED BY DIAPHRAGM WALLS,	

IS SHOWN IN LIGHT BROWN COLOR. BOTH CROSS SECTIONS SHOW THE MAXIMUM EXCAVATION AND THE REQUIRED DEWATERING SYSTEM.	66
FIGURE 32. NUMERICAL MODEL MESH AND BOUNDARY CONDITIONS.	69
FIGURE 33. MONITORED POINTS BY LEVELLING. LEVELLING TIME SERIES GROUPED BY LOCATION.....	71
FIGURE 34. INSAR DISPLACEMENT VELOCITY MAP (ABOVE). INSAR DISPLACEMENT TIME SERIES GROUPED BY LOCATION (BELOW).	74
FIGURE 35. INSAR (BLUE), LEVELLING (RED) AND NUMERICAL MODEL (ORANGE) RESULT COMPARISON.	75
FIGURE 36. DECISION FLOW DIAGRAM WITH SOME CODE COMMENTS RELATED TO THE APPENDIX.	83
FIGURE 37. PUMPING TEST WELLS AND PIEZOMETERS LOCATION.	85
FIGURE 38. FITTING CURVES OF THE NUMERICAL MODEL DURING THE PUMPING TEST.	86
FIGURE 39. GB-SAR, TRADITIONAL MONITORING DATA AND HYDROMECHANICAL MODEL RESULTS FOR ALL CROSS-SECTIONS.	88
FIGURE 40. GB-SAR, TRADITIONAL MONITORING DATA AND HYDROMECHANICAL MODEL RESULTS FOR ALL CROSS-SECTIONS.	89

List of Tables

TABLE 1. RESULTS SUMMARY FOR EACH SCENARIO AND DESIGN	42
TABLE 2. PARAMETERS OF THE HARDENING SOIL MODEL USED IN THE ©PLAXIS HYDROMECHANICAL MODEL. γ_T IS THE SOIL UNIT WEIGHT, c' IS COHESION, ϕ' IS THE FRICTION ANGLE, E IS THE YOUNG'S MODULUS, ν IS POISSON'S RATIO, m IS THE POWER FOR STRESS-LEVEL DEPENDENCY OF THE STIFFNESS, E_{50REF} IS THE REFERENCE YOUNG'S MODULUS AT 50% OF THE STRENGTH, E_{OEDREF} IS THE REFERENCE ODOMETRIC MODULUS, AND E_{URREF} IS THE REFERENCE UNLOADING-RELOADING MODULUS.....	51
TABLE 3. HYDRAULIC PARAMETERS OF THE AQUIFER LAYERS IN THE STUDY SITE.....	85

Chapter 1.

Introduction.

1.1. Motivation and objectives

The competition for space in urban areas due to an exponential population growth in cities means underground engineering plays a crucial role in the development of cities. Urban underground infrastructures are especially challenging because of the impacts generated by the interaction between underground infrastructures and groundwater, which can be maximized within high density populated areas (Pujades et al, 2012, Attard et al., 2016). The interaction between underground infrastructures and groundwater is two-fold: (1) groundwater may damage underground infrastructures or complicate their construction, and (2), underground infrastructures may impact aquifers.

On one hand, groundwater impacts are usually related to safety when they occur during the construction of underground infrastructures (Pujades et al, 2014a). Groundwater must be considered to guarantee the safety of the workers, the integrity of the construction, and the adjacent structures. During construction, the water table is usually lowered and controlled in order to be able to work in dry conditions and to avoid base level instabilities, such as hydraulic bottom uplift or liquefaction (Pujades et al, 2014b). After the construction, the water table returns to its original level, increasing the water pressure under the bottom slab (in cases of overpressure the bottom slab may break).

On the other hand, underground infrastructures may affect the quantity and the quality of the available water resources. In the case of low permeability underground structures, groundwater barrier effect is usually the main concern (Vázquez-Suñe et al., 2004). The underground infrastructure can act as a natural flow barrier, reducing the effective transmissivity of the aquifer and leading ideally to a rise in the water table upgradient and a lowering on the downgradient side. These modifications of the water table can have negative consequences (Deveughèle et al., 2010; Font-Capo et al., 2015). Rising water levels may flood basements, promote soil salinization, affect flora by rotting the roots of plants, reduce the bearing capacity of shallow foundations, expand heavily compacted fills under foundation structures, cause settling of poorly compacted fills upon wetting, increase loads on retaining systems or basement walls of buildings, increase the need for drainage in temporary excavations, and propagate contaminants contained in the partially saturated zone (Marinos and Kavvas, 1997; Tambara et al., 2003; Ricci et al., 2007; Paris et al., 2010). The lowering of heads on the downgradient side can cause seawater intrusion in coastal aquifers, ground subsidence, the drying of wells and springs and can kill off phreatophytes. Moreover, the difference of water pressure between both sides of the underground structure leads to asymmetric loading for which building foundations are seldom designed (Custodio and Carrera, 1989; Tambara et al., 2003).

In order to properly assess the potential impacts, it is important to characterize the site hydrogeologically (at geological, hydrochemical and hydrogeological level). Errors or inaccurate hydrogeological knowledge could mislead the final project or lead to unforeseen events. In fact, numerous accidents have occurred in recent years (for instance, the tunnel collapse in Barcelona - Spain, Van der Boom, 2011; or Köln - Germany, Van Baars, 2011). During the last few years, some regulations have appeared to control the impacts in both groundwater and infrastructures. In the case of Barcelona, the Municipal Environmental Ordinance of Barcelona ("*Ordenança municipal del medi ambient de l'Ajuntament de Barcelona*") collects and summarizes the following local and state regulations¹:

- Metropolitan regulation for water discharge
- Procedure H0309 - temporary water diversion. Catalan Water Agency.

¹

- Reglament metropolità d'abocament d'aigües.
- Procediment H0309 - Derivació d'aigües amb caràcter temporal. Agència Catalana de l'Aigua.
- Codi tècnic de l'edificació (CTE) - SE-C Cimentacions; 7.4 Gestió de l'aigua.
- RD 1514/2009, de 2 d'octubre, pel qual es regula la protecció de les aigües subterrànies contra la contaminació i el deteriorament.
- Llei 22/2011, de 28 de juliol, de residus i sòls contaminats.
- RD 9/2005, de 14 de gener, pel qual s'estableix la relació d'activitats potencialment contaminants del sòl i els criteris i estàndards per a la declaració de sòls contaminants.
- GISA: Plec de prescripcions per a l'assistència tècnica a la redacció d'estudis hidrogeològics.

- Technical Building Code (CTE) - SE-C Foundations; 7.4 Water Management.
- Decree 1514/2009, of 2 October, which regulates the protection of groundwater against pollution and deterioration.
- Law 22/2011 of 28 July on waste and contaminated soils.
- Decree 9/2005 of 14 January, establishing the list of potentially soil polluting activities and the criteria and standards for the declaration of soil contaminants.
- GISA: Specifications for technical assistance in the preparation of hydrogeological studies.

These regulations are only mandatory when the construction affects the water table and only require the performance of one pumping test to obtain aquifer parameters and to define the dewatering system. As a result, most of the underground constructions that interact with groundwater are performed with very poor knowledge on the hydrogeodynamics of the site.

The impacts on both aquifer and infrastructures must be limited, requiring construction designs that ensure safety compliance and preservation of the aquifer conditions. As a result, it is necessary to adopt corrective measures previous to, during, and/or after the construction that do not complicate the development of the construction and do not increase the total cost.

Urban underground infrastructures deal with variables such as cost, duration, safety, and management; faces political, social, economic and environmental issues; and guarantees future sustainability, maintenance, and energy efficiency. To do so, all these concepts and variables must be kept in mind during the whole construction process: (I) project design, (II) project construction and (III) project exploitation. The first stage "builds the project on paper", while the second and the third stages encompass the physical implementation of the project.

During the project design (stage I) previous data is collected, new data is generated, created (boreholes, field tests, chemical samples...) and processed, helping to understand the context and to design the infrastructure. The historical data can be used to design the first draft of the project. These data can be obtained from many different sources and can be structured and unstructured material in a wide variety of formats (text, numerical, multimedia, software, etc.). Since digital data collection, aggregation and integration have experienced an exponential increase (e.g. streaming in from a growing number of satellites and sensors, Internet, etc.), we are overrun by data.

The first draft of the project is used to define where and how additional new data must be generated (for instance, drilling new piezometers and/or wells, hydrochemical sampling or performing pumping tests). New data increases the data density in the underground construction area and allows defining the status quo of the groundwater (in terms of quantity and quality).

There are very advanced tools to store and process geological, hydrochemical and hydrogeological data, such as ArchHydro (Strassberg, 2007), H+ database (de Dreuzy et al., 2006) or HYDOR (Velasco et al. 2015). However, most of these tools are not common in infrastructure projects because most of the constructions only perform

the minimum legal requirement to characterize the context: a pumping test. Even if the pumping test usually leads to reliable hydraulic parameters estimation, its reliability greatly depends on the quality of the pumping test and the analysis, and on the accuracy of the geological and hydrogeological knowledge (Criollo et al., 2015). Therefore, there is a need to provide constructors with a set of tools based on software platforms they can feel comfortable with and which will allow them to increase the quality of their hydrogeological analysis. This will then allow early detection problems associated to the groundwater.

The use of spreadsheets is very common in construction since they are useful to store, process and plot any type of data. There are many examples of spreadsheets developed to assist hydrogeological calculations (e.g. Akin et al 2002, Locock et al 2008, 2014, Elmore et al., 2007, Molano, 2014). However, it is sometimes difficult to adapt them to be useful in a specific analysis. In this sense, there is not an easy methodology yet to allow non-experts and non-software developers to adapt existing geological, hydrochemical and hydrogeological tools and to offer the possibility of extending its functionalities.

As mentioned above, underground infrastructures can be especially challenging when the construction is under the water table and in urban environments due to the impacts on both aquifer and construction areas which usually require adopting corrective measures previous to, during, and/or after the construction.

The construction safety, cost and efficiency can be influenced by the decisions adopted during the design stage of the Project. Research shows that decisions concerning the design of projects have a major impact on cost and can eliminate a considerable percentage of construction damages (MacLeamy, 2004; Pujades et al., 2014). The Figure 1 illustrates MacLeamy Curve which relates the level of effort required, cost and effect over the infrastructure project stages. The blue line indicates the ability to impact project cost and performance, which sharply decreases as the project progresses. The red line shows how the cost of making and executing design changes is low during preliminary design, but sharply increases during the project.

For huge or complicated underground infrastructures, hydrogeological numerical models have become a frequently used tool for diagnosis, management and prediction of water behavior and ground deformation. These models are useful to estimate the hydraulic parameters of the aquifer, to predict and quantify head variations and soil deformation and to design solutions to choose the best dewatering system (Merrick and Jewell, 2003, Bonomi and Belleni, 2003, Ricci et al., 2007 and Paris et al., 2010). Historical and new data are analyzed and set up in the numerical models together with the infrastructure design to forecast groundwater evolution prior the construction.

These numerical models are also useful to quantify impacts and design mitigation measures. These mitigation measures are usually treated independently, resulting in a set of solutions (mitigation measures) in which each is associated to a specific problem. However, it is not the best praxis (Vázquez-Suñe et al., 2004). Sometimes impacts are generated or controlled by the same variable, for instance the groundwater level. This means that one independently solved mitigation measure can affect other solutions. For instance, a groundwater by-pass lowers the water table upgradient and raises the water level downgradient, and this water level variation changes the initial assumption of the bottom slab water pressure distribution design. From this example, it

seems illogical to design hydrogeological mitigation measures without considering all the mitigation measures depending on and affecting the groundwater level.

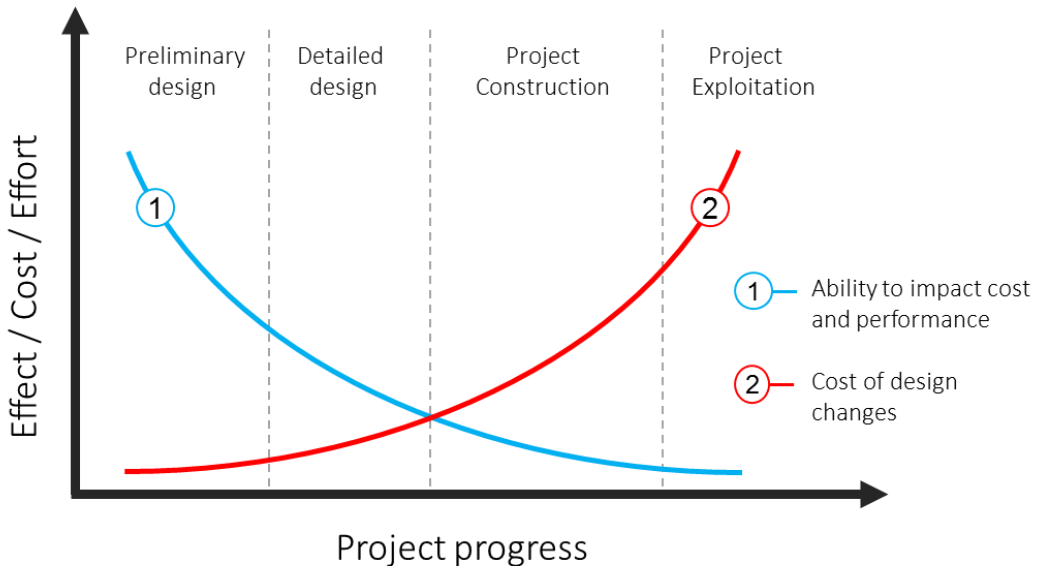


Figure 1. Modification of the “MacLeamy Curve” which illustrates the concept of making design decisions earlier in the project when opportunity to influence positive outcomes is maximized and the cost of changes minimized, especially as regards the designer and design consultant roles.

During the construction (stage II) a great amount of new data is generated. This data comes from land surveys and automatic measurement tools and is used to validate the numerical models and to prevent and detect unexpected events. Traditional infrastructure project monitoring is based on land surveys and geotechnical instruments. The most common topographic techniques include levelling, total stations, Differential Global Positioning System (DGPS), and robotic total stations, and the geotechnical techniques include pendulums, inclinometers, extensometers, piezometers, gyros, and optical fiber-based techniques (Dunncliff, 1988; Marchamalo et al., 2011). Some of these techniques, such as DGPS, robotic total stations and optical fiber-based methods, allow for automatic measurements and continuous monitoring. Although all of these techniques are widely accepted and used, they still allow only point-like measurements, requiring interpolation and extrapolation to achieve a complete measurement understanding.

In the last few decades, new technologies for assessing soil movements have evolved rapidly. Remote sensing imaging systems, such as synthetic aperture radar (SAR), now offer the ability to capture complete deformation patterns (2D information) and the possibility of both day and night operation, regardless of the

weather conditions (storm, wind, rain, and sun). The SAR sensors can be installed in satellites or on the ground (GB-SAR). While satellite acquisitions cover areas of 100 km by 100 km over longer time periods, ranging from days to weeks (depending on the satellite), ground-based systems allow for continuous monitoring in smaller areas (usually approximately 1-2 km²) and shorter revising times on the order of minutes. SAR systems presents some limitations, such as the necessity of measuring displacements perpendicular to the Line-Of-Sight (LOS) and the requirement for pixel coherence over time. Nevertheless, the SAR systems provide more capabilities compared with other deformation measurement techniques due to its heightened sensitivity to small deformations, its long-range measurement capability (up to several kilometres) and its simultaneous measurement of a vast number of points.

Both satellite and ground-based SAR systems have been used and tested in a variety of analyses. However, nobody has applied this technology as a monitoring tool during construction works yet.

In the light of the foregoing, the general objective of this thesis is **to demonstrate how the construction cycle deals with the various impacts produced by the interaction of underground constructions with groundwater at each stage of the process, with a view to providing improved processes**. Thus, the specific objectives of this thesis are:

- To provide constructors with a set of methods and tools to allow them to improve the quality of their hydrogeological analysis, allowing early detection of problems associated with groundwater.
- To propose new methods for optimizing underground infrastructure designs by combining solutions through numerical models during the design stage.
- To apply and develop new technologies and methods that have not been applied yet to monitor deformation in a construction environment during the construction stage. This thesis proposes the use of SAR (both ground-based and satellite sensors) to quantify deformation induced by dewatering and to improve the actual construction monitoring.

To do so, Adif (Administrator of Railway Infrastructures) provided the opportunity to test the developments of this thesis in the largest underground infrastructure of Barcelona (Spain): La Sagrera railway station.

1.2. Thesis outline

This thesis consists of five chapters. After the introductory chapter, the thesis continues with four chapters that were written as independent journal publications. Each chapter addresses one of the three specific objectives mentioned above.

Chapter 2 poses the problem of providing the constructors with a set of methods and tools to allow them to increase the quality of their hydrogeological analysis, which will allow early detection problems associated with groundwater. This chapter presents an approach to easily improve and customize any hydrogeological

software. The results of experience gained from updating several interdisciplinary case studies. The main insights of this approach have been illustrated by four examples: MIX (FORTRAN-based), BrineMIX (C++ based), EasyQuim and EasyBal (both spreadsheets based). The improved software has proven to be a better tool able to perform an enhanced analysis by considerably reducing the time-consuming input and output data files processing. All four examples are under the copyright protection of the Spanish Research Council (CSIC).

Chapter 2 is based on the paper: Serrano-Juan, A, Vázquez-Suñe, E., Alcaraz, M., Ayora, C., Velasco, V., Criollo, R. and Scheiber, L. How to improve and customize hydrogeological software. June 2016 - Hydrogeology Journal. *Under review*.

Also, the chapter is based on the following software registered by the Spanish National Research Council (CSIC): LAUNCH MIX (Reg. Num. CG3420733), EASYQUIM (Reg. Num. CG3420743), EASYBAL (Reg. Num. CG3420724), BRINEMIX (Reg. Num. CG3420764), all issued on March 31, 2015.

Chapter 3 provides an example of how the construction design can be optimized through numerical models analysis. This chapter presents an innovative groundwater by-pass design that enables the groundwater to flow through the structure and provide a homogenous distribution of the water pressure under the bottom slab. The new integrated design was applied to the largest underground infrastructure in Barcelona: La Sagrera railway station. A hydrogeological model was implemented to test the original and the integrated designs in three different scenarios. This new solution mitigates the groundwater barrier effect and optimizes the bottom slab, thus reducing the costs considerably and increasing safety during the construction stage.

Chapter 3 is based on the paper: Serrano-Juan, A., Vázquez-Suñe, E., Pujades, E., Velasco, V., Criollo, R., Jurado, A. Integration of groundwater by-pass facilities in the bottom slab design for large underground structures. May 2016 - Tunnelling and Underground Space Technology. *Under review*.

Chapter 4 is focused on the data acquisition during construction. This chapter aims to test the GB-SAR suitability to measure movements during construction. To do so, an experiment was performed in the future railway station of La Sagrera, Barcelona (Spain), in which GB-SAR was used to accurately quantify wall displacements induced by dewatering, and proved to be helpful in understanding structural deformations and identifying vulnerable areas. The results were compared to traditional monitoring data and numerical models to confirm the reliability of the GB-SAR measurements.

Chapter 4 is based on the paper: Serrano-Juan, A., Vázquez-Suñe, E., Monserrat, O., Crosetto, M., Hoffmann, C., Ledesma, A., Criollo, R., Pujades, E., Velasco, V., Garcia-Gil, A., Garcia-Alcaraz, M. GB-SAR interferometry displacement measurements during dewatering in construction works: the case of La Sagrera railway station in Barcelona, Spain. February 2016 - Engineering Geology. DOI: 10.1016/j.enggeo.2016.02.014.

Chapter 5 is also focused on the data acquisition during construction. This chapter analyses, compares and discusses levelling and InSAR measurements when they are used to measure the soil deformation induced by the dewatering associated with underground constructions in urban areas. To do so, an experiment was performed in the future railway station of La Sagrera, Barcelona (Spain), in which levelling and InSAR were used to accurately quantify ground deformation by dewatering. Results showed that soil displacements

measured by levelling and InSAR were not always consistent. InSAR measurements were more accurate with respect the soil deformation produced by the dewatering while levelling was really useful to determine the real impact of the construction on the nearby buildings.

Chapter 5 is based on the paper: Serrano-Juan, A., Pujades, E., Vázquez-Suñè, E., Crosetto, M. Levelling vs. Insar in urban underground construction monitoring: pros and cons. case of La Sagrera railway station (Barcelona, Spain). May 2016 - Engineering Geology. Under review.

Chapter 6 consists of a synthesis of the whole research. It contains the main conclusions by summarizing the answers to the three research-specific objectives addressed above. Furthermore, it provides an overall reflection on the conclusions, our contributions to the scientific and practical community are listed and recommendations for further research are provided.

In addition, there are **three annexes** with the supplementary material of the chapters and a list of publications related to this thesis.

Chapter 2. How to improve and customize hydrogeological software.

2.1. Introduction

Over the last few decades the rapid evolution of computer processing power has enabled the scientific community to solve different problems in the vast variety of geoscience fields such as mineralogy, petrology, geochemistry, geology, geophysics, hydrology, hydrogeology, among others. As a result, most scientists are aware of the importance of computer-aided analysis since geoscience algorithms manage many different variables, and this results in laborious calculations that are impossible to generate without a computer tool (Wang et al., 2012).

For decades scientists have searched to find repeatable and predictable processes that would improve productivity and quality of the computer architecture and programming languages in order to facilitate geoscientific calculations. The first programming languages such as FORTRAN (IBM, 1954), COBOL (Hopper, G, 1959), BASIC (Kemeny, John G. and Kurtz, Thomas E., 1964), etc. appeared in the mid 1960s and were widely

used until the 1990s. Most of them were devised to create individual programs to deal with specific tasks and short sets of data (at that time, data were limited and sometimes difficult to collect). The compilers generated the well-known “.exe”, which usually needed extra “.txt” files such as input, output or conditional data during the execution (Wang et al., 2013), resulting in a set of many different files containing the information for one analysis. Many geoscientists have developed tools based on these programming languages (e.g. Nath et al 2000, Akin et al 2002, Spada et al 2007, 2008, Agarwal et al 2008, 2010, Bea et al 2009, Prieto et al 2009, Toyokuni et al 2009, Alberti et al 2010, Jafargandomi et al 2013, etc.).

The development of new technologies in both computer architecture and programming languages continues apace, modifying the existing landscape. Current programming languages such as Matlab (MathWorks, Inc., 1984), Visual Basic (Microsoft, 1991) and Visual C (Microsoft, 1993) are known as visual languages, and are indeed more user friendly than their predecessors. Most of them integrate all the information required (input, output, sources, etc.) into a single file and enable the user to directly compute the whole analysis. Furthermore, greater computing power has corresponded to the increasing data. In the last few decades, digital data collection, aggregation and integration have experienced an exponential increase (e.g. streaming in from a growing number of satellites and sensors, Internet, etc.). Geoscientists are overrun by data and, at the same time, have access to ever-increasing computing power

Graphical User Interfaces (GUIs) are becoming common to assist rapid, rigorous and interactive analysis (Jones et al, 2014). Robin et al (1994) supported geoscience with graphical-user-interface Internet tools during the 90s. Since then, many examples of GUIs have been developed in geoscience (e.g. Sokos et al 2008, Mahabadi et al 2010, Phong et al 2012, etc.) in order to make the software more user-friendly (e.g. screen selection of the input, output arrangement for instant comprehension of the results...). Since new softwares are dynamic, visual and interactive, some old fashioned programming language-based software such as FORTRAN-based ones are becoming outdated owing to their complex analysis process (preparing input text files, analysing the output text files and displaying limited graphical options). However, despite the limitations of the aforementioned geoscientific software, they still are able to evaluate and solve successfully complex geoscience algorithms.

On the one hand, pre-existing software is being used to create new software systems rather than building new ones (Krueger, 1992). Research on technical issues such as repositories (Mili et al., 1997, 1998; Seacord, 1999; Guo and Luqi, 2000; Buregio et al., 2007), search-based tools (Lucredio et al., 2004) and domain-specific languages (Deursen et al., 2000) was the initial focus of the reuse community. However, as more experience became available for general software reuse (e.g. Endres, 1993; Griss, 1995; Joos, 1994; Frakes and Kang, 2005; Sherif et al., 2006; Lucredio et al., 2008, Bhandu et al 2013) and GIS reuse (e.g. Gordillo et al., 1999; Câmara et al., 2000; Lisboa Filho et al., 2002; Buccella et al 2013), not many reusing methodologies have been developed by the hydrogeological community. There still a lack of a simple general approach to easily reuse old fashioned hydrogeological software.

On the other hand, the combination of spreadsheets with Visual Basic for Applications (VBA) is widely used in the academic (e.g. International Journal of Engineering Education, 2004; Ibrahim, D., 2009; Palocsay et al., 2010; Wong et al., 2010) and scientific community (e.g. Asuncion, H. U., 2013) mainly because: (1) spreadsheet

interfaces are user-friendly and facilitate numerical and statistical computations, (2) data can be easily queried, analysed and visualized, (3) macro programming interface provides a good end-user guidance that helps the user in writing correct and more reliable programs (Cunha et al, 2014), (4) it saves time due to its low barrier since most researchers are already adept at manipulating spreadsheets, and (5) there are existing tools especially designed to fix potential errors (Jannach et al, 2014) and inconsistent data storage (Cunha et al, 2014). Consequently, it comes as no surprise then that nowadays a great variety of new tools exist that facilitates a number of geoscientific calculations (e.g. Zou et al 2004, Khan et al., 2006; Ayala et al., 2009; Ozcep, F., 2010; Choe et al., 2010; Aliane, N., 2010; Mayborn et al., 2011; Bonduá et al., 2012; Wang et al., 2010, 2012, 2012a, 2012b, 2012c, 2013, Jones et al 2014, etc). Specifically, in hydrogeology many spreadsheets have been developed in order to assist calculations in the analysis and interpretation of pumping tests, hydrogeochemical data, analytical and numerical solutions for groundwater flow and pollution problems, etc (e.g. Akin et al 2002, Locock et al 2008, 2014, Elmore et al., 2007, Molano, 2014), as well as benchmark analysis of existing tools (e.g. Torlapati et al., 2012).

Through this combination of spreadsheets and VBA, it is possible to reuse and update outdated programs and add new features and functionalities. This means that programs such as FORTRAN based ones can become user-friendly, dynamic and interactive. This combination also offers the possibility of adapting and personalizing the software by programming simple macros, which can run specific computing actions such as arranging input or output data to easily connect them to other software platforms, database management systems (DBMS) and GIS platforms (e.g. Velasco et al., 2014).

This chapter presents **an approach to easily reuse, customize and extend old fashioned hydrogeological software. It is the result of the experiences collected from updating several case studies.** The main insights of this approach have been illustrated by four examples: EasyQuim, EasyBal (both spreadsheets based), MIX (Carrera et al, 2004) (FORTRAN-based) and BrineMIX (PHREEQC - Parkhurst and Appelo, 1999) (C++ based). However, only the MIX will be largely discussed to allow the reader easily to follow a step by step process application of the presented approach. This chapter also wishes to answer the following research questions: **Q1** is it possible to easily update any hydrogeological program following this approach? **Q2** Is it possible that new updates lead to fewer errors during the analysis when compared to the original ones? **Q3** Are end users more efficient when using an updated spreadsheet-based program than using the original one?

2.2. Methodology

2.2.1. General systems development

Developers frequently use Object-Oriented Analysis (OOA) to analyse a task and then develop a conceptual model that can be used to complete that task. The main difference between object-oriented analysis and other forms of analysis is that the object-oriented approach requirements are organized around objects, which integrate both behaviours (processes) and states (data).

Similarly, the Systems Development Life Cycle (SDLC) is a term used to describe a process for planning, creating, testing, and deploying an information system, also commonly used in the computer programmer community. It consists of a set of phases in which each phase of the SDLC uses the results of the previous one. The SDLC comprises important phases that are essential for developers, such as planning, analysis, design, and implementation. A number of SDLC models have been created: waterfall, fountain, spiral, build and fix, rapid prototyping, incremental, and synchronize and stabilize. For example, the waterfall model shows a process, whereby developers have to follow these phases in order: (1) Requirements specification (Requirements analysis), (2) Software design, (3) Implementation and Integration (4) Testing (or Validation), (5) Deployment (or Installation) and (6) Maintenance (Kay, 2002). The object-oriented analysis (OOA) also states similar phases: (1) Analysis, (2) Design and (3) Coding.

In both Object-oriented analysis (OOA) and systems development life cycle (SDLC) the program creation can be rewritten as the following flow process:

$$ID \rightarrow GUI \rightleftharpoons DT/RUN$$

Where ID is the IDentification of the problem (SDLC (1), OOA (1)), GUI means the Graphical User Interface (SDLC (2), OOA (2)), DT represents the required Data Treatment and RUN describes the solution computation (SDLC (3-5), OOA (3)). The maintenance phase of the SDLC has not been included.

The first step is the **problem identification (ID)** which helps to understand the problem and answer questions such as what is available and what is desired. It is only when the programmer truly understands the nature of the problem that it becomes possible to identify steps such as which information is necessary and available, how to display it, how to arrange it, how to request it and which options should be offered. After identification, the **graphical user interface (GUI)** should be designed. Through this interface, the program requests the input data, visualizes the output data and offers the possibility of setting up any option the program offers. Finally, all the requested data in the GUI could require more or less **data treatment (DT)** to achieve the proper format to be computed (**RUN**). Afterwards, the output data should be again displayed in the GUI, maintaining a continuous interaction between the GUI and the computation of the program.

2.2.2. The Updating Approach

This chapter presents an approach to easily reuse, customize and extend outdated software. This approach is the result of the experiences collected from updating several case studies. It has been built as a decision flow chart (following the UML standards) as every software is different and requires different kinds of update. This chapter follows Figure 2; **Error! No se encuentra el origen de la referencia.** decision flow chart describing each step and discussing its different flow options. It is important to mention that all the presented codes have been developed to run in a MS Excel environment.

Problem identification (ID). In order to truly understand the problem, four main issues should be answered: (1) *input data and output data*, (2) *computation*, (3) *improvements* and (4) *communication*. **(1) INPUT DATA AND OUTPUT DATA.** What is computed? It is necessary to have a clear idea on all the involved data during the

process, not only considering that required but also that which is available. **(2) COMPUTATION**. How is it computed? Which softwares are involved in the computation? Is it possible to recompile the existing code (access to the source code)? At this step, the developer should understand how the program works. Particularly, some aspects such as the complexity of the algorithm, the accessibility (i.e. open code access or not) or the possibility to combine various software, can define different software configurations. **(3) IMPROVEMENTS**. Any changes needed? Possible improvements? The idea is not just to reuse and adapt outdated software, but to add new features and functionalities that will improve the performance of the analysis (e.g allowing data storage, enhancing graphic outputs or connecting the results to other software platforms such as GIS). **(4) COMMUNICATION**. What do I know? What does the final user know? Finally, it is necessary to understand who will use the software, taking into account factors such as background knowledge (both in computer and science), language, etc. It is significant how to ask for or how to display information. The problem identification process requires longer as it will define the future graphical user interface, the input and output data treatment and how the solution will be computed.

An appropriate **graphical user interface (GUI^{IN})** should request and display the adequate data (Phong et al, 2012), while being aesthetically pleasing, comprehensible, simple and responsive. **(5) INPUT DATA AND OUTPUT DATA**. Where is the input information coming from? In hydrogeology the information is commonly available from maps (use of GIS), tables (use of matrix), independent numbers (use of cells or Input Boxes) or is a selection from an existing dataset (use of buttons, lists...). The process is similar with the output, where results of the analysis are commonly displayed in maps (GIS) or tables (matrix). **(6) COMPUTATION and IMPROVEMENTS**. How to Setup the analysis? VBA offers a large set of options such as button clicks or events (e.g. when adding information or modifying a cell content). **(7) COMMUNICATION**. Again, who is the final user? There are many different options to display information or to order and select it. The MS Excel environment can greatly improve the power of the analysis by considering whether results should be static (e.g. simple tables or maps) or dynamic (e.g. pivot tables and charts). Finally, it is necessary to adapt all the new program capabilities depending on the final user knowledge.

The **input data (ID)** are usually the available data, not necessarily those that are required. As these available data are not always provided in the correct order, **(8) input data treatment (DT^{IN})** is essential. Depending on each program, filters, calculations, unit conversions and data rearrangement will sometimes be necessary to prepare the required input for analysis, whereas in other programs the input will be already in format. Non-Excel-based programs will need to **(9) export the input data (EX^{IN})** into different formats and call external executables to perform the analysis, whereas Excel-based programs (e.g. solvers, macros) will **(10) run (external – RUN^{EXT}; internal – RUN^{INT})** as a matter of course. By contrast, depending on the computational core format, **(11) output data will be imported (IM^{OUT})** into the GUI or prepared to be computed by another external program. As not all the output needs to be presented in GUI, the **Output data (OD)** can also be partially disregarded, rearranged in new tables and plotted. This **(12) output data treatment (DT^{OUT})** is usually necessary to fulfil the **(13) GUI (GUI^{OUT})** output requirements. Occasionally, it will be interesting to **export the results** to other software or platforms to obtain additional results and to perform in-depth analyses (e.g. connecting to GIS platforms adds a time-space dimension). Common considerations during the data treatment process are the decision to use code to evaluate formulas and create objects or to use pre-set formulas and

charts in the spreadsheets. Usually, data storing (input/output) will be necessary before it will be recalled by the GUI or exported into different formats.

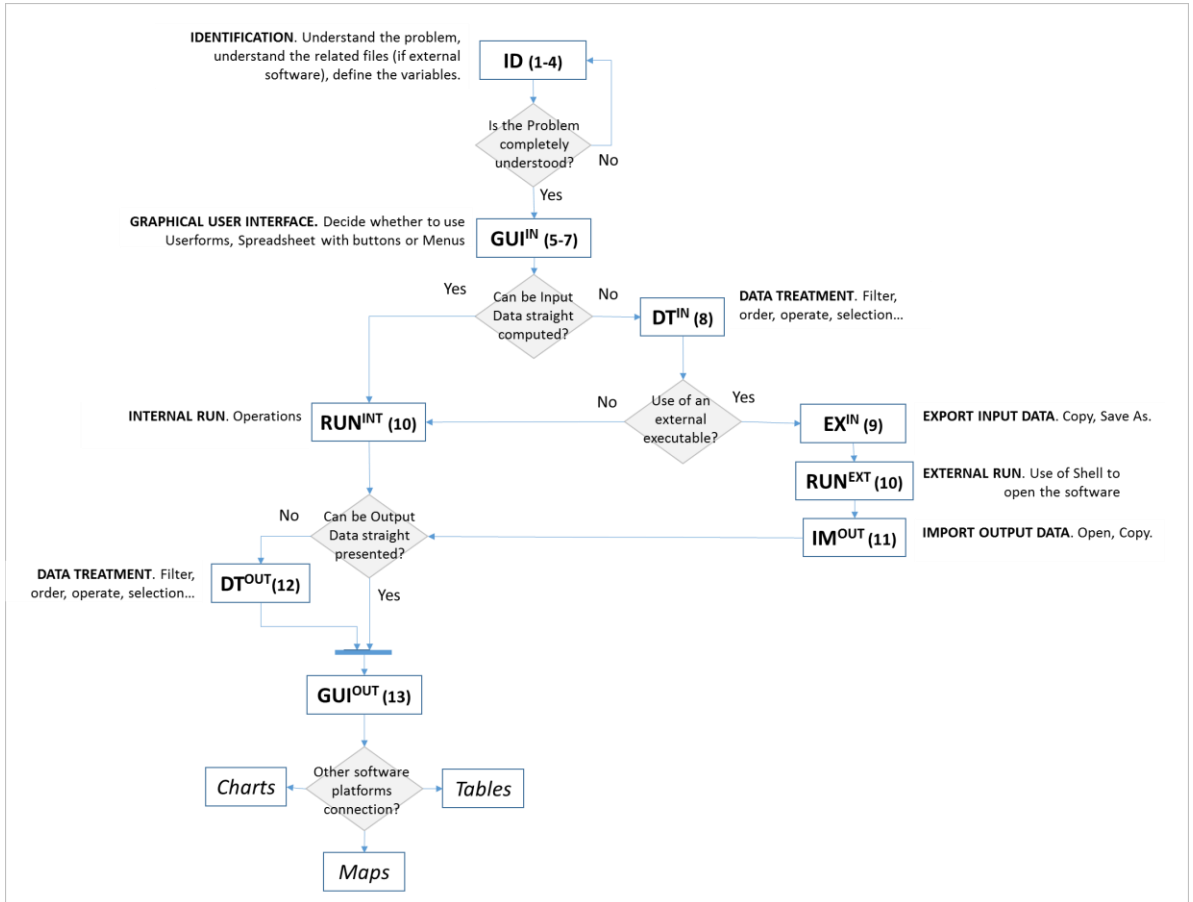


Figure 2. Decision Flow Diagram: Programming steps.

Verplank et al (1985) and Marcus et al (1995) defined some general principles of Graphical User-Interface Design and its effectiveness in visual communication. There are also many reliable resources in the Internet such as *jiscdigitalmedia* British website.

Figure 2 shows the Decision Flow Diagram mentioning possible code actions at each step. The Appendix presents another figure (Figure 36) and a list of specific code sentences that could help future program developers to perform each step of the process.

Additionally, during the reusing process the time needed to develop each step was analysed. The analysis shows that the conceptual model design (identification of the problem, designing the GUI and evaluating which data treatment is necessary) requires longer time than coding. In this line, Buccella et al (2013) presents similar time distributions during their reusing development case study in GIS, which is also similar to the Rational Unified Process (RUP) (Kruchten, P., 2003) hump chart and the Unified Process (Jacobson et al., 1999). Even if the user experience can impact in a significant manner in the total time necessary to reuse any software, the time task distributions usually remain the same.

2.3. Application examples

Several application examples have been created and tested to develop the presented approach. However, only the MIX will be discussed at length to allow the reader to follow a step by step process application of the presented approach. This example will be useful to emphasize the improvements to its previous versions, e.g. automatic and instant graphical output interaction, automatic formula refill to avoid heavy documents, connection to non-Excel-based software such as FORTRAN or GIS, automatic graphical output generation and automatic data selection and its rearrangement.

The other three update examples, will be shortly describe to provide better understanding on how spreadsheet-based and C++ based software can be also reused, customized and extended by following the same approach. All of these examples have become new tools that have been registered by the Spanish National Research Council (CSIC): LAUNCH MIX (Reg. Num. CG3420733), EASYQUIM (Reg. Num. CG3420743), EASYBAL (Reg. Num. CG3420724), BRINEMIX (Reg. Num. CG3420764) all issued on March 31, 2015.

2.3.1. MIX 2.0

(ID). MIX (MIX, 2013) was created in 2003 by Carrera et al,2004 to assess a methodology to compute mixing ratios with uncertain end-members. **(1) INPUT DATA AND OUTPUT DATA.** The input file contains information about the water samples (which can be split into “Sources” or “Wells”), their end-member concentration values and its covariance. Additional information such as restrictions or initial conditions can also be set. **(2) COMPUTATION.** Given that the software was developed in FORTRAN, it requires one input file and generates two output ones, both files being very long (output files can longer than 10.000 lines). MIX considers three different degrees of freedom to generate the input matrix: number of sources, number of wells and number of end-members. This matrix plus the user decision to include initial solutions and restrictions results in a complex input generation. Moreover, the input file is very sensitive to any typing error. The source code is not available to recompile any change. **(3) IMPROVEMENTS.** The first requirement is the automatic input file generation to handle the typing errors. The new MIX should also offer the possibility of using the main input matrix as a Database, offering the possibility of selecting which sources, wells or end-members the user wants to use in the analysis. A selection of the analysis results should be automatically displayed in the spreadsheet. **(4) COMMUNICATION.** The final user should reduce or avoid the feeling that he or she is working with different platforms (in this case, MS Excel and FORTRAN). Moreover, output files can be lengthy and monotonous to

read with some unnecessary information for the analysis. For standard analysis, only a data selection of these files should be displayed by tables and different kinds of charts.

In order to design the **GUI**, both spreadsheet and UserForm were chosen. This allows the user to predefine the magnitude of the problem in the UserForm and to set the input data in the spreadsheet as a matrix. **(5) INPUT DATA AND OUTPUT DATA**. In this case, input data tables are set in different spreadsheets (concentrations, standard deviations, initial solutions and restrictions) and are activated when the user navigates through the buttons of the UserForm. The input information can be directly set in the matrix or can be imported from a GIS (macros that allow the spatial selection and fill the matrix). This GUI also offers the possibility of interacting with Windows by opening some folders and existing files.

(6-7) COMPUTATION, IMPROVEMENTS and COMMUNICATION. After introducing the data, selecting those data that will be suitable for analysis and setting up the desired options, **(8) input data treatment** transforms all these data into a single text file, changing formats, data types and units, etc. This is the real input file that is **(9) exported** and then called by the "FORTRAN-based program MIX" out of the Excel environment **(10) (ERUN)**. The "FORTRAN executable" is automatically called by Excel giving the user the impression that he or she is not working with two different software programs (e.g. using the Shell statement). See the appendix for further information regarding to the code.

COMMUNICATION. To **(11) import** the results, **(12) output data treatment** is required despite being difficult to manage. Storing the input number of sources, wells and end-members in variables and using the functions to find key words enable us to select the information that is worth using. After the data treatment, two different plots are generated: pie charts to show the proportion of the water sources in each well and Scatter plots of measurements versus calculated values for each end-member. Moreover, other results such as contributions to the objective function and the eigenvalues are also presented in form of tables. If the user wishes to revise the two complete output files, these files are imported to two spreadsheets even if it also enables us to access the MIX windows folder where all files are stored.

One of the advantages of this case study is that the number of automatically generated plots and tables changes depending on the input data set by the user. Another advantage is that the new version is connected to the GIS-based software QUIMET (Velasco et al, 2014). This enables us to **(13) export** some data to their spatial representation in GIS and also to **(3) import** the input temporal and spatial GIS environment data selection to fill the input data tables for analysis in the new MIX. Also, the program allows storage of large amounts of data (use as a Database) and to select part of it to compute the analysis. Lastly, a Userform has been included that automatically appears when the program starts to show the title, the logo and the designers of the program. The Userform can be set to disappear when the user clicks a button, or it can automatically vanish after a few seconds. All the presented Userforms can be minimized in order not to trouble the user when he or she is checking the data. Figure 3 and Figure 4 compare the input and the output software environments between the old and the new versions.

Old

```

1  Run_name Run_well Run_pos n_incent Itaild named
2  10 10 11 0 1001
3  First_00000000 add 1000 wells
4  *C:\com\11\1\Run_name Run_well Run_pos n_incent Itaild named
5  10.000000E+0 09.800000E+0 11.240000E+0 66.210000E+0 70.000000E+0 11.800000E+0 -271.511000E+0 09.879700E+0 07.300200E+0 01.7280400E+0 Sour_1
6  14.447800E+0 09.150000E+0 10.041200E+0 49.261000E+0 78.700000E+0 09.840000E+0 -28.546000E+0 10.179500E+0 07.7826300E+0 13.219900E+0 Sour_2
7  90.522000E+0 09.421000E+0 02.381770E+0 10.449000E+0 04.400000E+0 42.200000E+0 -271.970000E+0 10.134800E+0 14.488700E+0 20.449000E+0 Sour_3
8  01.075900E+0 01.180000E+0 03.084200E+0 -02.020000E+0 01.500000E+0 42.800000E+0 -271.651000E+0 10.394900E+0 06.968000E+0 07.288000E+0 Sour_4
9  09.010101E+0 07.1405680E+0 02.211471E+0 07.281944E+0 13.847800E+0 09.880000E+0 09.890000E+0 06.802000E+0 04.180000E+0 04.280000E+0 Sour_5
10 30.4173930E+0 09.200000E+0 49.156970E+0 00.0932490E+0 02.300000E+0 24.640200E+0 -271.287400E+0 09.324810E+0 07.880800E+0 10.029712E+0 Well_1
11 02.132494E+0 03.180000E+0 09.058327E+0 01.4602390E+0 09.400000E+0 09.8028339E+0 -28.3484142E+0 10.000000E+0 19.1951411E+0 01.117420E+0 Well_2
12 39.351307E+0 09.200000E+0 01.5040110E+0 43.2074710E+0 01.700000E+0 20.000468E+0 -271.959707E+0 09.261513E+0 06.183000E+0 13.174802E+0 Well_3
13 01.988478E+0 09.460000E+0 02.479346E+0 02.078424E+0 07.100000E+0 01.049433E+0 -271.931719E+0 10.200000E+0 18.461388E+0 01.017030E+0 Well_4
14 01.712377E+0 09.890000E+0 05.846193E+0 11.4449310E+0 31.000000E+0 02.642337E+0 -28.1593411E+0 10.340187E+0 28.242907E+0 08.448343E+0 Well_5
15 44.284898E+0 01.200000E+0 77.414894E+0 39.739246E+0 02.400000E+0 22.419248E+0 -271.182113E+0 10.000000E+0 08.373253E+0 12.073211E+0 Well_6
16 34.071074E+0 01.120000E+0 71.324611E+0 35.292715E+0 09.200000E+0 20.000468E+0 -271.127421E+0 10.000000E+0 06.339920E+0 Well_7
17 02.332478E+0 02.800000E+0 09.173997E+0 02.428995E+0 10.000000E+0 09.994293E+0 -28.546984E+0 10.000000E+0 19.729207E+0 Well_8
18 04.324611E+0 06.220000E+0 04.732945E+0 02.382867E+0 20.000000E+0 01.464432E+0 -28.3484142E+0 10.000000E+0 21.008442E+0 Well_9
19 02.439992E+0 02.470000E+0 09.439424E+0 16.151976E+0 09.000000E+0 08.984118E+0 -27.742946E+0 10.078686E+0 18.536293E+0 Well_10
20 27.748044E+0 09.200000E+0 20.398021E+0 05.409240E+0 11.000000E+0 07.486238E+0 -28.101892E+0 10.207793E+0 01.289627E+0 Well_11
21 07.140568E+0 02.720000E+0 02.211471E+0 07.281944E+0 04.400000E+0 44.078302E+0 -271.878703E+0 10.202817E+0 13.967302E+0 Well_12
22 02.381770E+0 09.400000E+0 02.791361E+0 02.426471E+0 10.000000E+0 46.011213E+0 -28.252839E+0 10.289210E+0 18.890774E+0 Well_13
23 13.488498E+0 09.800000E+0 09.788471E+0 49.4402350E+0 44.000000E+0 01.412190E+0 -28.167248E+0 10.384812E+0 18.174004E+0 Well_14
24 05.354924E+0 04.400000E+0 10.194894E+0 19.073938E+0 22.000000E+0 02.171249E+0 -28.012431E+0 10.499717E+0 27.137046E+0 Well_15
25 04.721045E+0 09.200000E+0 09.121028E+0 09.793020E+0 20.000000E+0 01.757474E+0 -28.543293E+0 10.478080E+0 24.990389E+0 Well_16
26 09.497008E+0 04.890000E+0 05.441192E+0 10.305499E+0 31.000000E+0 02.084878E+0 -28.734497E+0 10.000000E+0 28.182230E+0 Well_17
27 04.288012E+0 09.140000E+0 05.083162E+0 09.489212E+0 21.000000E+0 01.908233E+0 -28.012431E+0 10.499717E+0 24.476030E+0 Well_18
28 12.581485E+0 09.200000E+0 14.293994E+0 69.451039E+0 01.000000E+0 11.933824E+0 -28.928211E+0 09.393761E+0 04.046291E+0 Well_19
29 09781480E+0
30 44.413123E+0 08.742000E+0 31.498900E+0 10.348031E+0 12.200000E+0 01.922930E+0 01.892137E+0 24.442512E+0 13.504646E+0 Well_20
31 12.182033E+0 08.200000E+0 25.202484E+0 04.000000E+0 13.448222E+0 02.009340E+0 02.004004E+0 27.181732E+0 05.347008E+0 Well_21
32 20.439582E+0 02.800000E+0 01.644880E+0 04.000000E+0 04.640000E+0 04.492100E+0 01.954054E+0 24.312120E+0 82.136471E+0 Well_22
33 20.949004E+0 33.408000E+0 29.387142E+0 01.024740E+0 24.300000E+0 09.764304E+0 01.904389E+0 27.013303E+0 20.110202E+0 Well_23
34 41.181392E+0 09.140000E+0 20.000000E+0 04.448400E+0 04.000000E+0 04.000000E+0 04.000000E+0 04.000000E+0 04.000000E+0 Well_24
35 14.415037E+0 04.304235E+0 47.826898E+0 01.168197E+0 29.000000E+0 06.238012E+0 91.213777E+0 08.178197E+0 64.000000E+0 Well_25
36 01.137038E+0 04.000000E+0 04.000000E+0 04.000000E+0 04.000000E+0 04.000000E+0 04.000000E+0 04.000000E+0 04.000000E+0 Well_26
37 19.143789E+0 04.304235E+0 24.246320E+0 01.282979E+0 25.000000E+0 04.000000E+0 96.734938E+0 08.130112E+0 01.000000E+0 Well_27
38 09.370148E+0 78.400000E+0 04.117923E+0 24.323605E+0 04.000000E+0 46.493947E+0 95.975118E+0 28.000000E+0 04.000000E+0 Well_28
39 20.439582E+0 02.740000E+0 09.128545E+0 05.244300E+0 04.000000E+0 04.470187E+0 01.201484E+0 09.989834E+0 04.000000E+0 Well_29
40 19.474802E+0 04.804200E+0 60.240723E+0 02.444874E+0 24.300000E+0 09.116490E+0 90.119149E+0 28.000000E+0 10.000000E+0 Well_30
41 12.847933E+0 07.400000E+0 08.878208E+0 09.272428E+0 24.300000E+0 04.000000E+0 90.148708E+0 28.000000E+0 04.000000E+0 Well_31
42 06.439786E+0 06.764600E+0 09.487197E+0 34.474941E+0 24.300000E+0 01.949113E+0 91.021601E+0 28.000000E+0 04.000000E+0 Well_32
43 01.000000E+0 01.703200E+0 01.000000E+0 05.497848E+0 01.000000E+0 02.737894E+0 01.054914E+0 28.000000E+0 04.000000E+0 Well_33
44 04.736892E+0 06.472890E+0 09.503394E+0 02.210313E+0 69.451000E+0 44.137147E+0 04.296335E+0 02.009320E+0 02.783126E+0 Well_34

```



New

MIX v2013

	CI	NH4	Na	Ca	I	Br	D	Iso_Sr	CE	Sr
Sour_1	1.50E+01	5.90E-02	1.13E+01	6.62E+01	7.00E-03	1.13E-01	-2.75E+01	9.88E+02	7.35E+02	1.73E+02
Sour_2	1.44E+01	5.76E+00	1.00E+03	4.94E+01	7.87E-01	1.57E+00	-2.86E+01	1.00E+03	1.75E+03	1.32E+03
Sour_3	9.05E+01	3.42E+00	2.58E+02	1.06E+01	4.40E-02	4.22E-01	-2.80E+01	1.01E+03	1.43E+03	2.04E+01
Sour_4	1.08E+02	1.16E+00	1.08E+02	-2.05E+00	1.50E-02	6.25E-01	-2.76E+01	1.04E+03	8.97E+02	8.73E+01
Sour_5	6.01E+00	9.71E+01	2.21E+02	9.73E-01	1.40E+03	5.88E+02	5.88E+02	6.08E+02	6.18E+02	6.28E+02
Well_1	CI	NH4	Na	Ca	I	Br	D	Iso_Sr	CE	Sr
Well_1	2.86E+01	8.30E-01	6.92E+01	5.01E+01	2.50E-02	2.46E-01	-2.72E+01	9.53E+02	7.88E+02	1.30E+03
Well_2	2.13E+02	3.18E+00	3.06E+02	1.48E+00	9.60E-02	9.28E-01	-2.83E+01	1.00E+03	1.96E+03	1.12E+02
Well_3	3.93E+01	8.30E-01	5.15E+01	4.53E+01	1.70E-02	2.01E-01	-2.80E+01	9.52E+02	8.16E+02	1.32E+03
Well_4	1.99E+02	3.36E+00	2.47E+02	2.08E+00	7.50E-02	8.10E-01	-2.79E+01	1.00E+03	1.85E+03	1.02E+02
Well_5	5.71E+02	5.99E+00	5.87E+02	1.14E+01	3.10E-01	2.58E+00	-2.86E+01	1.05E+03	2.82E+03	8.45E+02
Well_6	4.44E+01	1.03E+00	7.76E+01	3.37E+01	2.80E-02	2.26E-01	-2.72E+01	1.00E+03	8.37E+02	1.27E+03
Well_7	3.60E+01	1.12E+00	7.19E+01	3.39E+01	3.20E-02	2.01E-01	-2.71E+01	1.00E+03	8.34E+02	1.23E+03
Well_8	2.33E+02	2.85E+00	3.11E+02	2.42E+00	1.50E-01	9.40E-01	-2.89E+01	1.00E+03	1.97E+03	1.82E+02
Well_9	4.33E+02	5.22E+00	4.71E+02	2.38E+00	2.00E-01	1.65E+00	-2.93E+01	1.00E+03	2.10E+03	2.26E+02
Well_10	2.43E+02	2.87E+00	3.44E+02	1.65E+01	9.00E-02	1.01E+01	-2.77E+01	1.01E+03	1.85E+03	3.62E+02
Well_11	2.78E+03	9.00E-02	2.10E+03	5.41E+02	1.10E-01	7.49E+00	-2.15E+01	1.02E+03	1.29E+04	8.86E+03
Well_12	9.71E+01	2.72E+00	2.21E+02	9.73E-01	6.40E-02	4.49E-01	-2.79E+01	1.01E+03	1.40E+03	6.50E+01
Well_13	2.38E+02	2.80E+00	2.73E+02	2.63E+00	1.00E-01	8.60E-01	-2.83E+01	1.03E+03	1.89E+03	1.27E+02
Well_14	1.13E+03	9.63E+00	9.79E+02	6.97E+01	6.40E-01	5.41E+00	-2.85E+01	1.04E+03	5.82E+03	4.24E+03
Well_15	5.38E+02	6.40E+00	5.20E+02	1.91E+01	2.20E-01	2.17E+00	-2.90E+01	1.00E+03	1.27E+03	6.68E+02
Well_16	472.102	5.250	512.330	3.795	0.210	1.756	-29.543	1047.581	2499.058	301.702
Well_17	568.701	4.890	564.119	10.351	0.130	2.099	-28.716	1000.000	2858.223	891.068
Well_18	428.201	5.140	506.311	3.685	0.210	1.928	-30.014	1049.577	2467.803	300.795

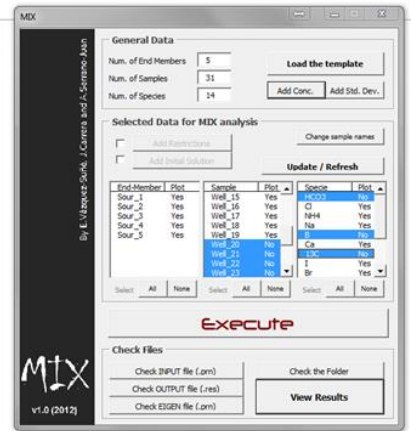


Figure 3. Comparison between the old MIX input file (top) and the new MIX v2013 input dynamic table (down).

To sum up, the new MIX version satisfies the need for GUI, proposing a GUI based on the MS Excel environment. This GUI prepares input templates based on the user's needs to perform the analysis in external software. Part of the generated output is plotted and rearranged in GUI, enabling the user to check the entire output data files. Other advantages are its potential use as a Database (providing the opportunity to select different combinations of sources, wells and end-members for analysis) and its connection to a GIS environment.

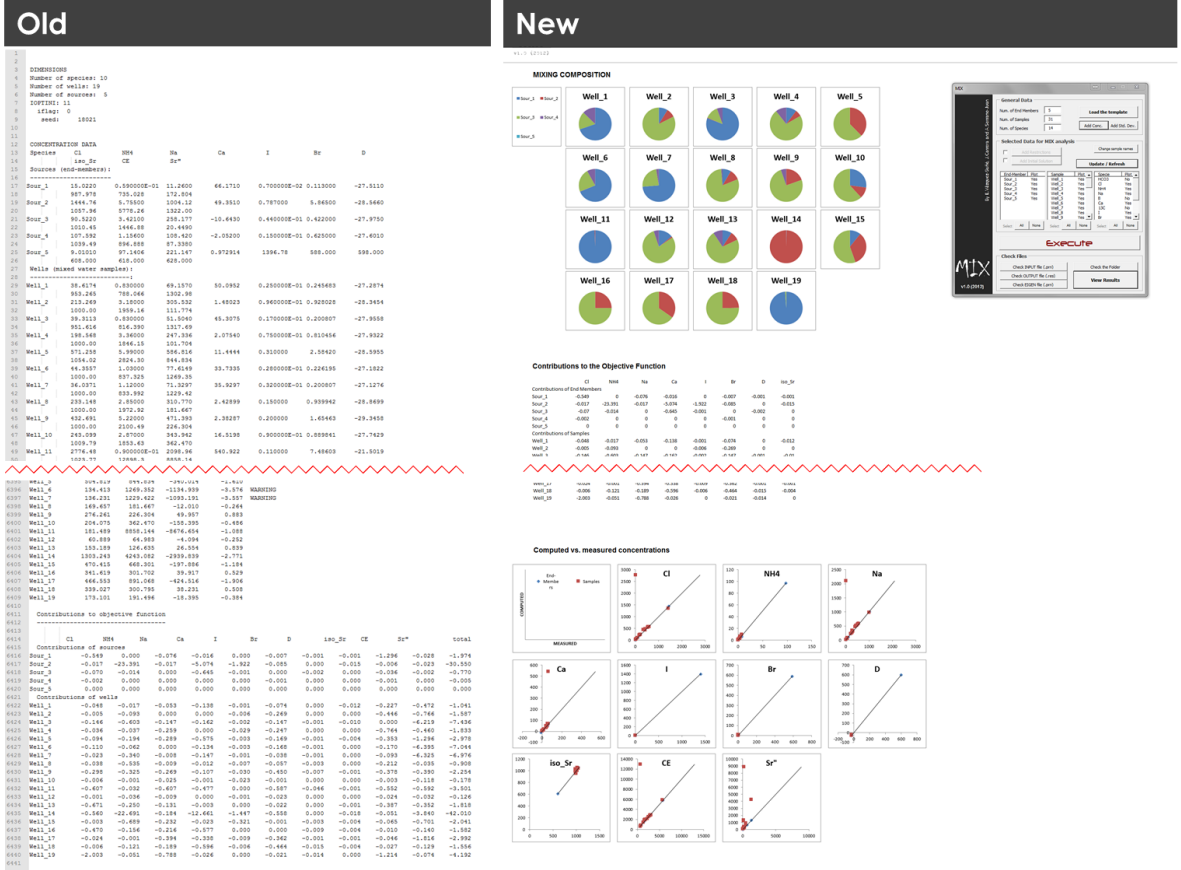


Figure 4. Comparison between the old MIX output file (with more than 6.000 lines) (left) and the new MIX v2013 output GUI (pie plots, data rearrangement and scatter plots) (right).

2.3.2. Other examples

EasyQuim (EasyQuim, 2013) was designed in 1999 to graphically represent hydrochemical data. It computes some calculations such as unit conversion, balance errors or ionic relationships. It also plots Piper, Schöeller-Berkaloff, SAR (Salinity) and Stiff diagrams of 24 samples and allows the user to select which to represent. Everything is set in spreadsheets with functions, except one small macro, which activates the “No representation of samples” and can only be activated once. The new version should provide three main advantages. The first advantage involves increasing the number of samples (up to 200), the second entails adding a “Sample Selector” and the third advantage involves the possibility of a space-time analysis. The “Sample Selector” provides a powerful tool to use the updated EasyQuim as a Database and to plot different sample combinations, whereas the connection to the GIS-based software QUIMET will allow analyses in the spatial and temporal dimensions.

EasyQuim is an example of how to energize a spreadsheet originally created to plot hydrochemical data analysis. The new version adds functionalities such as converting the main data spreadsheet into a database and creating a data selector, allowing the final user to decide which analyses are worth comparing. Additionally, new program connections such as the connection with GIS were set, allowing further temporal and spatial data analyses.

EasyBal (EasyBal, 2013) was designed in 1999 to evaluate water balance per unit of soil area as a function of precipitation, the potential evapotranspiration (or ETP), temperature and irrigation. Outputs are the deficit and the recharge of the aquifer. Older versions required up to six steps to introduce the input data into six different Excel sheets. All data analysis periods had to be between January 1970 and December 1997 and some calculations and adaptations were required if the user needed a different period. Each month only allowed for exactly 30 days instead of the real number of days. There is a need to solve the current data period restriction by allowing conditional sums that enable us to achieve automatic monthly and yearly totals. All functions should be reorganized to allow the autofill of the formula in a single line. These improvements enable the user to perform the analysis simultaneously and to obtain all the results so that they are clearly structured and organized in a single Excel sheet. Some extras should also be included in the new EasyBal version. On the one hand, the user can select the program language, English or Spanish. On the other hand, the ETP can be introduced as input data or can be automatically calculated (using the Hargreaves and Thornthwaite methods) and graphically compared with the input data, allowing the user to select the best option in the menu or graph.

EasyBal is an example of how to improve a current calculation spreadsheet. In this case, the performance involved reorganizing all data functions to achieve automatic formula refill, adding the language selector and the ETP graph selector. By changing some formulas, it was possible to accept any input data period and to automatically add up monthly and yearly totals.

In contrast to earlier examples, BrineMIX (BrineMIX, 2013) is a new program, not an update. In this case, BrineMIX seeks to create a GUI that automatically generates the input and reads the output of PHREEQC for a specific water mixing analysis. In the input only the chemical water samples, the mixing percentage and the mineral selection are set, whereas the output shows the chemical composition of the final water and its chemical precipitates. The purpose of this new program is to simplify a specific PHREEQC analysis for the user who does not usually work with it.

BrineMIX is an example of how to externalize part of a bigger software. PHREEQC can perform many different analyses but not all its possibilities are necessary for non-chemical users. BrineMIX was created to simplify some specific analyses through an Excel environment assisting these users to perform them.

Figure 5 shows the flow diagram paths followed by each of the presented case studies: EasyQuim, EasyBal, MIX and BrineMIX.

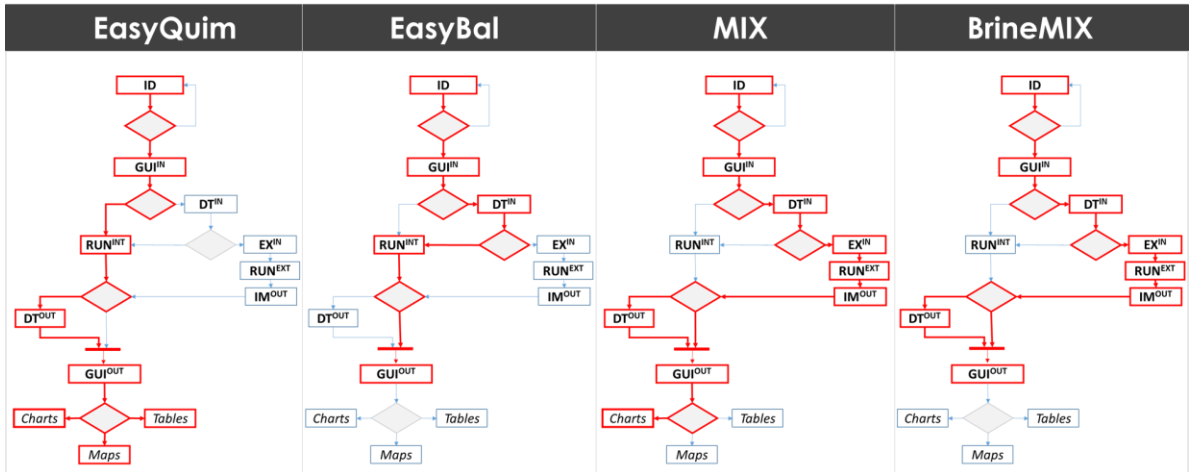


Figure 5. Flow diagram paths followed by each of the presented case studies: EasyQuim, EasyBal, MIX and BrineMIX.

2.3.3. Reused software validation

When software reuse is based on science and engineering it is usually treated as an empirical discipline (Frakes and Kang, 2005). Metrics were developed to quantitatively and qualitatively measure the improvement of the software (Suri and Carg, 2009). Empirical studies, in both industry and academia, with the aim of assessing the relationship between software reuse and different quality and cost metrics have been reported in the literature. They are usually related to quality (such as error density, fault density, ratio of major errors to total faults, rework effort, module deltas, developers perception), to productivity (i.e. lines of code per effort) and to time-to-market (i.e. development cycle time).

In order to answer how is this approach able to (1) easily update any hydrogeological program by following this approach, (2) to lead to fewer errors during the analysis, and (3) to perform better user efficiency by using an updated spreadsheet-based program, quantifiable and qualitatively metrics have been used. Quantifiable metrics rely on achieving the same or better results with less operational time when compared to the original one (metric of time), but the increase of the system reliability can be also measured (i.e. by replacing the error prone human processes by automation them or by displaying warning when values are out of range). Qualitatively metrics can be the addition of new functionalities, input/output data treatment or showing results in a proper format to use in another analysis or to be directly add into a report.

On the one hand, the validity of the updated software remains in the logic of the new code with respect to the old one. As most of the codes cannot be recompiled, the time required to strictly compute the solution still the same. What makes the difference between the old and the new version is the total time required to compute the whole analysis. Preparing the input files, setting up the problem, reading the output files and preparing the output for a correct interpretation can be onerous work that can be automatically set, saving

time in preparing all the files and also by strongly reducing the errors during the process (e.g. FORTRAN based programs are very sensitive to any typing error). All four case studies have been tested to evaluate the necessary time to compute a complete analysis between old and new versions. EasyBal and MIX save at least three quarters of the time, while EasyQuim and BrineMIX save half of it. The main improvements rely on dynamic data comparison, wide data range of values, addition of GUI and the automation of the input and output data treatment.

On the other hand, this approach has been used in educational, research and technical projects. EasyQuim and EasyBal are taught in different international master courses by institutions such as the Technical University of Catalonia (www.upc.edu) or by non-profit other such as the FCIHS (www.fcih.org). Besides, their previous versions were widely used in the hydrogeological international community, especially in Latin American countries. Moreover, all four reused software have been applied in different technical (Scheiber et al 2013a, 2013b, 2013c, GHS, 2013) and research projects (Scheiber et al 2014a, 2014b, Velasco et al 2014), and Criollo et al. (2014) have applied this approach for reusing the Marial fortran-based program.

2.4. System requirements and program availability

Visual Basic for Applications (VBA) has been supported since the MS Excel 97 version in a Windows based environment. Although Windows and Macintosh (OS X) have a similar interface, the latter only supports VBA in its 2004 and 2011 versions, not in its 2008 version. The main limitation of using VBA in an OS X environment is that it relies on Application Programming Interface (API) calls, which only works in Windows.

VBA has evolved considerably since its inception and this is the main reason that some programs could cease working from version to version. This usually occurs when the code uses modern functions or graphics because the way to refer to them has slightly changed. Since MS Excel is the host application and depends on the user versions, the memory space length changes from the 32 to 64 bits versions. Although the difference affects some variable declarations, this problem can be sidestepped (See Appendix for further explanations).

The four software examples can be obtained by making a request to the author or by downloading it from the URL, <http://www.h2ogeo.upc.es/software>.

2.5. Summary and conclusions

This chapter presents a new approach to reuse, customize and extend current hydrogeological software, and illustrates the insights of the process by applying it in four case studies. Through them, the reader has realised how spreadsheet-based and non-spreadsheet-based software can be reused by the same approach. Moreover, this same approach also allows the creation of new graphical user interfaces to automatically generate input and read output files from other analysis. Finally, The MIX case study has been largely discussed to allow the reader to easily follow a step by step process application of the presented approach.

This chapter wishes to answer whether or not (1) it is possible to easily update any hydrogeological program by following this approach, (2) it is possible that new updates lead to fewer errors during the analysis when compared to the original ones, and (3) the end users are more efficient using an updated spreadsheet-based program than using the original one.

On the one hand, it is demonstrated that new versions are indeed more user-friendly and avoid errors such as typing mistakes. A MS Excel environment allows us to perform the same action in a variety of ways. This is very helpful since it enables the program developer to design anything he or she considers appropriate, resulting in very personalized programs. Moreover, VBA offers the possibility of using messages in pop-up windows or colour changes to caution the user; e.g. letting him or her know which values are out of range or that the required values are numbers instead of letters.

On the other hand, new versions easily generate input files and show, rearrange and plot the most important parts of the output. Through VBA it was possible to assess complex input matrix generation and difficult output selections, as well as generate several chart types. We also demonstrated how VBA interacts with Windows by executing other program and by opening Windows folders. In all cases, the Graphical User Interface is very important as it not only makes each program easier to manage but also improves its organization.

Additionally, this methodology was tested during the reusing process programs of several case studies resulting in a qualitatively general trend of the time distribution along the whole process. It corroborates that the conceptual model design requires longer time than the rest.

This approach has been used in education and research, as well as being applied in several technical projects. All of these examples have become new tools that have been registered by the Spanish National Research Council (CSIC): LAUNCH MIX (Reg. Num. CG3420733), EASYQUIM (Reg. Num. CG3420743), EASYBAL (Reg. Num. CG3420724), BRINEMIX (Reg. Num. CG3420764) all issued on March 31, 2015.

This approach achieves the objectives, providing the necessary steps to easily develop any hydrogeological software and to reinforce the current understanding in hydrogeology. The fact that the methodology is simplified in a decision flow chart, helps the program developer to assess every type of program. However, although this approach has been created for reusing hydrogeological software by hydrogeologists, it can also be applied to other fields, creating synergies among scientists and expert program developers.

Chapter 3.

Integration of groundwater by-pass facilities in the bottom slab design for large underground structures.

3.1. INTRODUCTION

The competition for space in urban areas due to an exponential growth of population makes underground engineering play a crucial role in the development of cities. New urban planning concepts, technology advances and innovative construction capabilities condition the implementation of larger and high efficient infrastructures.

This concept of efficiency must be kept in mind during all phases of a project: (I) project design, (II) project construction and (III) project exploitation. Each phase deal with variables such as cost, duration, safety and management; face political, social, economic and environmental issues; while guarantees future sustainability, maintenance and energy efficiency.

Most of the aforementioned concerns are directly or indirectly related with the hydrogeology. Impacts are generated when underground constructions interact with the groundwater (Pujades et al, 2012, Attard et al., 2016). Most of these impacts must be assessed during the first stages of the project (phases I and II), when it is usually easier, cheaper and more efficient. Errors or non-accurate hydrogeological knowledge could mislead the final project or lead to unforeseen events. In fact, numerous accidents have occurred in recent years (for instance, the tunnel collapse in Barcelona - Spain, Van der Boom, 2011; or Köln - Germany, Van Baars, 2011).

The interaction between underground constructions and groundwater is two folded: groundwater can impact in the underground construction and impacts in groundwater can be consequence of the underground construction.

On the one hand, impacts in underground construction as a consequence of the groundwater are usually related with safety (Pujades et al, 2014a). The design of an underground construction must guarantee the safety of the workers and the integrity of the construction and the adjacent structures by implementing measures that do not complicate the development of the construction and do not increase the total cost. During the construction phase, the water table is usually lowered and controlled to be able to work in dry condition and to avoid bottom instabilities such as bottom uplift or liquefaction (Pujades et al, 2014b). After the construction, the water table returns to its original level, increasing the water pressure under the bottom slab (Figure 6-1). At this step, it is necessary to homogeneously distribute the water pressure under the bottom slab and to limit overpressure to avoid a bottom slab break. Overpressure may be due to groundwater aquifer dynamics or due to anthropogenic factors (Pulido et al., 2012). The most common technique to distribute and limit the water pressure under the bottom slab is the use of gravel layers under an oversized bottom slab. This technique allows water to move through the gravel layer and distribute pressure under the bottom slab, and the oversized bottom slab ensures the structure resistance when pressure rise up to a specific value. However, this technique does not able to release water pressure when this maximum water pressure is overhead, arising the possibility of a bottom slab break. To avoid this risk, artesian wells can be drilled over the bottom slab, allowing a water pressure release by restraining the groundwater level to a certain value (Figure 6-2).

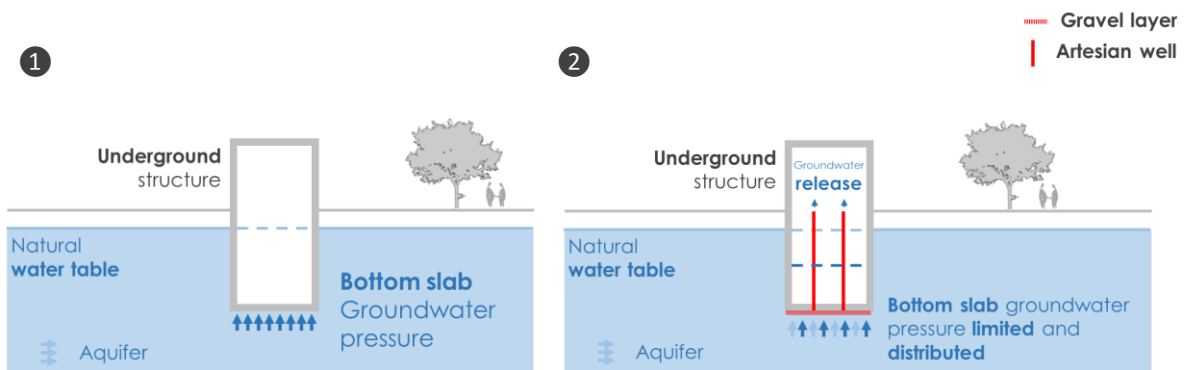


Figure 6. Bottom slab water pressure distribution scheme. (1) states the problem, (2) shows a possible solution.

On the other hand, groundwater can be impacted as a consequence of underground constructions. In case of low permeability underground structures, groundwater barrier effect is usually the main concern (Vázquez-Suñe et al., 2004). The underground construction can act as a natural flow barrier, reducing the effective transmissivity of the aquifer and leading to a rise in the water table upgradient and a lowering downgradient (Figure 7-1). These modifications of the water table can have negative consequences (Deveughèle et al., 2010; Font-Capo et al., 2015). Rising water levels may flood basements, promote soil salinization, flora affection by rotting the roots of plants, reduction of the bearing capacity of shallow foundations, expansion of heavily compacted fills under the foundation structures, settlements of poorly compacted fills upon wetting, increase in loads on retaining systems or basement walls of buildings, increase in the need for drainage in temporary excavations and propagation of contaminants contained in the partially saturated zone (Marinos and Kavvas, 1997; Tambara et al., 2003; Ricci et al., 2007; Paris et al., 2010). The lowering of heads on the downgradient side can cause seawater intrusion in coastal aquifers, ground subsidence, death of phreatophytes and the drying of wells and springs. Moreover, the difference of water pressure between both sides of the underground structure leads to asymmetric loading for which building foundations have seldom been designed (Custodio and Carrera, 1989; Tambara et al., 2003, Xu et al., 2012).

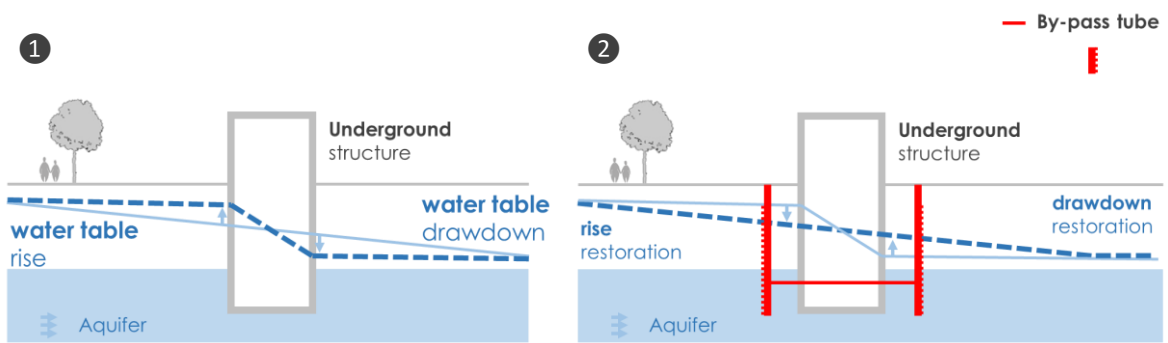


Figure 7. Groundwater barrier effect scheme. (1) states the problem, (2) shows a possible solution.

Groundwater barrier effect associated problems can be prevented by employing groundwater mitigation measures (Kusumoto et al., 2003; Hamate et al., 2003; Ribera et al., 2008; Nishigaki et al., 2010). Some authors have presented and discussed by-pass designs to allow groundwater pass from upgradient to downgradient (Akagi et al., 2004) (Figure 7-2). During the construction of the Kyoto's subway (Japan), semi-pervious wall were used to intake and recharge groundwater (Hashimoto et al., 2001). In a highway in Nerima, Japan, the upper parts of the cut-off walls were removed to allow the water cross the structure through a set of siphon pipes below the structure (Ueda, 1999). Similarly happened in the Barcelona's subway (Spain), where some parts of the cut-off walls and the space above the tunnel were filled with gravel (Malavia et al., 2008). During the construction of the High Velocity Train in Barcelona, groundwater was by-passed by horizontal pipes at two heights to avoid chemical clogging and enlarge durability (Lopez et al., 2009).

However, all the aforementioned designs present some drawbacks. The use of bentonites during the retaining walls construction lead to a reduction of the effective transmissivity, reducing the capacity to by-pass water when prefabricated permeable walls are installed (Figure 8-1) or when retaining walls are removed (Figure 8-2). Also, prefabricated permeable walls compromise the security of the facility due to the big volume of water and high hydraulic load that stands in the wall. Then, the use of wells seems to be a good option (Figure 8-3). However, it is necessary some space out of the structure to drill the wells and the saturated aquifer thickness limits their length. When this happens, the use of horizontal drains can solve the aforementioned limitations (Figure 8-4). However, and again, the length of the drain is limited due to technical issues (Santamaria et al., 2008).

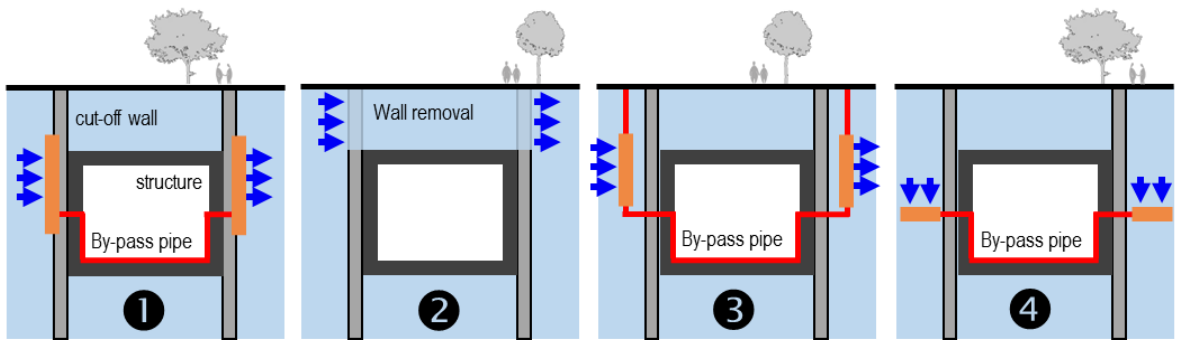


Figure 8 Groundwater by-pass designs. (1) Removal of cut-off wall, (2) intake and recharge pipes installed in drilled hole, (3) intake and recharge through permeable cut-off walls, and (4) intake and recharge wells. Modified figure from Akagi, 2004. Not to scale.

All the aforementioned impacts (bottom slab water pressure distribution and limitation, and groundwater barrier effect) are usually independently solved. While a proper bottom slab water pressure distribution and limitation design should homogeneously distribute and limit maximum water pressure, a proper barrier effect solution design should allow the groundwater to pass through the structure. In both cases, the groundwater level is the main variable to consider during the design of the solution. Again, the groundwater level is also the variable to be adjusted by both solution designs. Since it is illogic to design a solution without considering all the factors involved in the problem, all mitigation measures depending on and affecting the groundwater level should consider the groundwater level variation caused by the affection of other mitigation measures.

Then, the best option to deal with different problems that share common variables is to design integrated solutions (Figure 9). Bringing together designs allow to identify common points that can be usually combined or shared, increasing the efficiency of the solutions and reducing the costs of implementation. In this case, the groundwater pressure distribution and limitation and the by-pass should be design in a single integrated design. However, as far as the authors know, there is not in the literature any integrated design that brings together the bottom slab and groundwater by-pass designs in a single integrated solution.

Mitigation measures integration

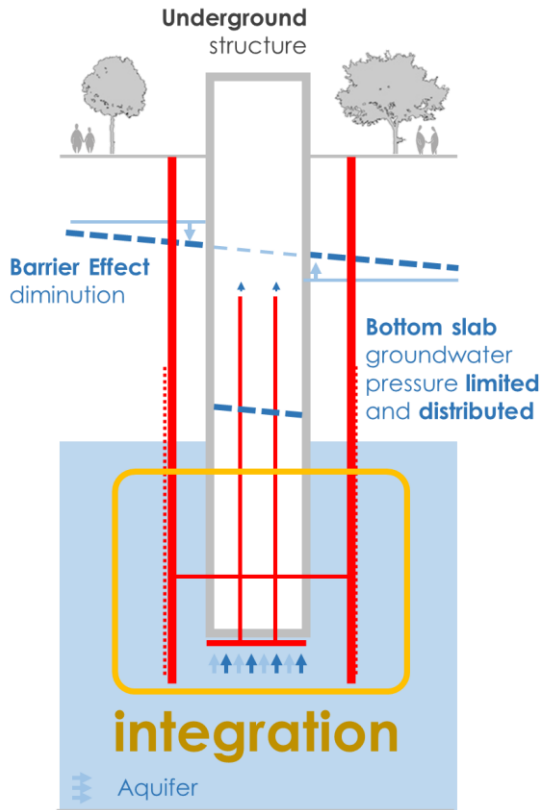


Figure 9. This figure shows how the bottom slab water pressure distribution and the groundwater barrier effect problems might be considered.

This chapter presents **an innovative groundwater by-pass design that enables the groundwater flow through the structure and provides a homogenous distribution of the water pressure under the bottom slab**. This new solution mitigates the barrier effect produced by the structure and optimizes the bottom slab by reducing considerably the costs. The new integrated design was applied to the largest underground infrastructure of Barcelona: La Sagrera railway station. La Sagrera railway station (Figure 10) is located in the metropolitan area of Barcelona (Spain) and aims to become the city's major intermodal transit hub, receiving more than 100 million passengers per year, combining high-speed trains, short- and medium-distance trains, four metro lines and buses (ADIF, 2015). The railway station construction began in 2010 and is planned to be completed by 2020. Now, the excavation stage is almost finished and the bottom slab construction is the next stage.

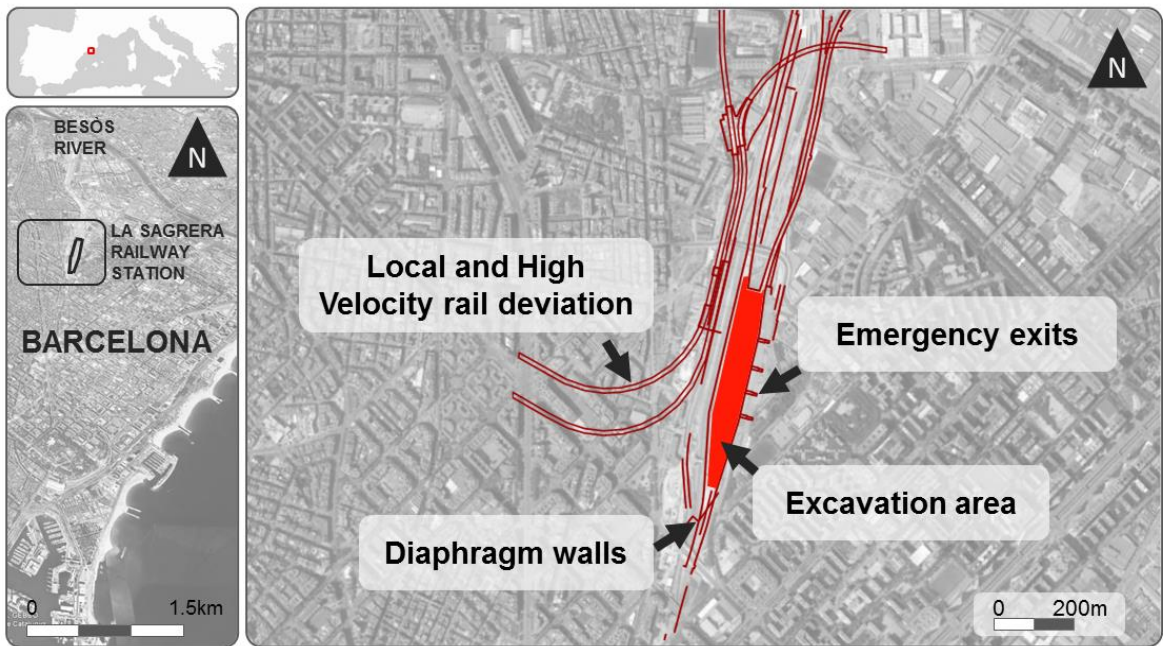


Figure 10. Geographical location of the study site.

3.2. MATERIALS AND METHODS

3.2.1. Geographical, geological, and hydrogeological description

The metropolitan area of Barcelona is located on the Mediterranean coast, on the northeast coast of Spain (Figure 11). Geologically, this area is formed by a coastal plain (The Barcelona Coastal Plain) (Vázquez-Suñé et al., 2016) bounded by two Quaternary deltaic formations corresponding to the Besòs (Velasco et al., 2012) and Llobregat rivers (Gámez et al., 2009) and an elevated area, the Catalan Coastal Ranges (mainly Paleozoic rocks composed of granite and metamorphic rocks) (Sanz, 1998; Solè et al., 2002). These ranges are the western onshore margin of the Valencia trough, which has a NE-SW orientation controlled by a group of faults that dip SE and have undergone repeated offsets throughout their history. This fault system is 400 km long and 200 km wide (Banda and Santanach, 1992). These extensional faults have been active since the late Oligocene, primarily during the Miocene, and are still active today (Roca and Guimerà, 1992). More concretely, the study site is located in the actual plain, which consists of Quaternary formations that overlie a substrate mainly formed by Palaeozoic and Cenozoic (Pliocene) series. The Quaternary formation presents a very heterogeneous pattern and can be divided into the Lower Quaternary (Pleistocene) and the Upper Quaternary (Holocene). The Pleistocene is made up of several cycles constituted by alluvial sequences. The upper Quaternary mainly consists of torrential, alluvial, and foothill deposits, where gravels and sands with a high proportion of clay matrix are present. All these quaternary deposits are 30 m thick. The pre Quaternary substrate consists of Pliocene series, mainly composed of marine blue marls, sandy marls, and Palaeozoic

granite. The whole study area is cut by many fractures that compartmentalize the pre Quaternary substrate; specifically, the construction area is crossed by a fracture (oriented NNW-SSE) that separates the two Pliocene series: Pliocene marls (south) and Pliocene sandy marls (north).

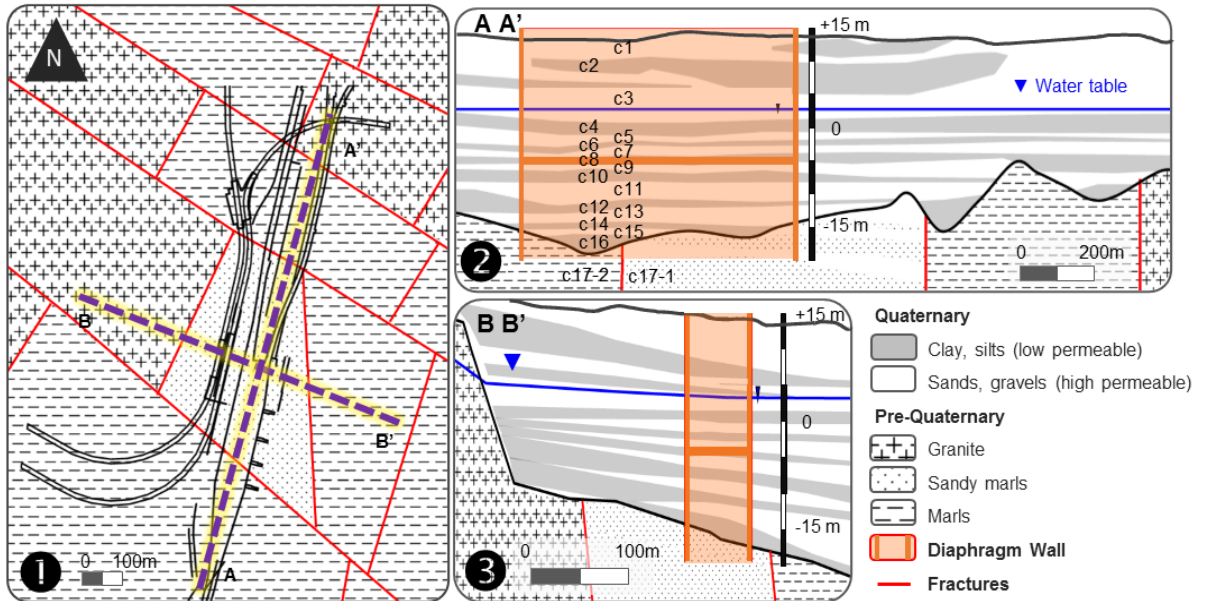


Figure 11. Detailed geological profile of the site. (1) Plan view of the geological basement, (2) Cross section A-B, (3) Cross section C-D. Excavation area, limited by diaphragm walls, is shown in light brown color. Both cross sections show the maximum excavation and the required dewatering system.

Hydrogeologically, the Quaternary and pre-Quaternary materials can be regarded as a layered aquifer with high vertical heterogeneity, with an effective transmissivity of 100-200 m²/d (Pujades et al., 2015). The hydraulic conductivity (K) of the Quaternary clay layers (low permeability layers) ranges from 0.001 to 0.01 m/d, the K of the Quaternary sand and gravel layers (high permeability layers) ranges from 0.1 to 10 m/d, the K of the Pliocene fine materials (marls) ranges from 0.001 to 0.01 m/d, and the K of the sands ranges from 0.1 to 10 m/d. These values were derived from the numerous hydraulic tests performed in the city of Barcelona during recent underground constructions (Pujades et al., 2012, Font-Capo et al., 2015; Serrano-Juan et al., 2016; Culí et al., 2016). Specifically, in the study site, the pumping tests undertaken before to start the constructions showed that the minimum hydraulic conductivity is 0.001 m/d and the maximum one is 700 m/d.

3.2.2. Basic concepts: Groundwater barrier effect.

The groundwater barrier effect (s_B) is defined as the increase in head loss along the flow lines caused by the reduction on conductance associated with an underground construction (Pujades et al., 2012) (Figure 12). In other words, the underground construction acts as a natural flow barrier, reducing the effective transmissivity of the aquifer and leading to a rise in the water table upgradient and a lowering downgradient. This can be written as

$$s_B = \Delta h_B - \Delta h_N \quad (1)$$

where Δh_B is the head drop across the barrier and Δh_N is the head drop under natural condition for the same points of measurement.

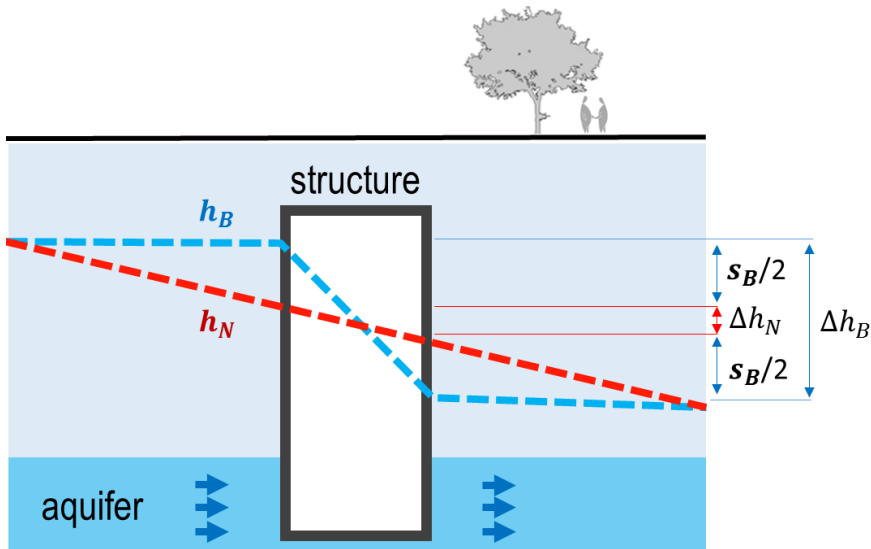


Figure 12. Cross section of a theoretical aquifer with a structure reducing its natural transmissivity. Groundwater barrier effect scheme. Modified from Pujades, 2012.

The groundwater barrier effect can be regional or local, depending on the distance between the measured points and the barrier (in this case, the structure). Boundary conditions also affect the barrier effect. If a Dirichlet boundary is downgradient, the barrier effect is mainly concentrated upgradient, while when the Dirichlet boundary is upgradient, the barrier effect is mainly concentrated downgradient. When boundaries are far enough, they do not affect the structure and the barrier effect is usually well balanced between the upgradient and the downgradient. A more detailed definition of the groundwater barrier effect is provided by Pujades et al., 2012.

3.2.3. Problem statement

The Sagrera station will occupy an area of approximately 70.000 m² and involves a 20 m deep excavation. The initial soil elevation is between +14 and +16 m.a.s.l. (meters above the sea level) and the water table natural position is between +3 and +4 m.a.s.l. The dewatering process is performed inside diaphragm walls (which bottom is at -20 m.a.s.l.) to reach structural requirements and also to reduce the water extraction and subsidence outside. The diaphragm walls have anchors on its upward side (upgradient) to support the railway lines (which have been deviated and are active during the whole process). The excavation bottom is at -8 m.a.s.l., requiring a water table drawdown of 12 m. There are 26 wells (which also bottom -20 m.a.s.l.) used during the dewatering phase and a network of 48 piezometers (20 inside and 28 outside of the excavation area) with different depths and screens to monitor the aquifer.

In order to mitigate the groundwater barrier effect and to distribute and limit the water pressure under the bottom slab, independent solutions were designed. On the one hand, a by-pass solution was designed to collect water upgradient and to discharge it downgradient through a pipe system. On the other hand, a fine gravel layer and a set of artesian wells were designed to homogeneously distribute the water pressure and to limit it in case of overpressure. As mentioned in the introduction, all mitigation measures depending on and affecting the groundwater level should consider the groundwater level variation caused by the affection of other mitigation measures. In this case, any of the solutions have considered the effects of the other one.

Figure 13 shows the original by-pass and bottom slab designs.

3.2.3.1. Groundwater By-pass

The groundwater by-pass consists in 4 PVC pipes of 80 m long with a diameter of 250 mm that cross transversally the station (Figure 5). All pipes are located inside the station in the lowest level, coinciding with every emergency exit corridor. Outside the diaphragm walls, 2 longitudinal pipes of 450 m long with a diameter of 210 mm connect the 4 transversal pipes to facilitate the groundwater to move from one pipe to another. In all pipe intersections there are gravel filled piles with a diameter of 1 m and 1 m depth with geotextiles in its upper part. This design allows a better water intake and discharge.

The bottom slab covers an area of 40.000 m² and it is 2.5 m thick to resist a maximum water pressure of 11.2 m.w.p. (meters of water pillar, 1 m.w.p. = 9806,38 Pa). The bottom slab is mainly flat at ground level -6 m.a.s.l. on its central part and sloping at the northern and southern edges, reaching ground levels at -1 m.a.s.l. and -4 m.a.s.l. respectively (Figure 5-2). Below the bottom slab there is a 0.2 m thick of fine gravels to allow a homogeneous water pressure distribution. Above the gravel layer there is a fine layer of 0.1 m thick of concrete and an asphaltic layer to isolate the bottom slab from the groundwater. In case of overpressure due to a rise of the water table, ten artesian wells were homogeneously drilled along the bottom slab to extract water when the groundwater head is higher than 5.2 m.a.s.l., which corresponds to a water pressure of 11.2 m.w.p.

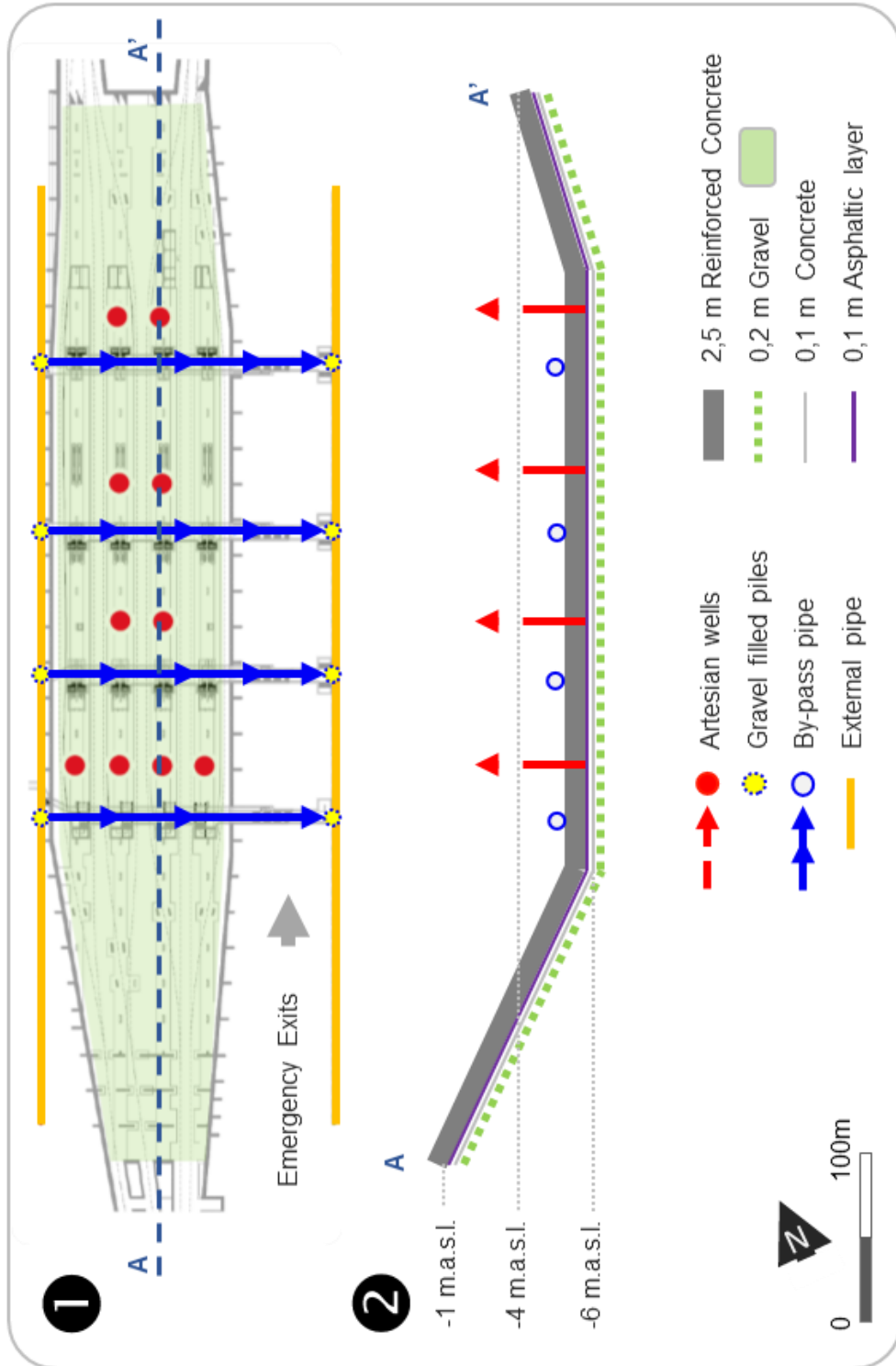


Figure 13. Original design scheme. (1) Plan view. (2) Cross section. Bottom slab

3.3. NEW INTEGRATED DESIGN

3.3.1. *Integrated Design description*

The integrated design aims to bring together the groundwater by-pass and the bottom slab designs into a single design. In order to do so, the original designs were modified to use the by-pass as a water pressure distribution net. Figure 14 shows the new design that integrates the by-pass and the bottom slab water pressure distribution net.

First, the original layer of gravels below the bottom slab were replaced by a gridded net of canals (4 longitudinal and 4 transversal) excavated below the bottom slab (Figure 14-1). Each canal has a section of 1 m² and is filled in gravel. This canal network is sufficient to homogeneously distribute groundwater pressure under the bottom slab by reducing the gravel volume from 8.000 m³ to 2.300 m³.

Second, all the transversal canals pierce the western and the eastern diaphragm walls. This design allows the canals to act as groundwater by-passes, collecting groundwater upgradient and in discharging it downgradient. The section of each by-pass increases 6 times, from 0.05 m² to 0.3 m² (the useful section is the result of multiplying 1 m² of gravel filled section with a gravel porosity of 0.3). Also, the 320 m PVC pipes with a diameter of 250 mm used in the original by-pass design are no longer needed, saving this line item in the budget.

Third, the pipes located outside of the diaphragm wall in the original design (upgradient and downgradient) were replaced by canals while the gravel filled piles still being the same from the original design: 2 longitudinal canals of 450 m long with a section of 1 m² and filled in gravel connect the 4 transversal gravel filled canals through gravel filled piles with a diameter of 1 m and 1 m depth with geotextiles in all canal intersections. Again, the 900 m PVC pipes with a diameter of 210 mm used in the original by-pass design are substitute by 900 m³ of gravel, reducing the cost of this line item in the budget.

Finally, two different designs of artesian wells distributions were proposed to release water in case of overpressure (water pressure higher to 11.2 m.w.p.): (1) Design 1, artesian wells inside the retaining walls; and (B) Design2, artesian wells outside the diaphragm walls (Figure 14).

3.3.1.1. Design 1: Artesian wells drilled inside the retaining walls

This design considers the same artesian well quantity and distribution than the project design: 10 artesian wells are homogeneously drilled along the bottom slab as shows Figure 14 (red dots). This distribution allows the water to be released very homogeneously inside the diaphragm walls.

3.3.1.1. Design 2: Artesian wells drilled outside the retaining walls

This design aims to keep the bottom slab totally impervious. This design proposes to move the artesian wells out of the diaphragm walls, locating them in the emergency exit tunnels (Figure 14– purple dots). The hydraulic connection from the inside to the outside of the diaphragm wall will be done through the gravel filled canals (by-passes). This connection will limit water pressure in the bottom slab by moving the water pressure from the inside to the outside.

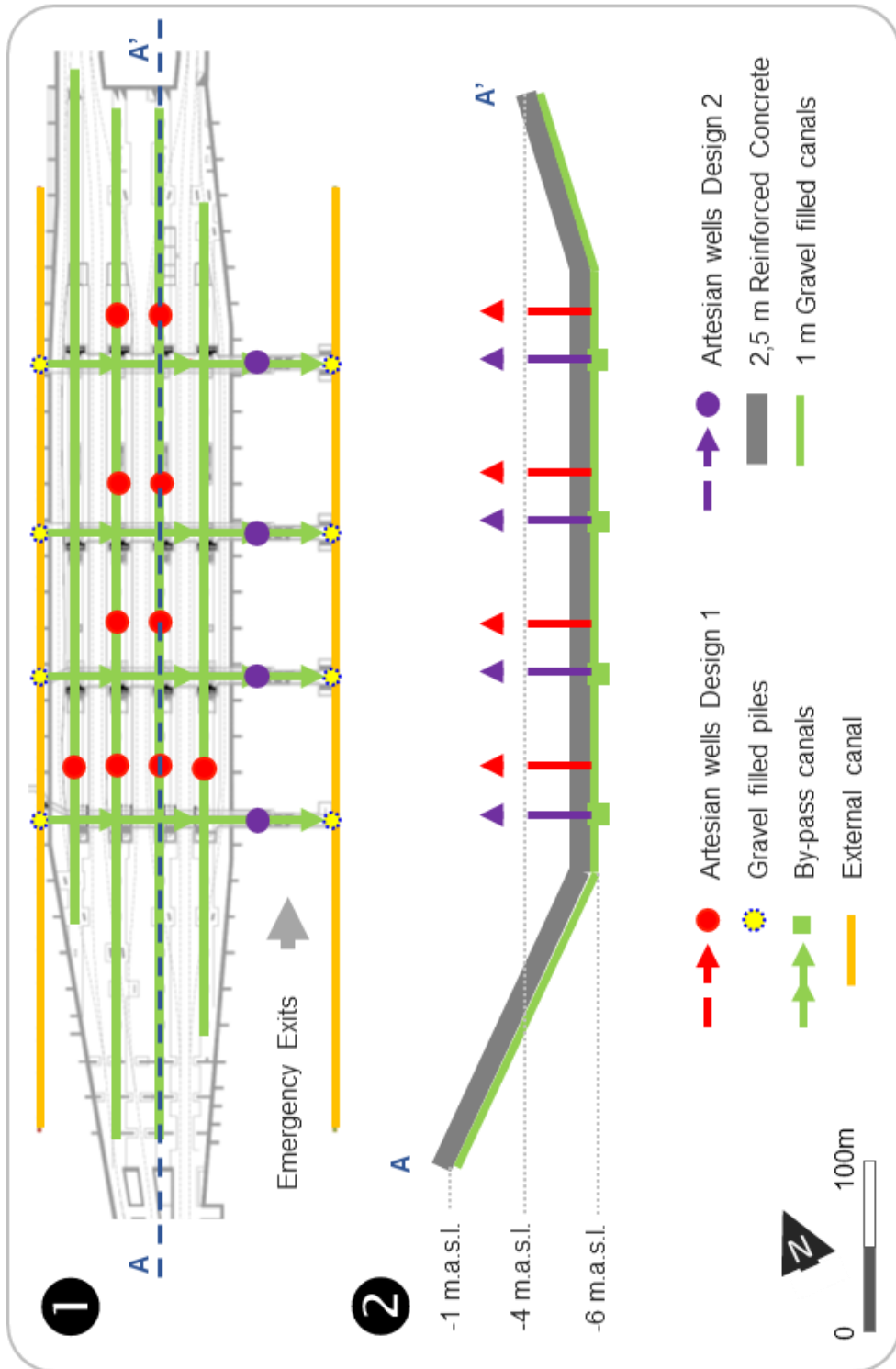


Figure 14. Integrated designs scheme. (1) Plan view. (2) Cross section.

This design reduces the number of artesian wells from 10 to 4 and avoids the necessity to drill the bottom slab and to place groundwater facilities in the train tracks yard.

3.3.2. Numerical model

The quantification and simulation of the groundwater dynamics and its related impacts was performed by a numerical model. The numerical model was built with the finite element code TRANSIN-IV (Medina and Carrera, 1996, 2003; Medina et al., 2000) that uses the visual interface of VISUAL TRANSIN (UPC, 2003). The numerical model is made up by 17 layers in the study site that simulate 17 strata with different properties (Figure 11). Three main geological formations are included in the numerical model: the Barcelona Plain (study site), the Besòs delta river (North, East and South-East) and the emerged (and altered) granites from the Palaeozoic (West). The geometry of the layers of the different formations was defined using data from the boreholes campaigns undertaken before starting the construction and also from geological data bases whose information has been recovered in the numerous projects developed in this area (Vázquez-Suñe et al., 2011; Pujades et al., 2012; Font-Capo et al., 2015; Serrano-Juan et al., 2015, 2016; Culí et al., 2016).

The hydrogeological boundaries of the numerical model were defined considering the natural boundaries of the aquifer and the piezometry of the area in natural conditions (Figure 15-1). Characteristics of the boundary conditions (BCs) adopted are as follows:

- The North-East side of the numerical model is bounded by the Besòs river at the East and by the Besòs river and the emerged Paleozoic that forms the Marina costal range at the North. The BC applied in the East zone of this boundary consists in a leakage (Cauchy BC), whose leakage coefficient is 10 d^{-1} . The BC adopted in the North zone was derived from the natural piezometry of the aquifer, where it is clearly observed that the emerged Paleozoic recharges the aquifer. Therefore, the BC implemented consists in a prescribed flow-rate whose value ($0.08 \text{ m}^2/\text{d}$) was calculated analytically from the piezometric distribution.
- The South-East side of the numerical model is bounded by the Mediterranean Sea. As a result, the BCs adopted consist in prescribed heads (Dirichlet BC). In this case, BCs were implemented at two different depths given the geometry of the Besòs delta river formation. This can be divided in three main units (Velasco et a., 2012, Vázquez-Suñe et al., 2016): the deep aquifer, the intermediate aquitard and the shallow aquifer. Prescribed head BCs were implemented in the two aquifers. The piezometric head was fixed at +0.3 and +1.3 m.a.s.l. for the shallow aquifer and deep aquifers, respectively. The piezometric head of the deep aquifer is higher because its discharge zone is located far away from the coastal line.
- Three different BC were applied in the West side of the model. These were defined from the natural piezometry of the aquifer. Firstly, the South-West zone belongs to the area where the Paleozoic emerges bounding the aquifer. The Paleozoic granites have a very low hydraulic conductivity and produce an abrupt change in the piezometric distribution. The applied BC consists in prescribe the head (Dirichlet BC) at +19 m.a.s.l. Secondly, the head was prescribed (Dirichlet BC) at +12 m.a.s.l. in the North-West zone. Finally, a no-flow BC was implemented between the two abovementioned

boundaries because the piezometric lines are perpendicular to this boundary zone, which indicates that none recharge occurs.

- The South-West boundary of the model, which crosses the Barcelona Plain formation, was delimited to avoid the complete modelling of the Barcelona Plain formation. This formation was not totally modelled to increase the precision of the predictions at the interest site (elements have to be bigger if the modeled area is larger). This boundary was also delimited from the natural piezometric distribution that defines a groundwater divisory along it. Therefore, a no-flow BC was implemented.
- Finally, the dewatering was simulated by implementing in the pumping wells a prescribed flow-rate which was measured during the dewatering stage. A turbine flow-meter was installed at each pumping well and daily measures were taken.

The hydrogeological parameters and the BCs adopted were calibrated and tested using (1) the natural distribution of the piezometric head and (2) the data measured during the pumping tests undertaken before the construction. The characteristics of the pumping tests and their interpretation (fitting curves and computed hydraulic parameters) are shown in the Appendix. Note that the representativeness of the predictions performed with this numerical model are supported by other studies and projects developed about the construction of La Sagrera Railway Station (Vázquez-Suñe et al., 2011, Serrano-Juan et al., 2015).

The piezometers and the pumping wells were introduced in the model considering the depth and length of their screens. The diaphragm walls of the enclosure were implemented considering the geometrical characteristics specified by the constructor and were simulated as areas with a low value of hydraulic conductivity ($K=10^{-4}$ m/d). This low value of hydraulic conductivity was corroborated with the interpretation of the WTAT. The tunnel of the Metro's L4 was also introduced as an area with a low hydraulic conductivity ($K=10^{-4}$ m/d) because it has not seepages.

To conclude, the used mesh (Figure 15-2) consists of 6924 triangular elements and 3495 nodes in each layer. The size of the triangular elements was discretized towards the study site, ranging from 100 m close to the boundaries to 0.5 m at the construction site.

3.3.1. Scenario simulation

Three scenarios were used to test and compare the original and new the designs 1 & 2 (Figure 16). The scenario A corresponds to the current groundwater conditions (groundwater head level approximately at +3 m.a.s.l.). The scenario B simulates a groundwater table rise enough to activate the artesian wells of the bottom slab, which corresponds to a rise of approximately +1.5 m and represents the maximum historical natural rise of the water table from 1996 to 2015. The scenario C simulates a rise of 7 m. This scenario was considered to study how designs 1 & 2 may respond when the difference of the water head between the inside and the outside of the diaphragm walls is very high. This scenario is worth to be considered to emphasize the difference between the outcome of the original design and designs 1 & 2 since designs 1 & 2 are more permeable (have bigger openings in the diaphragm walls) than the original design that allow the water to flow more easily under the bottom slab.

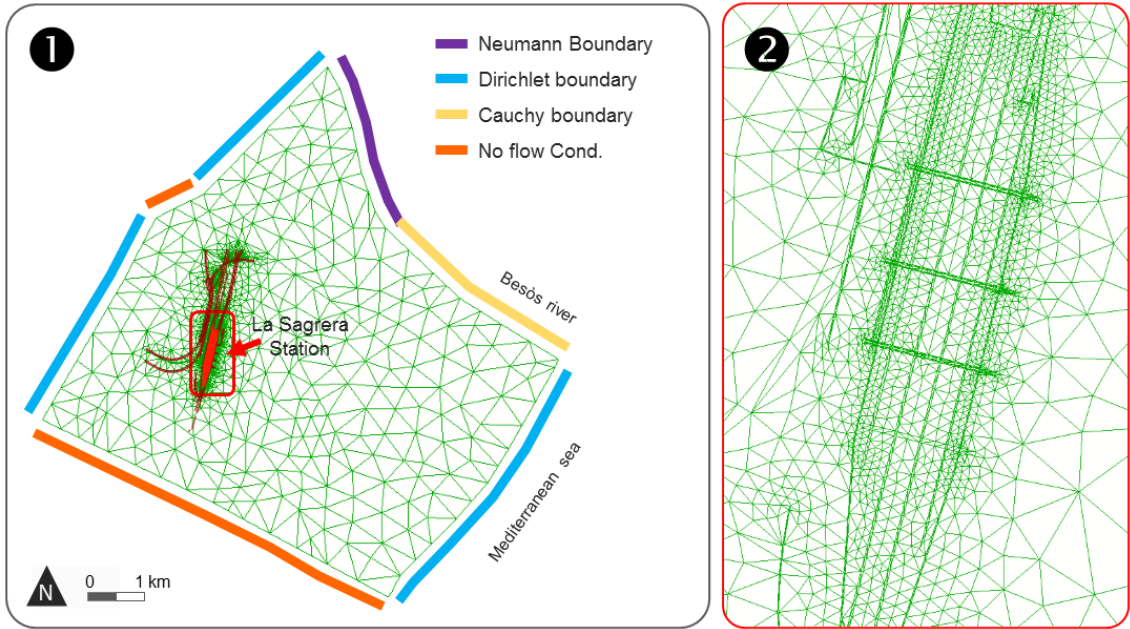


Figure 15. Numerical model mesh and boundary conditions.

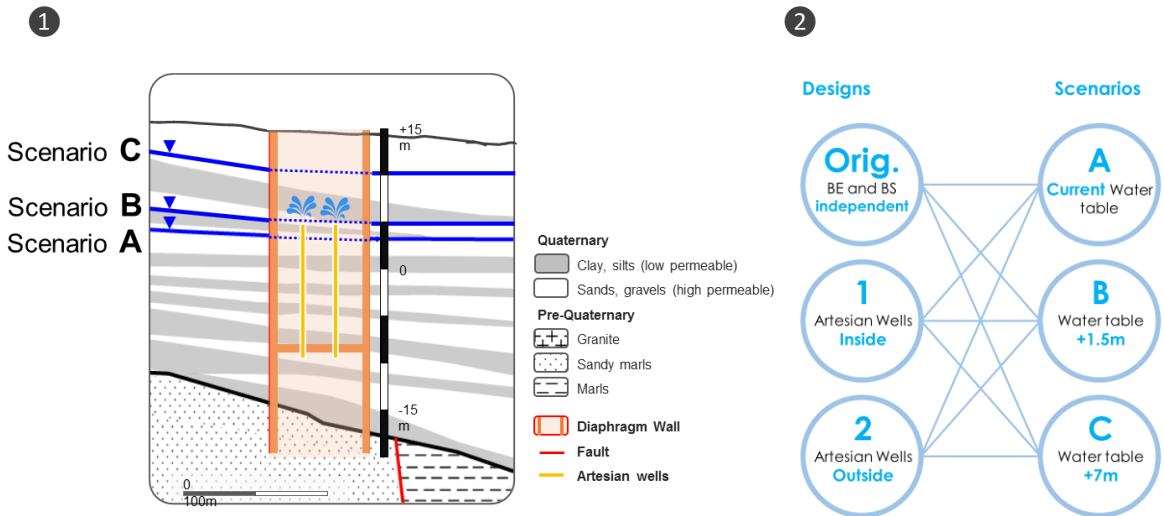


Figure 16. (1) Detailed water table location for each scenario. (2) Designs and Scenario evaluation.

3.4. RESULTS

The scenario A shows very similar results for all designs (Figure 17.A1-3). Actually, designs 1 & 2 show exact results since both designs only differ in the artesian well location and the piezometric level is not high enough to activate them. Only little variations close to the railway station can be appreciated among all designs. In this scenario the barrier effect is mitigated for all designs. The water head distribution below the bottom slab is also very similar, showing the highest water heads on the far south of the bottom slab.

Since the bottom slab is not entirely flat, when the piezometric level is constant the water pressure are not and change along the slopes (Figure 18.A1-3). In this scenario all water pressure distributions are very similar among all designs, being the maximum water pressure 9.3 m.w.p. in the major central part of the bottom slab, decreasing to 8 m.w.p. in the northern edge and to 5 m.w.p. in the southern edge. The water pressure distribution is linear from the central part to the edges of the bottom slab.

The scenario B shows a water table rise of 1.5 m, which is enough to activate the overpressure system (artesian wells). In terms of groundwater barrier effect, all designs are able to mitigate the groundwater barrier effect and result in very similar water head regional distribution, being the water head differences among the designs lower than 5 cm (Figure 17.B1-3).

The water head distribution under the bottom slab is different among the designs. Designs that have the artesian wells inside the station (original design and design 1) show similar results, with the maximum water heads in the northern and southern edges of the bottom slab. The artesian wells inside the station are sufficient to keep the interior water head at +4 m.a.s.l. in almost all the deepest part of the bottom slab by extracting 169 m³/d in the original design and 144 m³/d in the design 1 (reduction of 25 m³/d, each artesian well extracts approximately 17 m³/d and 14 m³/d respectively). In contrast, design 2 (with the artesian wells outside the diaphragm walls) shows a water head gradient of 0.2 m/m that flows from the north and south ends of the bottom slab to their central part. The maximum water head varies 0.5 m with respect to the other two designs. In this case, the four artesian wells are enough to release the necessary water to keep the water heads close to +4 m.a.s.l. in almost the whole central part of the bottom slab. A total of 124 m³/d are extracted through the four artesian wells, being approximately 31 m³/d the extraction by each of them.

In terms of water pressure (Figure 18.B1-3), the original design and design 1 (with inner artesian wells) show again very similar results. The canal network of design 2 shows almost identically results that a continuous layer of gravel of the original design. Maximum water pressure are 10.3 m.w.p. and are located where the bottom slab's slope change, close to the first and the fourth emergency exits. Design 2 (with outer artesian wells) presents differences with respect the other two. In this case, the maximum water pressure are located only close to the first emergency exit, reaching 11.1 m.w.p., which are very close to the maximum water pressure resistance of 11.2 m.w.p. that can hold the bottom slab before it breaks. In the central part of the bottom slab, the water pressure distribution shows a gradient that reflects how the water pressure is being released through the emergency exits. In all cases, minimum water pressure are close to 7 m.w.p. and are located in the bottom slab northern and southern ends.

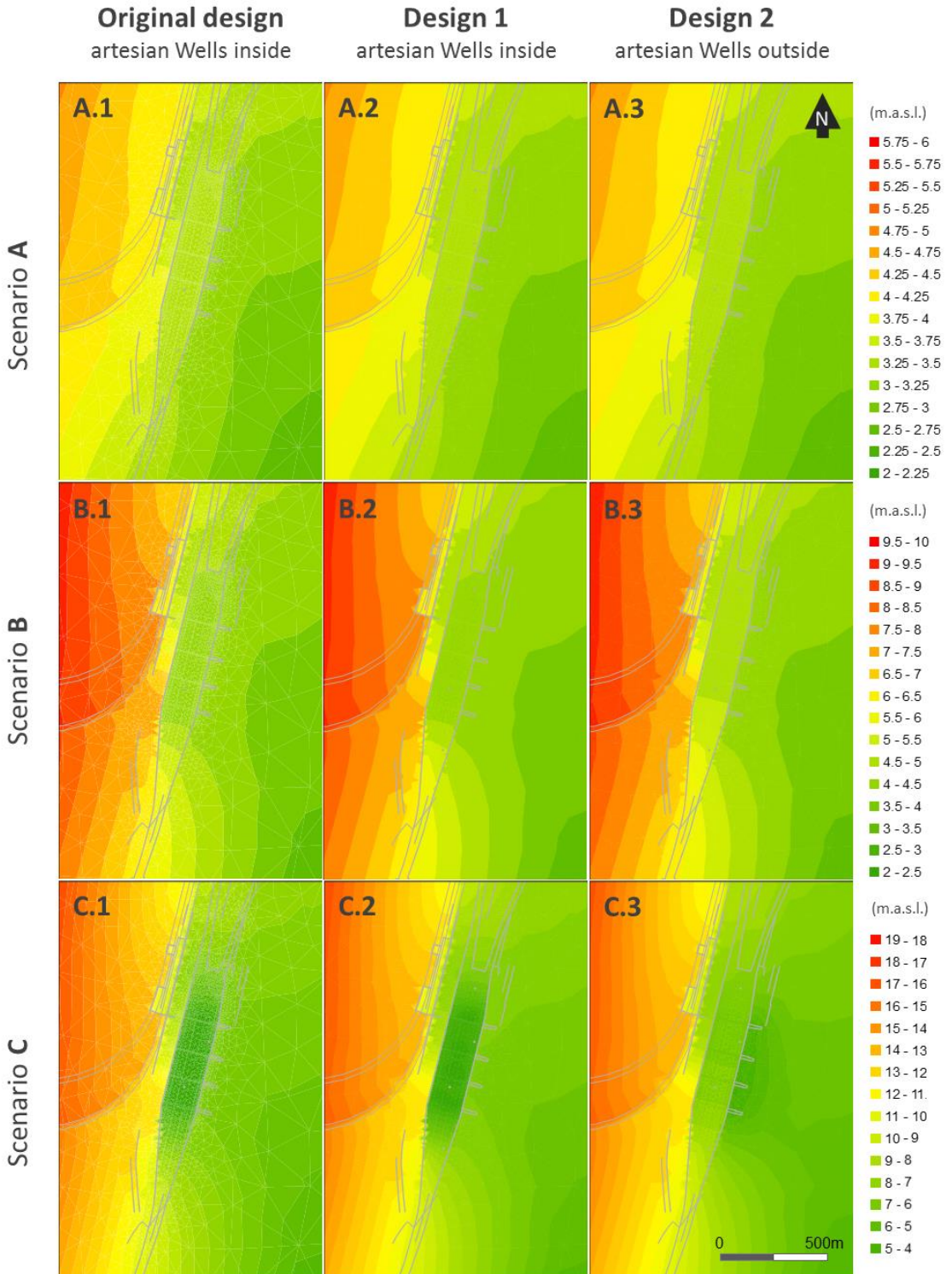


Figure 17. Simulation results: Water heads (in m.a.s.l.) for each scenario and design.

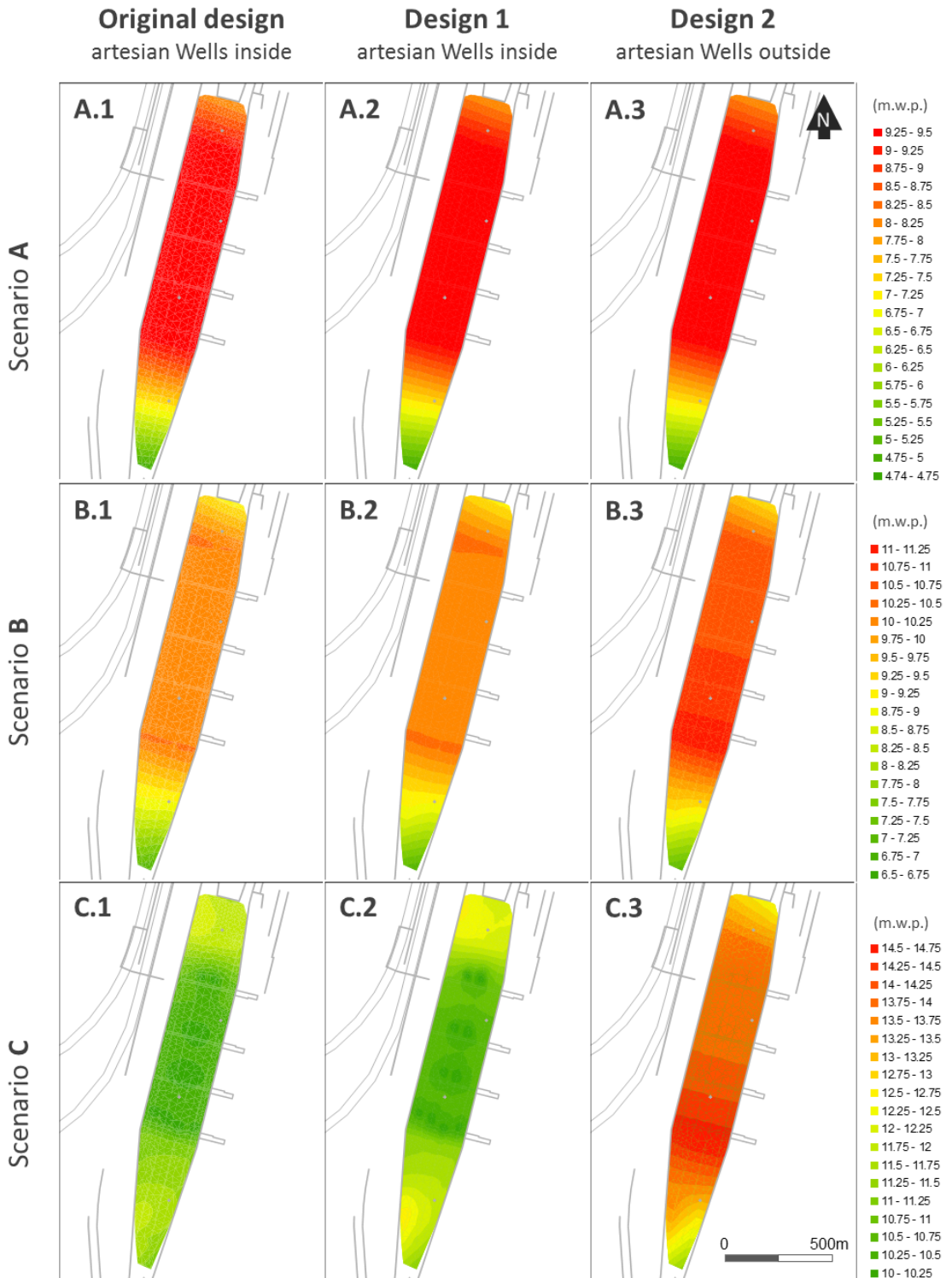


Figure 18. Simulation results: Water pressure (in m.w.p.) for each scenario and design.

In scenario C the water table rises 7 m. In terms of groundwater barrier effect, the inner (original design and design 1) and the outer (design 2) artesian well designs show very different results (Figure 17.C1-3). While the original design and design 1 produce a similar groundwater barrier effect, design 2 results in a very strong barrier effect. This is because the artesian wells are forcing the water head to be at +4 m.a.s.l. outside the enclosure (downgradient) while its natural condition would be higher. In terms of groundwater modelling, this situation is comparable to have a Dirichlet boundary condition at the emergency exits.

The water head distribution under the bottom slab is different among the designs. Similarly to the scenario B, designs that have the artesian wells inside the station (original design and design 1) show similar results. This slight difference in the water head distributions between the original design and design 1 is mainly due to the increase of the diaphragm wall openings. In the original design the enclosure has openings in both north and south edges, while in designs 1 & 2 they have also transversal openings (by-pass canals). In contrast, the artesian wells of design 2 force the water head at to be at +4 m.a.s.l. outside the enclosure (downgradient), inducing a strong flow gradient from the inside to the outside close to the emergency exits. In this case, the artesian wells do not mainly release the water coming from the by-passes (inside of the enclosure), they also release water from anywhere out of the enclosure, reducing the capacity of the artesian wells to keep the water head at +4 m.a.s.l. under the bottom slab.

Again, water pressure below the bottom slab are similar in the original and design 1 (Figure 18.C1-3). While the original design shows the best results with maximum water pressure of 12.2 m.w.p. (located close to the north and south bottom slab ends), Design's A maximum water pressure are 0.5 m higher than the original design. This design shows a water pressure rise of 0.3 m in between the artesian wells in the same section and over 0.5 m between artesian well sections. Design 2 shows the worst results, with maximum water pressure at 14.7 m.w.p. and minimum ones at 11.3 m.w.p. In fact, any design does not fulfil the maximum water pressure requirement of 11.2 m.w.p.

Table 1 summarizes the results for each scenario and design.

3.5. DISCUSSION and CONCLUSIONS

This chapter presents an innovative groundwater by-pass design that enables the groundwater flow through the structure and provide a homogenous distribution of the water pressure under the bottom slab. The new integrated design was applied to La Sagrera railway station, the largest underground infrastructure of Barcelona, and it was simulated to analyze its response to different scenarios.

Scenarios A and B showed similar results in all three designs. All designs are able to mitigate the groundwater barrier effect and none of them exceeded the maximum water pressure resistance of the bottom slab, being all three good options.

The water pressure distribution between the original design and design 1 (with inner artesian wells) in scenario B demonstrates that the canal network can distribute the water pressure almost equally that the continuous layer of gravel, but reducing four times the costs (gravel volume from 8.000 m³ to 2.300 m³). There are also collateral benefits in using gravel filled canals instead of a continuous gravel layer. For instance, prior the execution of the bottom slab, superficial water such as precipitation, water inflows or water pollutants can be easily collected and redirected by the canal network. This helps to increase safe and efficiency during the construction stage since the canal network maintains the workspace clean and dry.

Scenario B also presented very similar barrier effect responses among all designs. This demonstrates that the original design PVC by-passes can be replaced by gravel filled canals. The 320 m of PVC pipes with a diameter of 250 mm and the 900 m of PVC pipes with diameter of 210 mm are no longer needed which strongly reduces the costs. Additional benefits are the by-pass relocation out of the structure (under the bottom slab), which avoids flooding in case of breakdown. Also, the by-pass section increased 6 times (from 0.05 m² to 0.3 m²), reducing the necessity of maintenance and cleaning processes and also reducing the head loss due to the pipe inlet.

The artesian well section and extraction capacity is different between design 1 (the inner) and design 2 (the outer artesian well designs). While the first one should have 10 artesian wells with a minimum section of 10 mm (considering scenario B, a water velocity of 2 m/s and a coefficient discharge/area of 0.45 for Nominal Pipe Size (NPS) of 10 mm and 0.71 for NPS of 15 mm), the second only need 4 artesian well with a slight bigger section of 15 mm. The benefits of the outer artesian wells do not only rely on the cost reduction, but the possibility of keeping the bottom slab clean, which facilitates the maintenance processes and reduces de risk of accidents in the station.

The comparison among the three designs in the scenario C reveals that openings in the enclosure are critical when the difference of the water head between the inside and the outside of the diaphragm walls is very high. Other important factors are the artesian well quantity and location. In this sense, design 2 (with outer artesian wells) does not respond well to this scenario. The original design and the design 1 (with inner artesian wells) respond very similar, but none of them guarantee that the bottom slab does not break by overpressure. However, it is a very unrealistic scenario in La Sagrera, which maximum historical water heads have never overhead the ones simulated in the scenario B.

This chapter shows that design integration is useful to create more efficient solutions, to avoid over budgets and to increase safe previous, during and after construction. The example of La Sagrera railway station shows the pros and cons of implementing independent and integrated design solutions to avoid the groundwater barrier effect and to limit and distribute the water pressure below the bottom slab. The integrated solutions solve the barrier effect produced by the structure and optimizes the bottom slab, reducing considerably the costs and increasing safety during the construction phase.

Chapter 4.

GB-SAR interferometry displacement measurements during dewatering in construction works.

The case of La Sagrera railway station in Barcelona, Spain.

4.1. INTRODUCTION

Civil projects can be especially challenging when construction is under the water table and in urban environments. The impacts on both aquifer and construction areas must be limited, requiring construction designs that ensure safety compliance and preservation of the aquifer conditions. As a result, it is necessary to adopt corrective measures previous to, during, and/or after the construction. In all cases, these measures must be supervised by monitoring the hydraulic heads, soil movement (heaves and subsidence), and movements of adjacent buildings (these being the most common controlled parameters).

Traditional infrastructure project monitoring is based on land surveys and geotechnical instruments. The most common topographic techniques include leveling, total stations, Differential Global Positioning System (DGPS), and robotic total stations, and the geotechnical techniques include pendulums, inclinometers, extensometers, piezometers, gyros, and optical fiber-based techniques (Dunnicliff, 1988; Marchamalo et al., 2011). Some of these techniques, such as DGPS, robotic total stations and optical fiber-based methods, allow for automatic measurements and continuous monitoring. Although all of these techniques are widely accepted and used, they are susceptible to the weather conditions (i.e., they are difficult to use during a storm) and still allow only point-like measurements, requiring interpolation and extrapolation to achieve a complete measurement understanding (Figure 19).

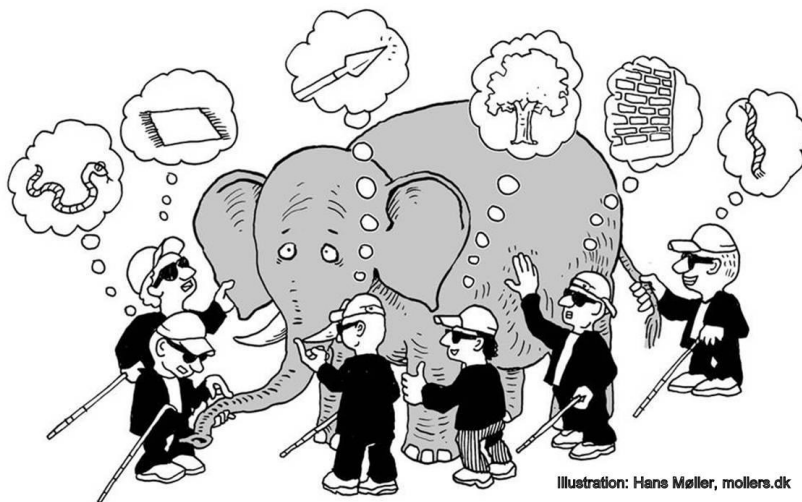


Figure 19. Illustration of Hans Møller to emphasize divergence in interpretations.

In the last few decades, new technologies for assessing soil movements have evolved rapidly. Remote sensing imaging systems, such as synthetic aperture radar (SAR), now offer the ability to capture complete deformation patterns (2D information) and the possibility of both day and night operation, independent of the weather conditions (storm, wind, rain, and sun). The SAR sensors can be installed in satellites or on the ground (GB-SAR). While satellite acquisitions cover areas of 100 km by 100 km at longer time periods, ranging from days to weeks (depending on the satellite), ground-based systems allow for continuous monitoring in smaller areas (usually approximately 1-2 km²) and shorter revising times on the order of minutes. GB-SAR presents some limitations, such as the necessity of measuring displacements perpendicular to the Line-Of-Sight (LOS) and the requirement for pixel coherence over time. Nevertheless, the GB-SAR system provides more capabilities compared with other deformation measurement techniques due to its high sensitivity to small

deformations, its long-range measurement capability (up to several kilometers) and its simultaneous measurement of a vast number of points.

GB-SAR has been successfully used, tested and accepted in a variety of applications. The most common applications include the monitoring of slope instability related to rockslides (Tarchi et al., 2005), landslides (Tarchi et al., 2003; Schulz et al., 2012), or volcanoes (Casagli et al. 2010). Other important GB-SAR applications are urban infrastructure and building monitoring (Pieraccini et al., 2004; Tarchi et al., 1997; Tapete et al., 2013), dam monitoring (Tarchi et al., 1999), dike monitoring (Takahashi et al., 2013) and glacial motion monitoring (Luzi et al., 2007). A general review of the GB-SAR technology is provided by Monserrat et al. (2014).

Due to the characteristics of GB-SAR, a very large variety of displacements can be accurately measured. However, GB-SAR has not yet been applied as a monitoring tool during infrastructure projects. This might be due to the difficulty of properly locating the sensor or to the lack of elements that remain coherent over time. Fortunately, these drawbacks can be overcome by combining the GB-SAR with traditional displacement measurements and by analyzing which structures are most vulnerable and should be monitored.

This chapter aims to **demonstrate how to use GB-SAR to continuously monitor infrastructure projects in time and space**. To demonstrate the utility of applying GB-SAR to structure monitoring, an experiment was conducted in the future railway station of La Sagrera, Barcelona (Spain). This experiment consists of the design, implementation, quantification and interpretation of a pumping test that allows the GB-SAR to measure the movements of a structure during the construction phase. Based on the geological, geotechnical, hydrogeological and construction knowledge of the work, the structures susceptible to movement in the next phase of the project were selected. The results of GB-SAR are compared with conventional monitoring measures.

4.2. PROBLEM STATEMENT AND GB-SAR EXPERIMENT DESIGN

4.2.1. GB-SAR BASICS

This section briefly reviews the most important characteristics of GB-SAR deformation monitoring. The GB-SAR is an imaging sensor based on the synthetic aperture radar (SAR) technique (Fortuny and Sieber, 1994). For each image pixel, a GB-SAR provides a complex number, which consists of the In-phase and Quadrature components of the received echo, from which the signal phase and amplitude can be derived. The amplitude is related to the power of the reflection of the observed scene, while the phase contains geometric information, which is related to the distance between the radar antenna and the given target. The main GB-SAR observation is given by the interferometric phase, which is obtained using the phase difference of images acquired at different times. The interferometric phase is directly related to the displacements of the observed scene in the time elapsed between two acquisitions, providing the displacements of individual image pixels. The displacement associated with a given pixel represents a weighted average of the displacement of all of the elements included in the pixel footprint. The weight is given by the amplitude of the response of each single element.

Figure 20 summarizes the main equations to acquire the displacement information.

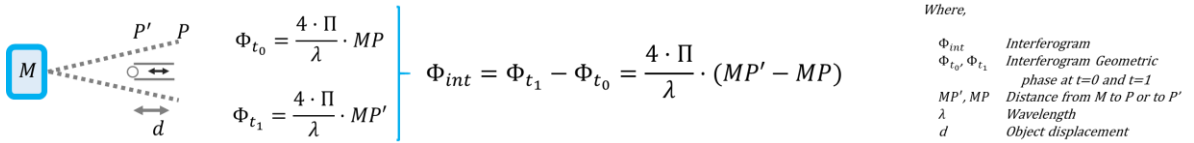


Figure 20. Ground-based SAR images treatment. The physics and the mathematics.

The main steps of GB-SAR data processing include the following: **(i)** acquisition of a stack of GB-SAR images; **(ii)** image co-registration; **(iii)** selection of the coherent pixels (the pixels maintain their relative position and phase, and it does not affect the degree of correlation between two images), i.e., the pixels that can be exploited for deformation monitoring; **(iv)** phase unwrapping; **(v)** phase integration, estimation and removal of the atmospheric phase component; **(vi)** estimation of the LOS deformation time series for each coherent pixel; **(vii)** computation of the three coordinates (e.g., East, North, and height) of each measured pixel; and **(viii)** (optional) transformation of the LOS deformation in the actual deformation direction (this can only be performed if the deformation direction is known).

The main shortcomings of GB-SAR deformation monitoring are as follows: **(1)** the pixel response must be coherent over time (i.e., between different image acquisitions); **(2)** the reconstruction of the interferometric phase (unwrapping phase (Ghiglia and Pritt, 1998)) is error-prone, especially for discontinuous GB-SAR measurements; and **(3)** the sensor measures displacement along the radar Line-of-Sight (LOS), and therefore, displacements oblique to the LOS can be computed while displacements perpendicular to the LOS cannot be measured.

PROS & CONS

- ✓ **2D deformation** measurement
- ✓ **Automatic process**
- ✓ **Submillimetric** precision
- ✓ Cover **areas of 1-2 km²** with very high **dense coverage**
- ✓ Independent to weather conditions

- ✗ The pixel **displacements** must be **coherent**
- ✗ Sensor **measures** in the **Line-Of-Sight (LOS)**

However, GB-SAR deformation monitoring presents many advantages. **(1)** The deformation monitoring process can be highly automated, independent of the weather conditions and the day-night cycle. **(2)** GB-SAR is able to monitor deformation phenomena, from a few millimeters per year up to 1 m per h, at distances of up to several kilometers (the precision ranges from sub-millimeters to a few millimeters, depending on the target characteristics, the sensor to target distance and the distance from the reference point). **(3)** A GB-SAR measurement can cover an area of 1–2 km², providing a dense measurement coverage of the observed scene (the GB-SAR instrument used in this study ranges from approximately four measurements/m² at 100 m to 0.4 measurements/m² at 1000 m). Finally, **(4)** GB-SAR can be used in two acquisition modes: continuous (the instrument is left installed in situ, acquiring data on a regular basis, e.g., every few minutes) and discontinuous (the instrument revisits a given site periodically, e.g., weekly or monthly) (Crosetto et al., 2014).

4.2.2. LA SAGRERA STATION EXCAVATION AREA

4.2.2.1. General situation

La Sagrera railway station (Figure 21) is located in the metropolitan area of Barcelona (Spain) and aims to become the city's major intermodal transit hub. The station is expected to receive more than 100 million passengers per year, combining high-speed trains, short- and medium-distance trains, four metro lines and buses (ADIF, 2015). The railway station construction began in 2010 and is planned to be completed by 2020. At the time of the experiment (February 2014), all diaphragm walls were built (finished in February 2013), the dewatering system was drilled and equipped (finished in November 2012), and the site leveling was completed (no excavation yet).

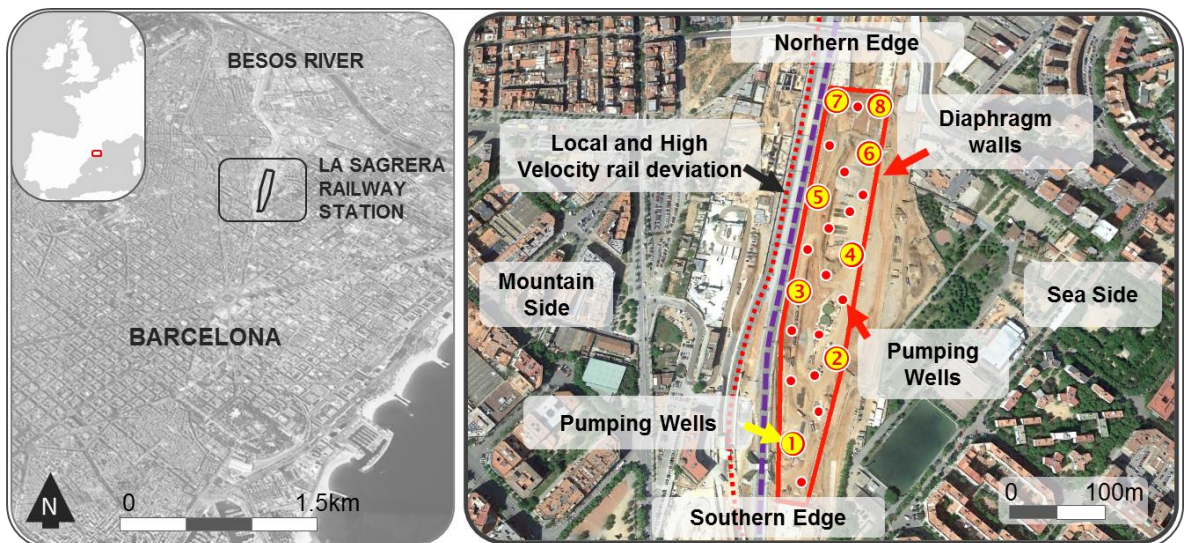


Figure 21. Geographical location of the study site. Yellow wells are activated during the pumping test.

4.2.2.2. Geological and hydrogeological settings

The metropolitan area of Barcelona is located on the Mediterranean coast of NE Spain. Geologically, this area is formed by a coastal plain (the Barcelona coastal plain) bounded by two Quaternary deltaic formations (corresponding to the Besòs and Llobregat rivers) and an elevated area, the Catalan Coastal Ranges (mainly Paleozoic rocks composed of granodiorite materials) (Sanz, 1988). More concretely, the study site is located in the actual plain, which consists of Quaternary formations that overlie a substrate mainly formed by Paleozoic and Pliocene series. The Quaternary formation presents a very heterogeneous pattern and can be divided into the Lower Quaternary (Pleistocene) and Upper Quaternary (Holocene). The Pleistocene is made up of several cycles composed of alluvial sequences. The upper Quaternary is mainly composed of torrential, alluvial and foothill deposits, where gravels and sands with a high proportion of clay matrix are present. All of these quaternary deposits are 30 m thick. The pre-Quaternary substrate consists of the Pliocene series, mainly composed of marine blue marls and sandy marls and Paleozoic granite. The entire study area is cut by many fractures that compartmentalize the pre-Quaternary substrate; specifically, the construction area is crossed by a fracture (oriented NNW-SSE) that separates the two Pliocene series: Pliocene marls (south) and Pliocene sandy marls (north).

Hydrogeologically, the Quaternary and pre-Quaternary materials can be regarded as a layered aquifer with high vertical heterogeneity, with an effective transmissivity of 100-200 m²/d. The hydraulic conductivity (k) of the Quaternary clay layers (low-permeability layers) ranges from 0.001 to 0.01 m/d, the k of the Quaternary sand and gravel layers (high-permeability layers) ranges from 0.1 to 10 m/d, the k of the Pliocene fine materials (marls) ranges from 0.001 to 0.01 m/d, and the k of the sands ranges from 0.1 to 10 m/d. These values were derived from the numerous hydraulic tests performed in the study area and from numerical models developed for calibration purposes.

The water table oscillations during the 20th century, due to extensive water extractions at the beginning of the century (drawdowns of approximately 10-15 m) and the water table recovery after the 1970s (Vázquez-Suñé et al., 2005), resulted in an over-consolidation of the soil, changing the soil deformation from plastic to elastic (Odometric curve). This behavior has been appreciated in the nearby High Velocity Railway shafts of Padilla (approximately 1,500 m) and Trinxant (approximately 500 m) in Barcelona, Spain (Pujades et al., 2014a, 2014b). Basic soil parameters were obtained from laboratory and field tests (see Table 1). The cohesion ranges from 0 to 70 kPa, the soil unit weight ranges from 20 to 21.5 kN/m³, the friction angle is in the range of 26° to 38°, and Poisson's ratio is between 0.3 and 0.4.

Figure 23 summarizes the hydrogeological and geological characteristics of the study area. Figure 22 shows a detailed view of the excavation and the rail retaining wall (west).

LITHOLOGY	PRE-QUATERNARY		QUATERNARY			
	GENERAL DESCRIPTION	PL1: Sandy soil with clay and silt interlayers	PL2: Clay	PQ1: Sand and gravel	PQ2: Clay and silt	QA1-QA2 fine: Clay and silt
PARAMETERS						
γ_t (kN/m ³)	20.5	20.5	21.0	21.0	21.0	21.5
c' (kPa)	20.0	70.0	0.0	30.0	30.0	0.0
ϕ' (°)	35.0	26.0	38.0	29.0	29.0	34.0
E (MPa)	40.0	40.0	25.0	20.0	20.0	18.0
ν	0.3	0.3	0.4	0.3	0.3	0.4
Hardening soil model						
m	0.5	0.5	0.5	0.5	0.5	0.5
E_{50}^{ref} (MPa)	31.0	31.0	25.0	20.0	20.0	24.0
E_{oed}^{ref} (MPa)	24.8	24.8	20.0	16.0	16.0	19.2
E_{ur}^{ref} (MPa)	93.0	93.0	75.0	60.0	60.0	72.0

Table 2. Parameters of the Hardening Soil Model used in the ©PLAXIS hydromechanical model. γ_t is the soil unit weight, c' is cohesion, ϕ' is the friction angle, E is the Young's modulus, ν is Poisson's ratio, m is the power for stress-level dependency of the stiffness, E_{50}^{ref} is the reference Young's modulus at 50% of the strength, E_{oed}^{ref} is the reference oedometric modulus, and E_{ur}^{ref} is the reference unloading-reloading modulus.

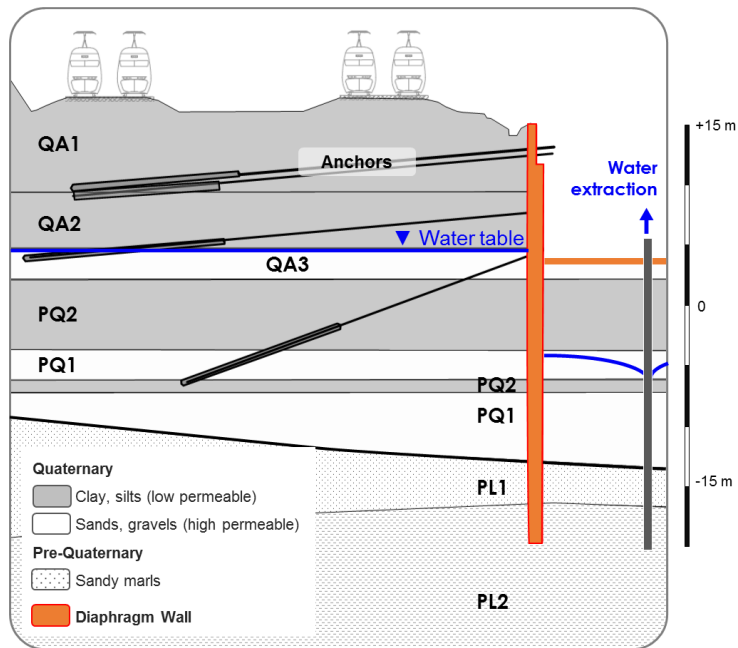


Figure 22. Soil and excavation profile corresponding to the transverse section A6 (see Figure 25 to locate the section) at the time of the experiment. A6 is also the transverse section of the hydromechanical model ©PLAXIS.

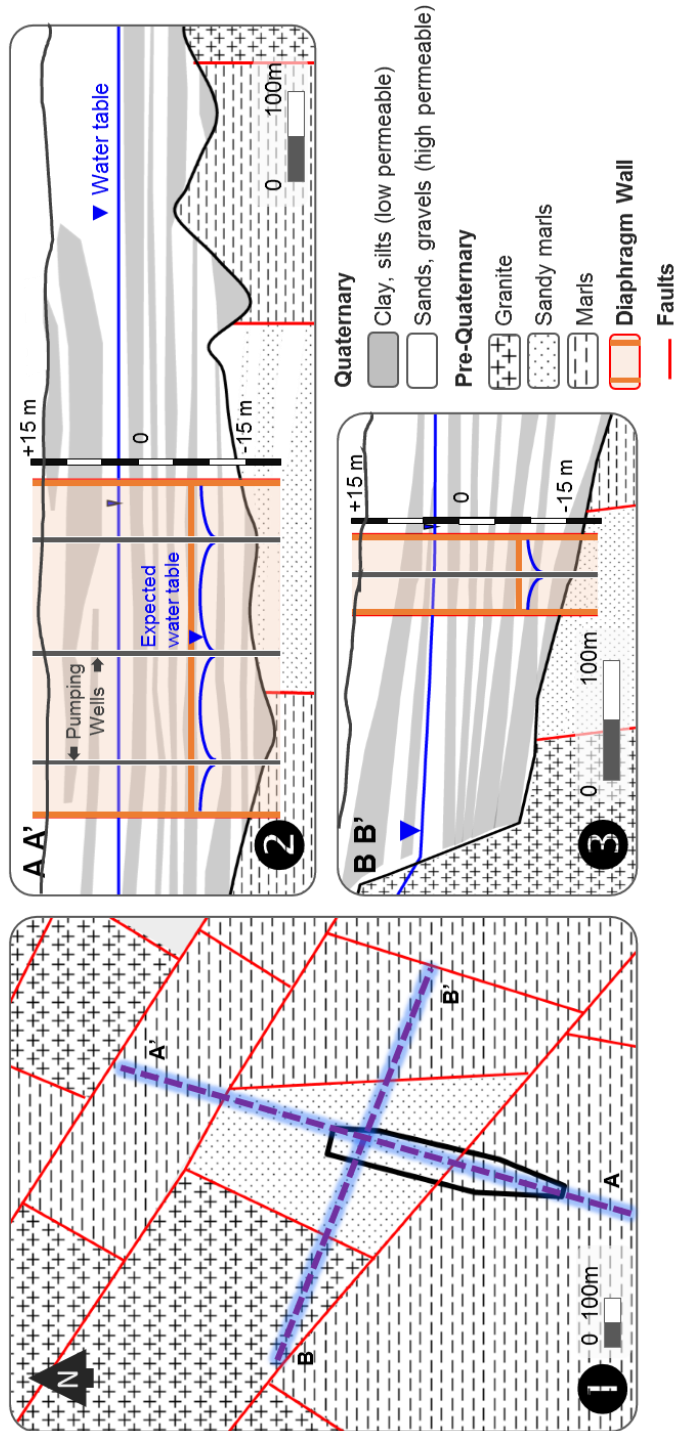


Figure 23. Detailed geological profile of the site. (1) Plan view of the geological basement, (2) Cross section A-B, (3) Cross section C-D. Excavation area, limited by diaphragm walls, is shown in light brown color. Both cross sections show the maximum excavation and the required dewatering system.

4.2.2.3. Construction characteristics

The Sagrera station will occupy an area of approximately 70.000 m² and requires a 20-m-deep excavation. The initial soil elevation is between +14 and +16 m.a.s.l. (meters above sea level), and the water table's natural position is between +2 and +4 m.a.s.l. The dewatering process is performed inside diaphragm walls (the bottoms of which are at -20 m.a.s.l.) to meet the structural requirements and to reduce the water extraction and subsidence outside. The diaphragm walls are anchored on their upward sides to support the railway lines (which have been deviated and are active during the entire process). The excavation bottom is at -8 m.a.s.l., requiring a water table drawdown of approximately 12 m. The first excavation phase involves extraction of the non-saturated soil (the bottom of which is at +2 m.a.s.l.). The second phase excavates the saturated soil, from +2 m.a.s.l. to -8 m.a.s.l. There are 26 wells (which reach down to -20 m.a.s.l.) and a network of 48 piezometers (20 inside and 28 outside of the excavation area) with different depths and screens to execute and control the dewatering process.

The construction stages are **(i)** design, **(ii)** diversion (any services on the site such as drainage, water and gas piped services, power and communication cables and traffic must be diverted before the construction starts); **(iii)** site clearing; **(iv)** diaphragm wall construction and non-saturated soil excavation; **(v)** dewatering and excavation; **(vi)** building construction; and **(vii)** building operation. At the time of this experiment (February 2014), all diaphragm walls were built and the dewatering system was ready (construction stage iv was finished).

See Figure 21 for the site study area and the construction details. Figure 22 shows a cross section at the moment of maximum excavation, and Figure 23 shows a detailed view at the time of the experiment.

4.2.3. EXPERIMENT SETUP

The current stage of construction presents a great opportunity to measure structural displacements (Figure 24). The experiment involves the following steps. **(1)** A pumping test is used to generate a controlled deformation: drawdowns in a pre-consolidated soil result in an elastic soil deformation behavior. **(2)** Numerical methods are used to design the pumping test (hydrogeological models) and to anticipate the soil and wall displacements (hydromechanical models). **(3)** GB-SAR measurements are spatially and temporally correlated with hydrogeological data (such as pumping rates and piezometric level evolutions) to evaluate the deformation produced by the dewatering. **(4)** GB-SAR measurements are compared with direct observations and other conventional displacement measurement techniques (such as total station measurements, inclinometers and extensometers). **(5)** Numerical models are calibrated with the real displacement and hydrogeological measures, and the results are compared with the GB-SAR measurements.

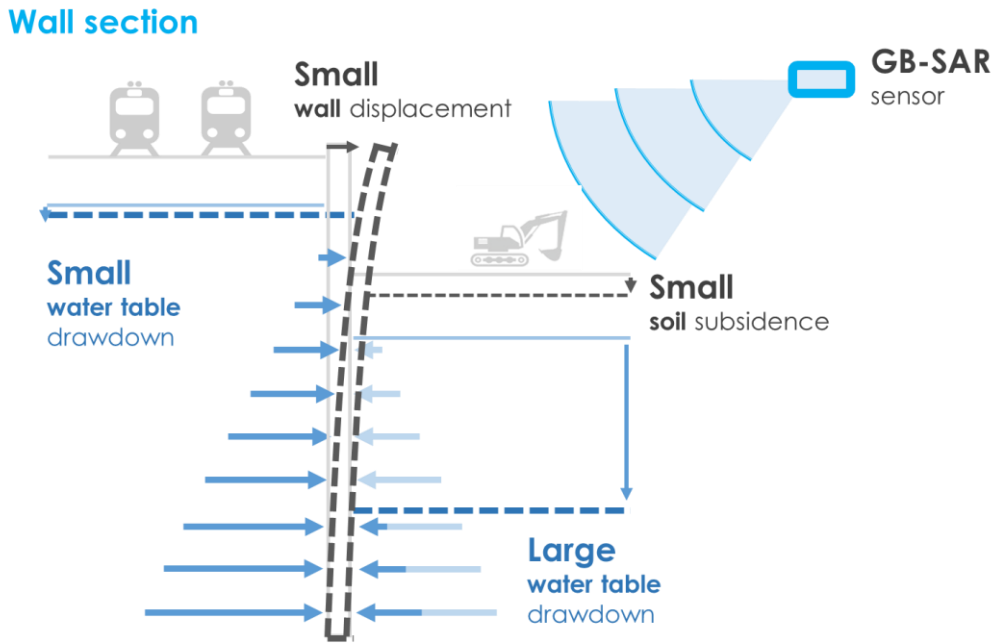


Figure 24. Scheme of the experiment and the expected wall deformation.

4.2.3.1. Pumping test

A 3-week pumping test was performed using eight pumping wells. Each pump extracted approximately 4 L/s, rising to 32 L/s when all eight pumps were extracting. Instead of starting the eight pumps simultaneously, the pumps were started sequentially (from the southern to the northern edge) to generate eight hydraulic steps. Every hydraulic step (when a pump starts) increased the water extraction, decreased the piezometric level and increased the soil deformation. The main advantages of this pumping test design rely on **(1)** the non-homogenous temporal and spatial deformation generation (which produces a complex deformation); **(2)** the limit of detection identification for every measurement technique; **(3)** the construction defects detection (i.e., open joints in the diaphragm walls - Vilarrasa et al., 2011, Pujades et al., 2012); **(4)** the numerical modeling calibration and validation; and **(5)** the dewatering system status inspection. The maximum drawdown was 8 m, increasing inside the pumping wells according to the head loss.

Figure 21 shows the position of all of the pumping wells, distinguishing those activated in this pumping test in yellow, numbered in the order of activation.

4.2.3.2. GB-SAR location

The position of the radar is a fundamental aspect as the sensor performs LOS measurements. In construction projects, where the imaged scene can vary considerably over time, the GB-SAR can only be used to monitor those elements, buildings and structures that remain coherent over time. To measure all of the horizontal

(structures) and vertical (soil) displacements, the GB-SAR sensor must be located at sufficient height and distance to have a LOS inclination as close as possible to 45°. The geometry of the study site allowed us to obtain a low LOS elevation (ranging from 2° to 8°). This quasi-horizontal LOS resulted in a good sensitivity to horizontal displacements and limited sensitivity to vertical displacements. The radar was located perpendicular to the northern diaphragm wall and was able to measure approximately two-thirds of the construction area. Figure 25 shows the radar location and the field of view.

4.2.3.1. GB-SAR measurements

The radar measurements were performed using a Ku-band interferometer, IBIS-L, manufactured by IDS Spa. IBIS-L uses a radar wavelength of 1.74 cm. The measurements were taken using a range resolution of 0.5 m and an azimuth resolution of 4.4 mrad (which, for example, corresponds to 0.44 and 0.88 m at 100 and 200 m, respectively). Additional information related to the sensor is provided in Bernardini et al. (2007), IDS (2013), Monserrat et al. (2014) and the IDS web page (www.idscorporation.com). The SAR images were acquired over a time period of 5 min. For each measured point, the displacements were estimated corresponding to the date of each acquired SAR image. The GBSAR data processing followed the steps listed in Section 2.1. In particular, the phase unwrapping was based on the Minimum Cost Flow algorithm (Costantini, 1998), and the estimation and removal of the atmospheric phase component were based on stable areas that surround the deformation area of interest.

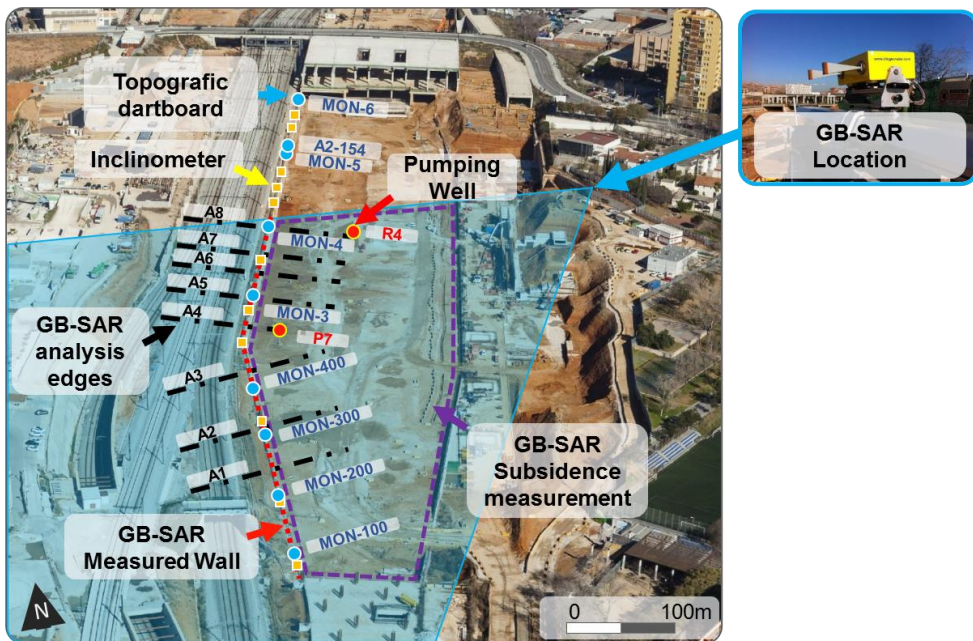


Figure 25. Radar position, GB-SAR analysis area, manual acquisition data targets (blue circles, MON) and inclinometers (yellow squares), pumping well positions (red circles) and GB-SAR (black dashed lines) and ©PLAXIS (red dashed line) section analysis.

4.2.3.2. Other measurements

The soil and diaphragm wall displacements were monitored by a system composed of extensometers, inclinometers and topographic targets located inside and outside of the enclosure. In the zone of interest, the subsidence in the excavation area was measured by four incremental extensometers, and the wall displacements were controlled by 10 inclinometers and 10 topographic targets. The total station was a TCRP 1202 R100 Leica model and measured both the soil subsidence inside the enclosure (using manual target-prism) and the topographic targets on the wall. The periodicity of the measurements ranged from days to months, depending on the progress of the construction project. During the experiment, measurements were expected to be taken at least three times: previous to, during (at the maximum pumping rate) and after the pumping test. Figure 25 shows the location of all of the extensometers, inclinometers and topographic dartboards at the experiment site.

4.2.3.3. Hydrogeological and hydromechanical numerical models

Numerical models are necessary to simulate and understand the mechanisms that control the structural movements: for the design of the pumping test (hydrogeological models) and for prediction of the soil and wall displacements (hydromechanical models).

The finite element code TRANSIN-IV (Medina et al., 2000; Medina and Carrera, 2003) is used with the visual interface of VISUAL TRANSIN (UPC, 2003) to build the hydrogeological model. A 3D model is constructed and divided into 17 layers. This distribution enables us to represent the station accurately in its real depth. Borehole and piezometer screens are located in their corresponding layers. A more detailed information about the model is presented in the section 3.3.2. Numerical model.

The finite element model, based on the ©PLAXIS commercial code, is used to establish the hydromechanical model. This model simplifies the shape of the excavation to a rectangle of 500-m length and 80-m width and cuts the rectangle into a series of 2D transverse sections, defined at distances of approximately 35 m, which require 35 sections to simulate the entire diaphragm wall (sections 6 to 23 are measured using the GB-SAR during the experiment). Every section contains the structural elements of the retaining structure (cast-in-place diaphragm walls and anchors). Additional configurations are set up in some sections when special features (geometric, structural, or geotechnical) required them. The Hardening Soil Model within the ©PLAXIS code is selected as a mechanical constitutive law, as was shown to be convenient for simulating the behavior of the Quaternary and Tertiary soils in Barcelona (Pujades et al., 2014b). Figure 22 shows a detailed soil and excavation profile of the hydro-mechanical numerical model corresponding to the transverse section A6 over the period of the experiment.

4.3. RESULTS AND DISCUSSION

The experiment was performed from January 28th to February 18th, 2014. The pumping test lasted three weeks: two weeks of pumping (from January 28th to February 10th, 2014) and another week to observe the drawdown recovery. Four pumps were activated during the first week (daily, from Monday to Thursday), and the rest

were activated during the second week (Figure 26). Water pressure data were collected manually (five times per day) and automatically (every 5 min) from 29 points; four dartboards were measured previous to, during, and after the experiment; over 33,000 coherent points were collected every 5 min by the GB-SAR radar. In this analysis, only the night GB-SAR data are used for two main reasons: (1) to reduce the effect of the traffic in the construction area and increase the number of coherent points and (2) to reduce atmospheric effects (such as changes in humidity or temperature) in the measured SAR data. Multiple interferograms were processed to check the consistency of the phase unwrapping.

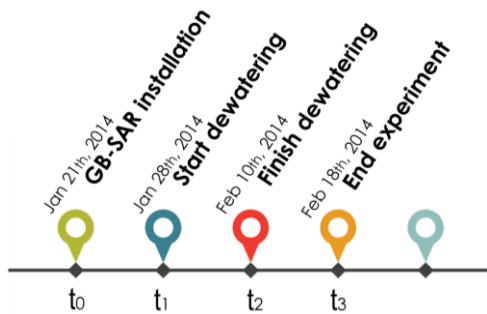


Figure 26. Summary of the experiment dates.

Two displacement maps (Figure 28) compare the original soil and wall positions at the maximum drawdown time step (Figure 28-2) and after the drawdown recovery (Figure 28-3). In Figure 28, the LOS displacements are color-coded. The black colored pixels represent pixels with no coherence. When the water pressure is reduced inside the enclosure during the pumping test, the water pressure out of the enclosure pushes the wall toward the interior of the enclosure (in this case, toward the radar) and produces a deformation of the wall (see Figure 28-2). When the dewatering ceases, the water pressure increases inside the enclosure, pushing the wall in front of the sensor and restoring the original wall position. The accumulated displacements are shown in Figure 28-3. An intermediate interferogram (from the maximum deformation up to the end of the experiment) is very similar to the map shown in Figure 28-2 but with opposite displacement values. In this figure, one may observe that the wall connection to the railway lines on its upward side results in a very rigid structure (the wall and the railway) that moves together. Eight sections (A1 to A8) were analyzed to determine the sensitivity of the wall to the drawdown: they undergo maximum horizontal displacements that range between 2.7 and 3.7 mm (see Figure 29). The negative values demonstrate that the wall was moving closer to the radar sensor (the LOS distance is decreasing). The displacement distribution along the wall was not constant (see Figure 29); this is logical because both anchors in the diaphragm walls and the drawdowns induced by the progressive pumping test were not constant either (see Figure 27 and Figure 29). The GB-SAR radar position was not high enough, and only a quasi-horizontal LOS was achieved (see the bottom parts of Figure 28-2 and Figure 28-3). The soil displacement results were discarded due to the weak radar sensitivity to vertical displacements and the lack of coherence inside the diaphragm walls.

A spatial-temporal correlation analysis between the measured GB-SAR displacements and hydrogeological parameters was conducted. Pumping rate evolutions, piezometric level time series and wall displacements were correlated in Figure 30. The graph shows a strong cause-and-effect relationship over time among all of the variables. The pumping and piezometric level recovery periods coincide with the displacement trends: the distance to the radar sensor was reduced when pumping, and the original distance was recovered after the pumping stopped.

Water levels of -4 m.a.s.l. (occasionally below that inside the pumping wells, due to head losses) were measured during the experiment. From a hydromechanical point of view, the soil responds with an elastic

behavior, with very little variation during the pre-pumping, post-pumping and recovery cycle (Figure 28 and Figure 30). However, due to a power outage, the GBSAR system stopped acquiring data during the drawdown recovery (represented as a dashed line in Figure 30); therefore, it was not possible to obtain the measurement of the exact wall response when the pumping ceased. This measurement was only possible at the end of the campaign (when we were able to make the last measurements). In principle, this last measurement could contain unwrapping errors, but they would be multiples of $2p$, i.e., multiples of $1.74/2$ cm in terms of displacements. We consider such displacements rather improbable.

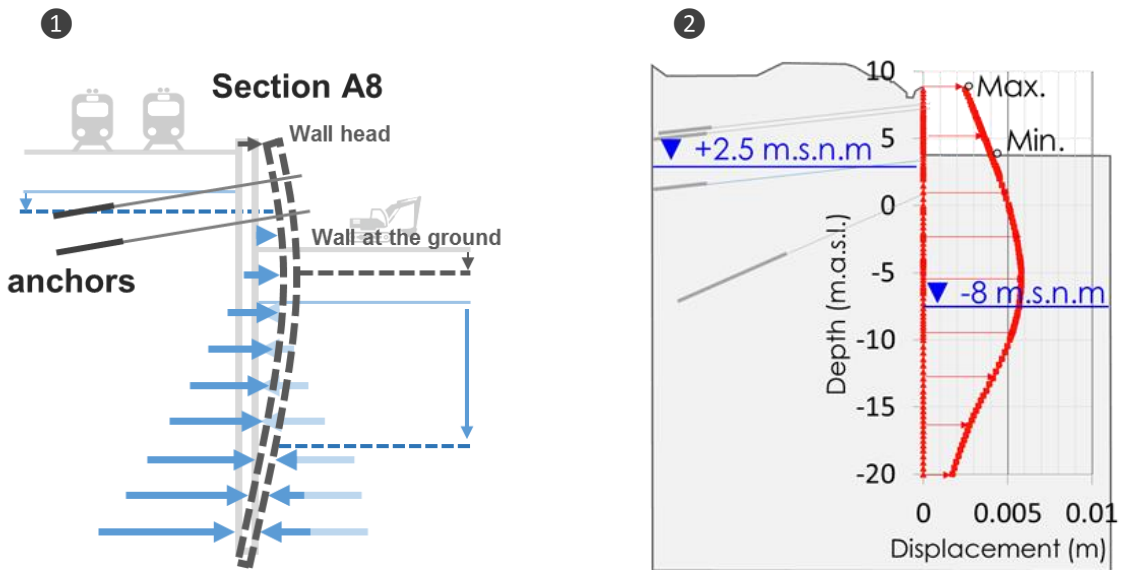


Figure 27. Hydromechanical model (©PLAXIS) results. Cross section: horizontal displacement induced by dewatering calculated in the model for section A6. (1) Scheme, (2) model results.

The northern side of the diaphragm wall was completely measured before, during, and after the experiment, and the rest of the wall was partially measured. Inclometers installed in the diaphragm wall were not read during the pumping test. Despite the few available data points and the small displacements (very close to the limit of detection), the GB-SAR measurements (right side edge) and the manual measurement of target MON4 (measurement with total station) obtained coincident values: MON4 measured 3.12 mm, and A8 measured 3.16 mm. The rest of the acquired manual data were used to validate the hydromechanical model.

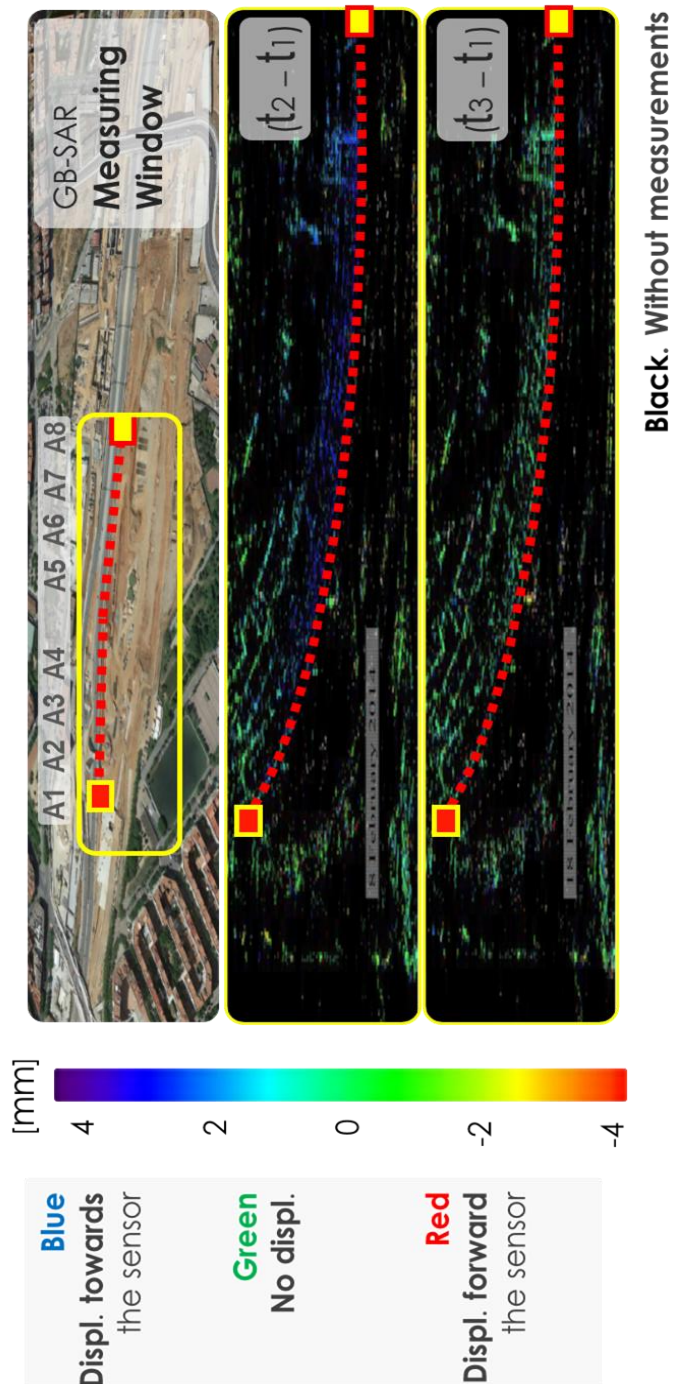


Figure 28. Radar output: displacements estimated by the GB-SAR. All pixels with discarded data due to the lack of coherence are shown in black. The red dashed line represents the measured diaphragm wall. Negative values represent movements towards the sensor.

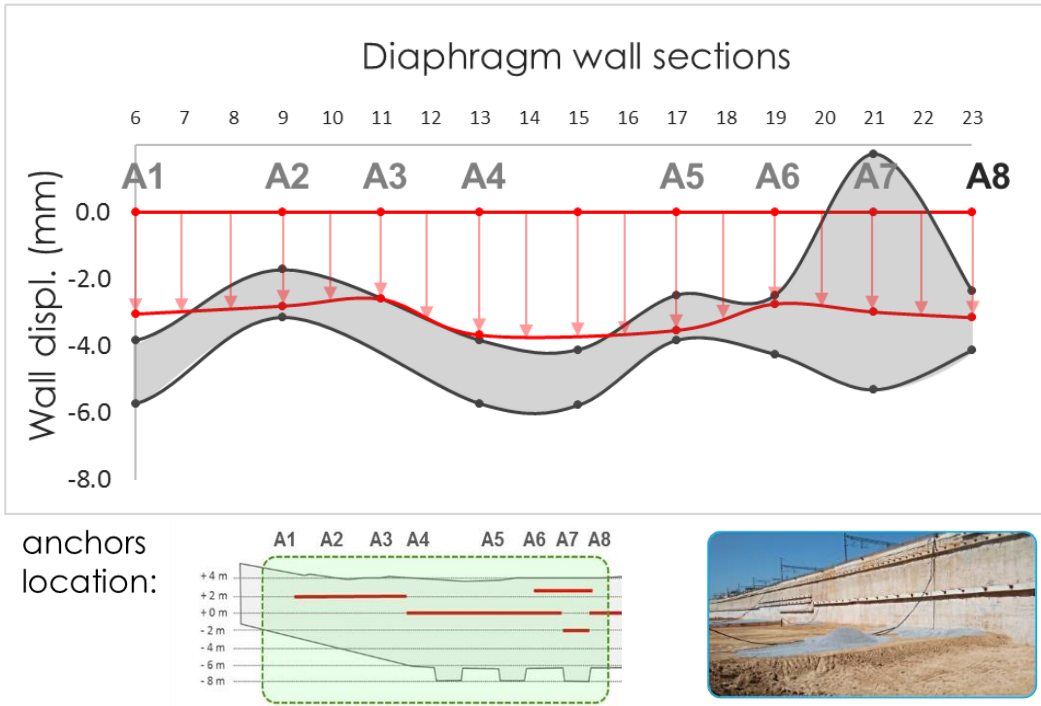


Figure 29. Plan view: computed (gray band) and measured (red arrows) horizontal displacements for the mountain side retaining wall in all sections considered. (3) Cross section: locations of the anchors.

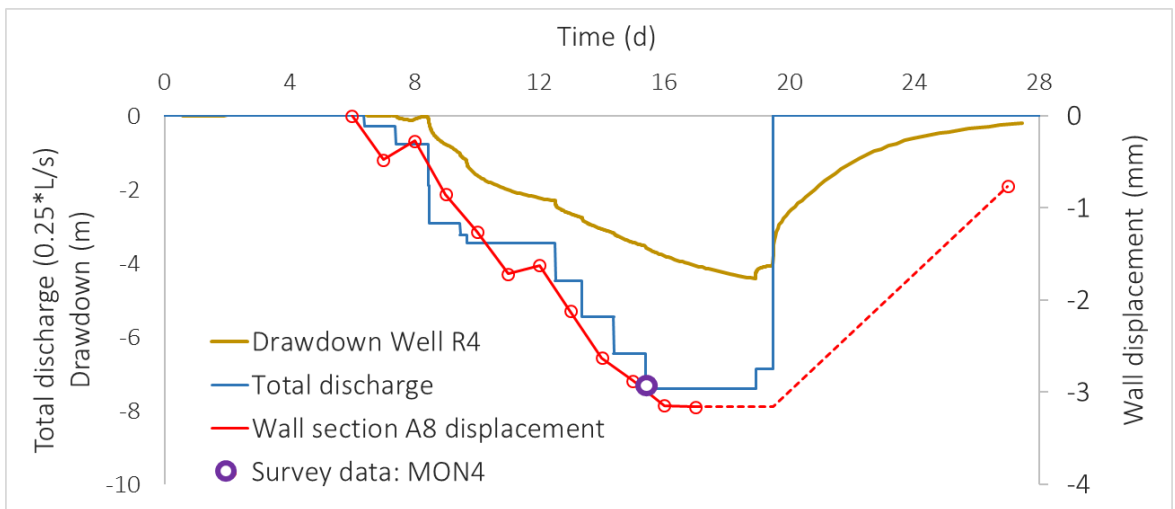


Figure 30. Multi-parameter correlation: pumping rates, drawdowns and GB-SAR wall horizontal displacements. The measurements are shown in circles. The dashed line represents a data gap. The rest of the cross-sections are included in the Appendix.

Finally, a hydromechanical model was used to check whether the displacement distribution was similar along the wall and of the same order of magnitude. Wall displacements induced by dewatering inside the excavation were calculated for different sections. The ground level was assumed to be at +3.00, which corresponds to the reported level at the time of the test. The ground water level inside the excavation varied, depending on the section and based on the levels measured during the pumping test. An example of a calculated horizontal displacement section is shown in Figure 27 (section A6). The use of anchors in the upper part of the wall decreases the head displacements, producing an arched deformation shape, locating the maximum movement at approximately 6 m.a.s.l. The shape of this arch varies in each section, depending on the distribution of the anchors and the foot wall depth.

The computed and measured horizontal displacements for the western retaining wall are shown in Figure 29. Horizontal displacements computed at the top of the wall and at ground level are presented in all sections. The results show that the measured displacements are in the range of 3 mm, which is in good agreement with the lower range of the computed values (approximately 4 mm). Considering that no particular adjustment of the model was made and that only groundwater levels were locally adjusted, the calculated results validate the measured displacements: the measured and predicted results appear to be in very good agreement, and only local discrepancies are observed. These discrepancies can be explained by changes in geometry and anchor distribution. In some sections, the complex vertical deformation shape obtained in the ©PLAXIS model (Figure 27) corresponds to a single point measured by means of GB-SAR, which makes the comparison difficult.

4.4. CONCLUSIONS

The experiment conducted in the La Sagrera railway station showed that GB-SAR can measure movements during the construction stage. GB-SAR has precisely quantified the horizontal wall displacements induced by dewatering. Manual data and numerical models have confirmed the measurements with a correlation analysis and by comparing measurements and deformation patterns, which produced similar results. Knowledge of the geology, hydrogeology, geotechnics and construction processes was found to be fundamental to design, perform and interpret the experiment. The results of this experiment are satisfactory. However, more detailed data obtained from the total station, extensometers and inclinometers would improve the reliability of the GB-SAR measurements.

From this study, the following conclusions were drawn. First, the sensor location represents a critical aspect because, in construction projects, the imaged scene can vary considerably over time, and GB-SAR can measure only those elements, buildings and structures that remain coherent over the observed period. Second, due to the high sensitivity to small displacements, the coverage of large areas, and the dense quantity of measurements over the observed scene, the GB-SAR can be helpful in understanding the mechanisms that control structure deformations and to identify vulnerable areas. For example, the La Sagrera case study showed different wall displacements, depending on the position of the anchors and a strong connection between the wall and the railroad tracks. Finally, the GB-SAR automation allows for obtaining high density temporal coverage. Depending on the expected deformation response, the radar data acquisition can be automatically realized every few minutes (as in the case of La Sagrera), hours, or days.

Chapter 5.

Levelling vs. Insar in an urban underground construction monitoring: pros and cons.

The case of La Sagrera railway station in Barcelona, Spain.

5.1. INTRODUCTION

Underground engineering plays a crucial role in the development of urban areas. New underground infrastructures are usually constructed below the water table to not interfere with the existing ones. Consequently, dewatering is generally required to facilitate the construction process (i.e. work in dry conditions) and it is necessary to assure safety conditions (i.e. avoid bottom instabilities such as bottom uplift or liquefaction) (Pujades et al., 2012a and 2016). However, dewatering reduces the piezometric head that may produce ground subsidence (i.e. pumping settlements) (Terzaghi, K., 1943; Bear and Corapcioglu, 1981a and 1981b). This subsidence is really feared (specially in urban areas) because they may damage nearby buildings

and structures (e.g. see His and Small, 1992, Gue and Tam, 2004, Forth, 2004, Roy and Robinson, 2009). Consequently, when pumping is mandatory, pumping settlements are predicted in advance to avoid unexpected events and if they are not acceptable, corrective measures (sometimes over-dimensioned) are adopted to minimize them (Vázquez-Suñé et al., 2004; Pujades et al., 2014a). However, predictions could not be accurate and therefore it is mandatory to monitor the groundwater levels and the ground deformation during the construction process to anticipate problems and verify the previous predictions (Lan et al., 2012; Culi et al., 2016).

Concerning the ground deformation, there are a wide range of techniques to measure it. The most accurate and spread used one is levelling, which can detect sub-millimetric deformations (Pelzer et al., 1984). This point-like surveying technique allows for tens of discrete in-situ measures per squared kilometer (Karila et al., 2013). Levelling is a relative measurement technique that need to be tied to a stable point whose elevation is known. The accuracy of the measurements depends on the levelling instruments and the surveying team (Pelzer et al., 1984; Kahmen and Faig, 1988). The periodicity of the measurements depends on each project, ranging from days to years.

Another emerging technique for mapping soil deformation is the Interferometric Synthetic Aperture Radar (InSAR). InSAR uses two or more Synthetic Aperture Radar images of the Earth's surface that are collected from orbiting satellites (Gabriel et al., 1989; Crosetto et al. 2016). The accuracy of this technique has been rapidly improved in the last few years, being now able to detect millimetric ground changes. InSAR has been already proved as an useful tool to measure subsidence in urban areas (Schmidt and Bürgmann 2003; Ferretti et al. 2004; Zerbini et al. 2007; Bell et al. 2008) and more specifically to measure changes in existing buildings and infrastructures (Herrera et al., 2009; Lan et al. 2012; Sousa and Bastos 2013; Crosetto et al. 2015; Wasowski et al. 2015, among many others). Recently, InSAR has been revealed as a powerful tool in the field of underground constructions, e.g. Liu et al. (2014b) have used InSAR to detect ground deformation during the drilling of a tunnel by a tunnel boring machine (TBM) in Düsseldorf (Germany) and Serrano-Juan et al, (2016) proved that Ground-based SAR interferometry can be useful to monitor construction works.

Levelling is currently the most common and precise technique to measure elevation changes (Karila et al., 2013). However, InSAR provides better spatial point density and more extensive spatial coverage, which is important to monitor the structures under construction but also the nearby area. In addition, InSAR is cheaper and a higher frequency of monitoring is possible. Some authors have compared and discussed both techniques in terms of cost, frequency and point density (i.e. Odijk et al., 2003; Zhou et al., 2003; Raucoules et al., 2007; Tomas et al., 2013) and have validated the InSAR as a proper tool to measure continuous subsidence phenomena. However, they have not compared both techniques in construction environments. This comparison is mandatory to ascertain the most suitable technique to measure the induced ground displacements by underground constructions and its effects on nearby structures. Disparity between both techniques is expected because they are based different principles. Levelling usually monitors relative deformation measurement of metal bolts attached to existing buildings and structures from the ground, while InSAR captures a different scene from space, including buildings, structures and streets. As a result, measurements are usually different because buildings, structures and ground may not behave alike as consequence of thermal effects, existence of deep foundations, etc.

This chapter **analyses, compares and discusses levelling and InSAR measurements when they are used to measure the soil deformation induced by the dewatering associated to underground constructions in urban areas**. This study was carried out in the largest underground infrastructure of Barcelona (Spain): La Sagrera railway station (Serrano-Juan et al., 2016). This underground infrastructure will combine high-speed trains, short- and medium-distance trains, four metro lines, and buses, becoming the city's major intermodal transit hub with more than 100 million passengers per year, (ADIF, 2015). The railway station construction began in 2010 and is planned to be completed by 2020.

5.2. MATERIALS AND METHODS

5.2.1. Geographical, geological and hydrogeological description

The metropolitan area of Barcelona is located on the Mediterranean coast, on the northeast coast of Spain (Figure 31). Geologically, this area is formed by a coastal plain (The Barcelona Coastal Plain) (Vázquez-Suñe et al., 2016) bounded by two Quaternary deltaic formations (corresponding to the Besòs - Velasco et al., 2012 - and Llobregat rivers - Gámez et al., 2009) and an elevated area, the Catalan Coastal Ranges (mainly Paleozoic rocks composed by granodiorite materials) (Sanz, 1988, Banda and Santanach, 1992, Roca and Guimerà, 1992, Solè et al., 2002). More concretely, the study site is located in the actual plain, which consists of Quaternary formations that overlie a substrate mainly consists of Pliocene series, mainly composed of marine blue marls, sandy marls, and Paleozoic granite. The whole study area is cut by many fractures that compartmentalize the pre Quaternary substrate generated during the Alpine orogeny as shown in Figure 31. As a result, all the Quaternary materials can reach 30 m thick. The Quaternary formation presents a very heterogeneous pattern and can be divided into the Lower Quaternary (Pleistocene) and the Upper Quaternary (Holocene). The Pleistocene is made up of several cycles constituted by alluvial sequences. The Holocene mainly consists of torrential, alluvial, and foothill deposits, where gravels and sands with a high proportion of clay matrix are present. More in detail, the construction area is crossed by a fracture (oriented NNW-SSE) that separates the two Pliocene series: Pliocene marls (south) and Pliocene sandy marls (north).

Hydrogeologically, the Quaternary and pre-Quaternary materials can be regarded as a layered aquifer with high vertical heterogeneity, with an effective transmissivity of 100-200 m²/d. (Pujades et al., 2015). The hydraulic conductivity (K) of the Quaternary clay layers (low permeability layers) ranges from 0.001 to 0.01 m/d, and the K of the Quaternary sand and gravel layers (high permeability layers) ranges from 0.1 to 10 m/d. As regards the Pliocene materials, the K of the fine materials (marls) ranges from 0.001 to 0.01 m/d, and the K of the sands ranges from 0.1 to 10 m/d. These values were derived from the numerous hydraulic tests performed in the city of Barcelona during recent underground constructions (Pujades et al., 2012b, Font-Capo et al., 2015; Serrano-Juan et al., 2016; Culí et al., 2016). Specifically, in the study site, the pumping tests undertaken before to start the constructions showed that the minimum hydraulic conductivity is 0.001 m/d and the maximum one is 700 m/d.

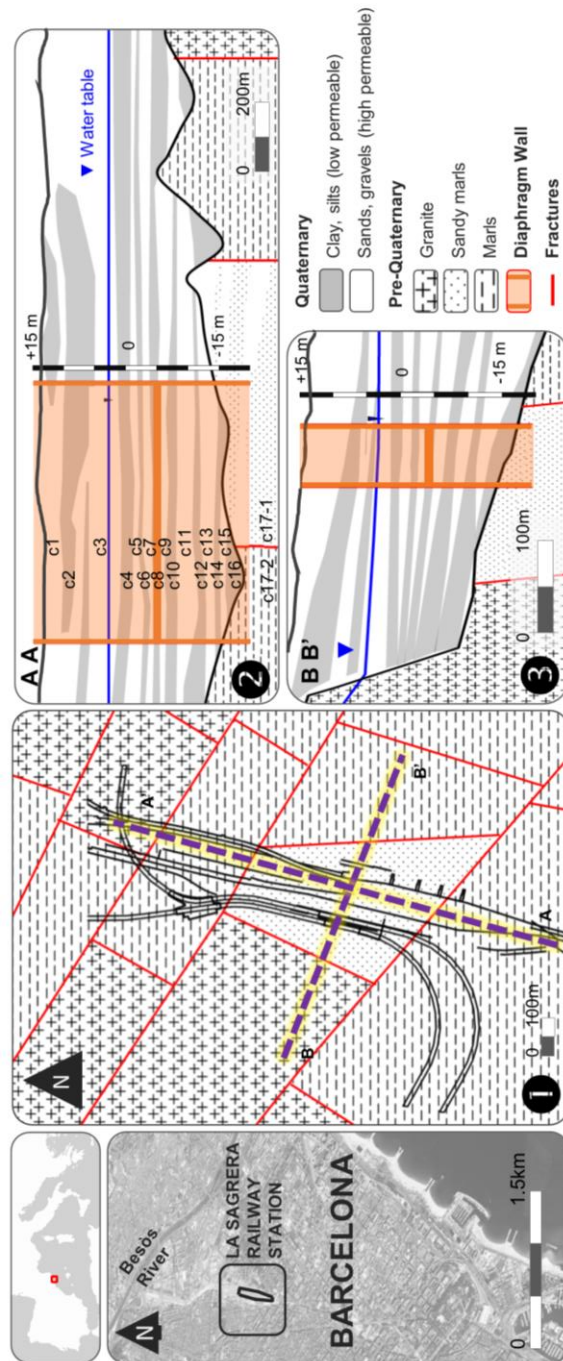


Figure 31. Geographical location of the study site and detailed geological profile of the site. (1) Plan view of the geological basement, (2) Cross section A-B, (3) Cross section C-D. Excavation area, limited by diaphragm walls, is shown in light brown color. Both cross sections show the maximum excavation and the required dewatering system.

5.2.2. Construction characteristics

The Sagrera station will cover an area of approximately 70.000 m² and a 20-m deep excavation is required to its construction (Serrano-Juan et al., 2016). The original soil height was between +14 and +16 m.a.s.l. (meters above sea level), the water table's natural position was between +2 and +4 m.a.s.l and the excavation bottom was at -8 m.a.s.l. (requiring a piezometric head drop of 12 m to excavate in dry and safe conditions). An excavation between diaphragm walls was designed to meet the structural requirements and to reduce the dewatering impacts outside (i.e. drawdown and subsidence). In this case, the diaphragm walls gradually bottom from -8 m.a.s.l to -20 m.a.s.l., where the maximum diaphragm wall depth is at the center of the station and the minimum ones at both ends. The upward sides of the northern diaphragm walls are anchored to support the railway lines (which have been deviated and are active during the construction). 26 pumping wells (whose bottom is located at -20 m.a.s.l.) were drilled to undertake the dewatering. Additionally, 20 piezometers were drilled inside and 28 outside of the excavation area to monitor the groundwater evolution during the dewatering stage. Piezometers were screened at different depths to know the piezometric evolution in the different geological layers.

A 3 weeks Watertightness Assessment Test (WTAT) (Pujades, et al., 2014a) was performed before the dewatering stage. The objectives of this test were to check the status of the dewatering system (wells were drilled and pumps were installed some months before the dewatering) and to assess the state of the diaphragm walls. WTATs allow identifying defects in enclosures to avoid unexpected groundwater inflows during excavation (Pujades et al., 2012a and 2016; Vilarrassa, et al., 2012). Pumps were started sequentially (from the southern to the northern edge) to generate eight hydraulic steps and extracted a maximum of 32 L/s when all eight pumps were operative. Results of the test showed that diaphragm walls were in good conditions and that the dewatering stage could be performed without problems. The dewatering stage started a short recovery period after the WTAT. The duration of this period was not enough to allow the complete recovery (until its initial position) of the piezometric head. The dewatering started with 15 pumping wells extracting 4.000 m³/d. Two weeks later stopped 2 pumping wells on the low permeable Pliocene and started 4 from the high permeable Pliocene.

5.2.3. Levelling

The construction board monitors 27 points with high precision geometric levelling out of the excavation area (Figure 33). All topographic targets are attached to facades of nearby buildings and are installed in every campaign. The characteristic of the targeted buildings vary noticeably: their number of floors ranged from a single floor to 10-floor buildings, and from buildings without underground to ones with 3 underground parking floors. Consequently, ground deformations could affect them differently.

A closure check is performed in each survey assuring a high accuracy. This can be performed either with a complete loop back to the starting point or else closing on a point whose elevation is known. The periodicity of the measurements during the construction ranged from few per month to some months, depending on the progress of the works.

5.2.4. InSAR

The InSAR deformation monitoring over la Sagrera area was based on very high resolution SAR images acquired by the TerraSAR-X sensor (Figure 34). This type of images has a pixel footprint of about 3 m². However, it is worth underlining that only a fraction of the pixels of these images can be exploited to derive deformation measurements. In urban areas, InSAR based on TerraSAR-X images can deliver several thousand measurement points per square kilometer. Given a location on the Earth, TerraSAR-X has a revisiting time of 11 days. However, in this study the average temporal frequency of the SAR images is one image every 26 days.

The InSAR deformation measurements discussed in this work were derived using 22 TerraSAR-X images that cover the period from March 2013 to October 2014. The InSAR processing was based on an advanced InSAR technique called PSIG (Persistent Scatterer Interferometry chain of the Geomatics Division of CTTC), which is described in Devanthéry et al. (2014).

5.2.5. Calculation of the pumping settlements (numerical model and analytical equations)

Pumping settlements were computed analytically and compared with those measure by levelling and InSAR. Settlements were calculated using the numerical drawdown computed from a hydrogeological numerical model. The numerical model was built with the finite element code TRANSIN-IV (Medina and Carrera, 1996, 2003; Medina et al., 2000), with the visual interface of VISUAL TRANSIN (UPC, 2003). The numerical model is made up by 17 layers in the study site that simulate 17 strata. The mesh has 6924 elements and 3495 nodes in each layer (Figure 32). Borehole and piezometer screens were located in their corresponding layers. The hydraulic parameters were automatically estimated (using inverse problem or back analysis) from data measured during previous pumping tests.

All boundaries of the numerical model were located far enough from the construction site to not affect the drawdown evolution during the dewatering simulation. Neumann and Cauchy boundaries (leakage coefficient of 10 d⁻¹) were used to simulate the Besòs river in the NE. No flow is considered on the west. A Dirichlet boundary was considered upgradient (ranging from +19 to +12 m.a.s.l.) and downgradient (+0.3 m.a.s.l. for the upper aquifer of Besos' delta and + 1.3 m.a.s.l. for the lower aquifer of Besos' delta). All boundary conditions were determined as a function of the natural groundwater flow prior to the construction. A more detailed information about the model is presented in the section 3.3.2.Numerical model.

Note that the representativeness of the predictions performed with this numerical model are supported by other studies and projects developed about the construction of La Sagrera Railway Station (Pujades et al., 2012b, Font-Capo et al., 2015; Serrano-Juan et al., 2016; Culí et al., 2016).

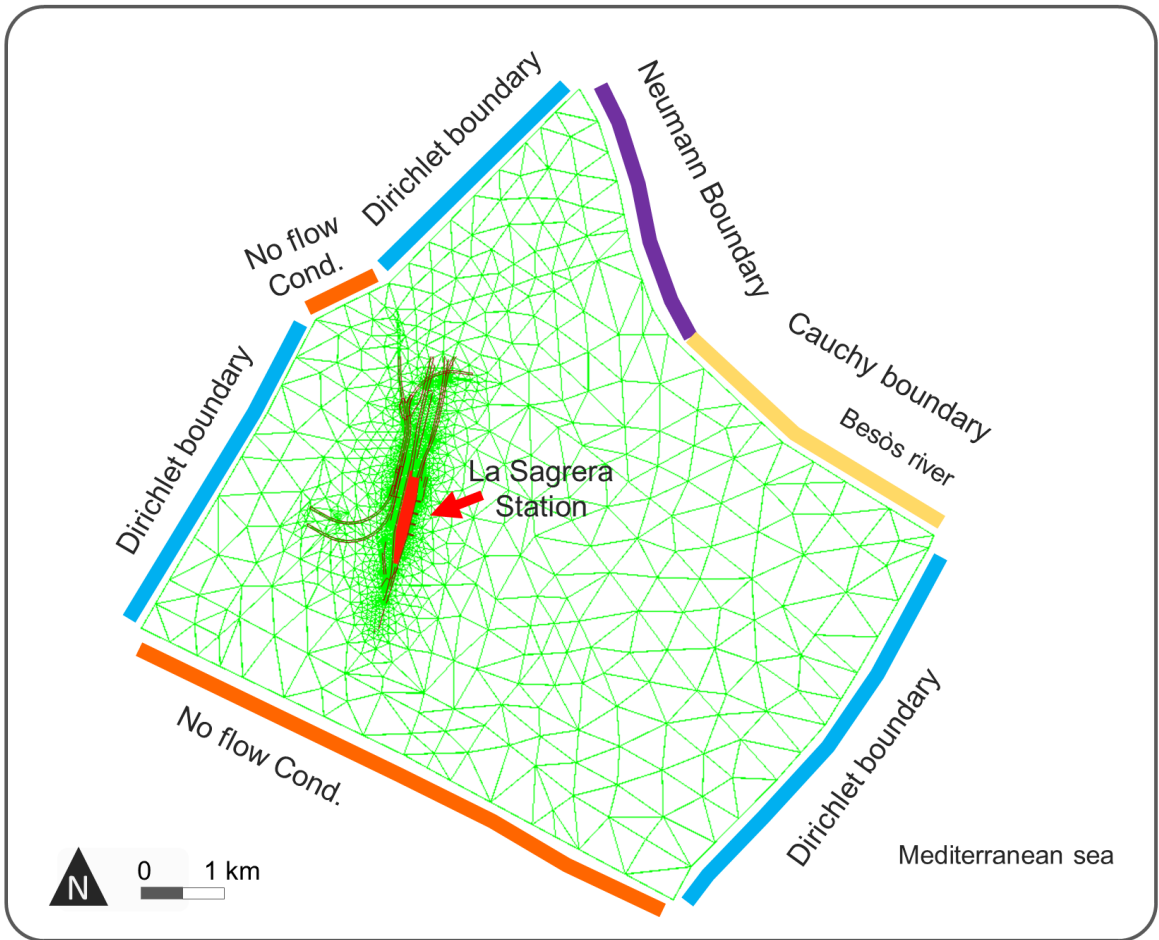


Figure 32. Numerical model mesh and boundary conditions.

Once drawdown was computed numerically, pumping settlements were calculated by applying the following equation (Cashman and Preene, 2001):

$$\rho_i = \gamma_w s_i D_i \alpha_i$$

Where ρ_i is the settlement of layer i , γ_w is the specific weight of the water, s_i is the drawdown at each layer i , which is expressed in meters of water column, D_i is the thickness of layer i and α_i is the soil compressibility. α_i was derived from the storage coefficient of each layer (s_i) taking into account that the soil is preconsolidated in the study site and behaves elastically (Vazquez-Suñe et al., 2004; Serrano-Juan et al., 2016). Applying the equation proposed by Jacob (1950) and cited by Ferris (1962) for elastic aquifers

$$S_i = \gamma_w \theta_i D_i \left(\beta + \frac{\alpha_i}{\theta_i} \right)$$

Where θ is the porosity and β is the water compressibility. It is possible to consider that $S_s = \alpha$, assuming that β is very small compared to α , where S_s is the specific storage coefficient, which can be obtained from the interpretation of pumping tests. Settlements were computed considering the S_s of each layer obtained from the numerical interpretation of pumping tests performed before starting the construction. Although this methodology assumes exclusively vertical movements, which is not always the case, it allows us to approximate the displacements with an acceptable error (Pujades et al., 2014a and 2014b). Settlements were calculated when the computed steady state was practically reached (214 days of simulation/dewatering).

5.3. RESULTS and DISCUSSION

5.3.1. Levelling

The first levelling survey was performed on 5 March 2014, one day before starting the dewatering stage. Since then, 54 surveys were performed. Figure 33 shows soil displacements evolution at several levelling points. Measurements can be classified in 3 categories depending on the soil response: (1) final pumping settlements lower than 1 mm (green), (2) final pumping settlements between 2 and 4 mm (red), and (3) pumping settlements between 1 and 2 mm during early times in which an uplifts is observed on the later times (yellow). It is important to mention that the accuracy of the geometric levelling in a construction environment is 1 mm.

The green area (Figure 33) is mainly covered by buildings with more than 7 floors plus 2 underground parking floors. The underground floors act as deep foundation sustaining the building motionless when small soil deformation occurs. As a results, it was not possible to measure the actual ground settlements produced by the dewatering because the topographic targets were installed in the building's facades. However, the trend of the measured pumping settlements reflects the dewatering evolution, but the absolute magnitude of the measured displacements was lower than the actual one. Levelling in the green area measured the building's affection due to the dewatering.

The red area (Figure 33) corresponds to pedestrian streets and low buildings (some of them with just 1 floor) and without underground floor parking. In this case, the building's response to the dewatering was similar than that of the ground and thus, measured settlements were bigger than the observed in the green area (higher buildings). In addition, the diaphragm walls of the excavation are shallower in this area. Consequently, outside dewatering impacts were higher.

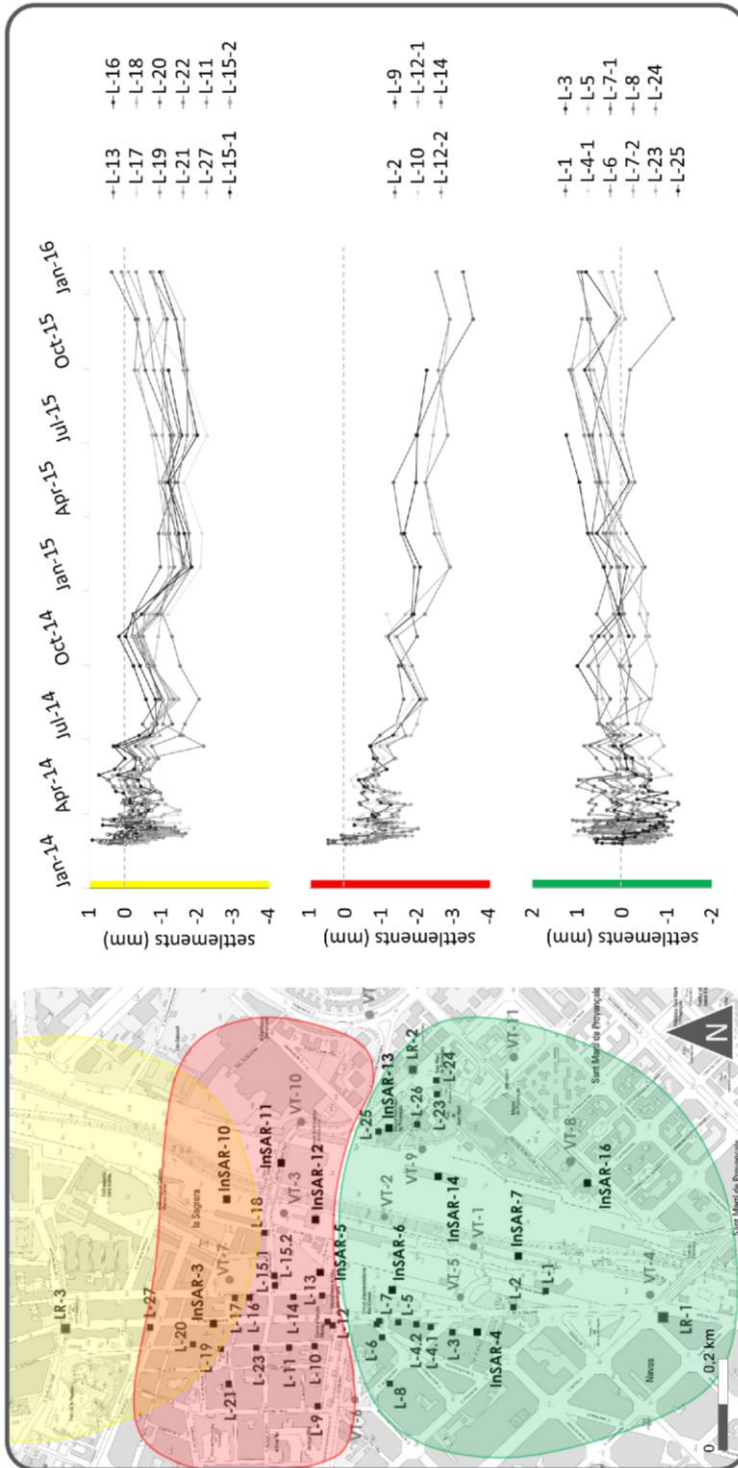


Figure 33. Monitored points by levelling. Levelling time series grouped by location.

The pumping settlements evolution observed in the yellow area (Figure 33) is similar to the measured in the red one during the early times. However, in the yellow one, settlements decreased during latter times. This behavior can be explained by the proximity to the yellow area of a large shaft associated to the Metro's line 4 of Barcelona that is named "Macro Pou" and that requires a constant pumping to avoid seepage problems. During the monitoring period the flow rate of the pumping associated to the "Macro Pou" was reduced, resulting in a general piezometric head recovering. Consequently, given the elastic properties of the soil in the study site, a soil uplift occurs in the surrounding area affecting the yellow area. The uplift can be observed in the soil movement evolution during the latter times.

In terms of absolute values, maximum settlements of 3.5 and 2.3 mm were measured on the red and yellow areas, respectively. These values were calculated from a reference point whose high should be stable. However, reference points used in the levelling monitoring were clearly inside of the influence area of the dewatering (Figure 33). Thus, all measurements could have been minored with an unknown constant which may range from 1 to 3 mm.

Measured soil response to pumping was instantaneous. However, a small and transitory uplift can be observed during the early dewatering times. This behavior could be related with horizontal displacements produced by pumping. Drawdown during early times is higher in the layers located below the bottom of the diaphragm walls because those located above need more time to be drained. Consequently, horizontal pumping displacements (contraction towards the pumping wells) will be higher in the layers located below the bottom of the diaphragm walls. This contraction of the lower layers squeeze the upper ones, which caused the water pressure to increase inside them and their vertical expansion because of the Poisson effect. This effect that can be related to the Noordbergum effect (Kim and Parizek, 1997), which disappears when the upper layers are drained vertically.

5.3.2. InSAR

22 acquisitions were taken between 27 March 2013 and 20 October 2014. An image taken previously to start the dewatering (69 days before) was used to determine the reference position of the soil and to compute the soil displacements from the subsequent acquisitions. InSAR measured several thousand points, both from the ground and from buildings and structure, providing a dense 2D representation of the soil deformation, see Figure 34.

InSAR measurements can be shown as velocities or as time series (Figure 34). In both cases, all measurements were coherent with the dewatering: the closer the measurement to the construction site, the higher the settlement. Maximum settlements were between 6 and 8 mm, while minimum ones were under 3 mm, with exception of almost no soil displacements in measurements of very deep foundation structures (e.g. the point 14 that measures the diaphragm wall vertical displacement).

There is a strong relationship between the soil behavior and the water table evolution. Like in the levelling measurements, a transitory heave of approximately 1 mm was measured by the InSAR during the early times of the dewatering. Note that, trend changes in time series may not agree with the exact time when the events occur because InSAR acquisitions were every few weeks. As a result, some events occurred earlier or later to

the acquisition time. In this sense, time series must be treated carefully. For instance, the first and last InSAR acquisition during the WTAT was on 9 February 2014, and the next acquisition (on 25 March 2014) measured the settlements occurred after the first two weeks of dewatering. Consequently, the expected soil uplift during the recovery period between the WTAT and the start of the dewatering stage could not be observed. In the same manner, there is not an InSAR acquisition at the exact time when the pumping test started (28 January 2014), when it reached its maximum drawdown (18 February 2014), or when the dewatering started (6 March 2014). In our case study, it was not possible to increase the frequency of the acquisitions during the dewatering (TerraSAR-X satellite). However, there are new satellites like Sentinel 1A and 1B that will be soon able to acquire images every 6 days, increasing the time resolution.

5.3.1. Levelling vs. InSAR

Even if levelling is more precise than InSAR in ideal conditions, in construction environments their precision are similar. While the levelling accuracy depends on the used instrument, the target device and the human factor, the InSAR accuracy depends on the data processing, which aims to separate the deformation from the phase noise, the atmospheric effects and the so-called residual topographic errors (Crosetto et al., 2016). In this study, both levelling and InSAR measured the same ground displacement events, which correlated with the hydrogeological events. Both techniques measured an instantaneous response of the soil to the dewatering and a transitory uplift during early pumping times.

Contrariwise, the maximum pumping settlements measured with InSAR were higher than those observed by levelling. On the one hand, the difference could be related with the fact that both methods do not measure the same targets. While levelling measured data from discrete targets on building's facades, which may be altered by the building characteristics, InSAR acquired a full 2D displacement field, which includes points located on the ground, on buildings or structures. On the other hand, the lower pumping settlements measured by levelling could be also explained by the position of the reference point, which was clearly inside of the influence area of the dewatering.

Analytical settlements were computed at different points around the construction site (Figure 35) to be compared with the measured displacements and to evaluate the method (levelling or InSAR) that measured the more representative pumping settlements. Analytical settlements were computed when the steady state was practically reached. Therefore, they are compared with the measured soil displacements after 214 days from the start of dewatering stage. Maximum analytical pumping settlements range between 5 and 8 mm. Thus, they are more similar to the soil displacements measured with the InSAR technique when the monitored points are coincident with deep foundation structures. This results confirm that levelling measurements were affected (1) by buildings characteristics (underground floors) because the analytical calculations do not consider them, and (2) by the position of the reference point, which was influenced during the pumping.

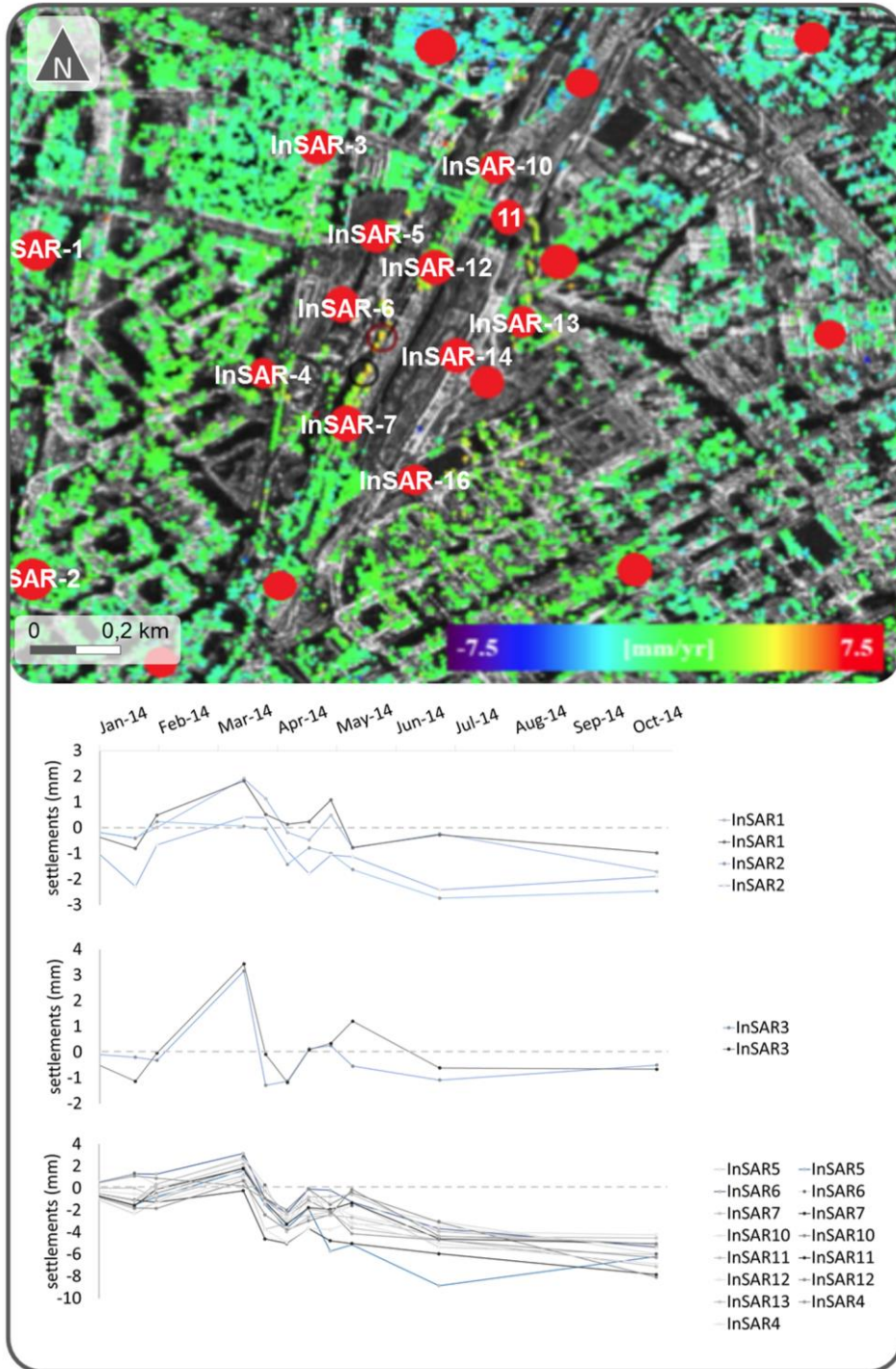


Figure 34. InSAR displacement velocity map (above). InSAR displacement time series grouped by location (below).

5.4. CONCLUSIONS

Monitoring the soil displacements produced by dewatering underground constructions is essential to anticipate problems and verify the predictions. Levelling is the most common technique used in construction environments to measure soil displacements. However, InSAR is acquiring importance during the last years because it allows obtaining the displacements distribution in 2-D instead of the punctual measures obtained by levelling. Both techniques were used to monitor the soil behavior during the dewatering undertaken to construct La Sagrera railway station in Barcelona. This study compares the measurements taken by levelling and InSAR to ascertain the main advantages and limitations of both techniques. The main conclusions are summarized below:

- Both levelling and InSAR measurements have a coherent settlement evolution. All measurements can be explained and related with the hydrogeological events.
- Levelling and InSAR measurements differ on the absolute settlement values. Measured settlements by InSAR are higher than those observed by levelling. Analytical settlements agree with the InSAR measurements suggesting that levelling displacements are lower than the real ones. This fact is produced because:
 - The levelling discrete targets are installed on building's facades and most of these buildings have deep foundations (at least 1 or 2 underground parking floors), which mitigates the pumping settlements. Conversely, InSAR acquires a full 2D displacement field, including points located on the ground, on buildings or structures.
 - Levelling calculated the soil deformation using reference points that was located inside the dewatering influence area. Thus, absolute values may be lower than the real ones.
- Although InSAR measurements are more appropriate to measure (quantify) the soil deformation, levelling is extremely useful to achieve one of the main objectives of the constructions monitoring, which is to know the impact caused by the pumping on the nearby buildings.
- The monitoring frequency is a limitation of the InSAR technique.
- Both techniques measured a heave of the soil during the early times of the pumping. The nature of this behavior is the same that the Noordbergum effect. Layers not drained horizontally (upper ones) expand vertically because of the Poisson effect when they are squeezed by the horizontal contraction occur in the layers drained horizontally (lower ones).

Chapter 6.

General Conclusions

This thesis aims to demonstrate how the construction cycle deals with the various impacts produced by the interaction of underground constructions with groundwater at each stage of the process, with a view to providing improved processes. To do so, this thesis has contributed to data storing and data analysis software which implies new and significant developments to increase the quality of the hydrogeological analysis; it has provided new approaches to address the groundwater corrective measures definition during the design stage; and it has developed and applied new methods of infrastructure monitoring using ground-based and satellite SAR sensors during the construction stage.

Chapter 2 presents a new approach to reuse, customize and extend current hydrogeological software, and illustrates the insights of the process by applying it in four case studies. This approach allows the creation of new graphical user interfaces (GUIs) to automatically generate input, execute the calculus, and show, rearrange and plot the most important parts of the output from spreadsheet-based and non-spreadsheet-based software.

This approach achieves the objectives, providing the necessary steps to easily develop any hydrogeological software. The fact that the methodology is simplified in a decision flow chart, helps the program developer to assess every type of program. However, although this approach has been created for reusing hydrogeological

software by hydrogeologists, it can also be applied to other fields, creating synergies among scientists and expert program developers. The MIX case study has been largely discussed to allow the reader to easily follow a step-by-step process application of the approach presented. This approach has been used in education and research, as well as being applied worldwide in numerous technical projects. Moreover, four new software have been registered by the Spanish National Research Council (CSIC)

Chapter 3 presents an innovative groundwater by-pass design that enables the groundwater to flow through the structure and provides a homogenous distribution of the water pressure under the bottom slab. This chapter showed the necessity of integrating designs to create more efficient solutions, to avoid going over-budget and to increase safety prior to, during, and after construction. The example of the La Sagrera railway station shows the pros and cons of implementing independent and integrated design solutions to avoid the groundwater barrier effect and to limit and distribute the water pressure below the bottom slab. The integrated solutions solve the barrier effect produced by the structure and optimize the bottom slab, reducing the costs considerably and increasing safety during the construction phase.

Chapter 4 shows the experiment conducted in the La Sagrera railway station which showed that GB-SAR can measure movements during the construction stage. GB-SAR has precisely quantified the horizontal wall displacements induced by dewatering. Manual data and numerical models confirmed the measurements with a correlation analysis and by comparing measurements and deformation patterns, which produced similar results. Knowledge of the geology, hydrogeology, geotechnics and construction processes was found to be fundamental for design, performance and interpretation of the experiment. The results of this experiment were satisfactory. However, more detailed data obtained from the total station, extensometers and inclinometers would improve the reliability of the GB-SAR measurements. Moreover, the addition of an alert system to the GB-SAR sensor would ensure the continuous acquisition of the data.

Chapter 5 compares the measurements taken by levelling and InSAR techniques when monitoring the soil behavior during the dewatering undertaken to construct La Sagrera railway station in Barcelona to ascertain the main advantages and limitations of both techniques. Both levelling and InSAR measurements could be explained and related to the hydrogeological events. However, levelling and InSAR measurements differed on the absolute settlement values. Levelling monitored relative deformation of metal bolts attached to existing buildings and structures from the ground, while InSAR captured a different scene from space, including buildings, structures and streets. Analytical settlements agree with the InSAR measurements suggesting that levelling displacements are lower than the real ones. Although InSAR measurements were more appropriate to measure the soil deformation, levelling is extremely useful to achieve one of the main objectives of construction monitoring, which is to know the impact caused by pumping on nearby buildings.

Specific pros and cons of both ground-based and satellite SAR sensors were discussed in their respective chapters.

APPENDIX

6.1. Supplementary material Chapter 2

This appendix provides a compilation of the most basic code sentences that allows any program developer to create and design any similar software comparable to that presented above. Every title contains different code examples for performing the title action. Figure 36 locates each action in the decision flow diagram steps.

'Select a Cell A1
 Range("A1").Select
 Cells(1, 1).Select
 Range("B2").Offset(-1, -1).Select

'Select a range A1:C1
 Range("A1:C1").Select
 Range("A1", "C1").Select

Range(Cells(1, 1), Cells(1, 3)).Select
 Range("A1").Resize(1, 3).Select

'Concatenate words and variables
 Variable = "C"
 Range("A1:" & Variable & "1").select
 'Select final value in a row or column
 FinalRow = Cells(Rows.Count, 1).End(xlUp).Select


```

FinalColumn = Cells(1,
Columns.Count).End(xlToLeft) .Select

'Avoid repetition
Cells(1, 1).Select
Selection.Value = "Test"

'Use straightforward
Cells(1, 1).Value = "Test"

'Error management
On Error Resume Next
On Error GoTo 0
On Error GoTo Label1
Label1:

'Hide many Rows and Columns at once
Range("A2:AA2").SpecialCells(xlCellTypeFormulas,
xlTextValues)
.EntireColumn.Hidden = True
Range("B1:B50").SpecialCells(xlCellTypeFormulas,
xlTextValues)
.EntireRow.Hidden = True

'Open
Workbooks.Open
Filename:=Application.GetOpenFilename(, "Title")
Workbooks.Open ("C:\ OutputFile.out")

'Save as
New_file_name =
Application.GetSaveAsFilename("C:\ ")
ActiveWorkbook.SaveAs Filename:=fname,
FileFormat:=xlNormal

'Another way of saving is printing line by line
Open thisfile For Output As #1
For j = 1 To FinalRow
    Print #1, Cells(j, 1).Value
Next j
Close

'Execute external software
Variable = Shell("C:\Launch MIX\MIX_2.exe ",
vbMaximizedFocus)
Call Shell("C:\ Program.exe C:\InputFile.txt", 1)

'Find
Cells.Find(What:="Word To Find", After:=ActiveCell,
LookIn:=xlFormulas, _
    LookAt:=xlPart, SearchOrder:=xlByRows,
SearchDirection:=xlNext

'Working with charts
'Add charts
Charts.Add
'Add data to the chart
ActiveChart.SetSourceData = Range("A1:A5")
'Define the chart type
ActiveChart.ChartType = xlColumnClustered
'Very important, store its name somewhere to
future references to the chart
ActiveChart.Location Where:=xlLocationAsObject,
Name:="Sheet1"

'Fasten the code
Application.ScreenUpdating = False
Application.Calculation = xlCalculationManual
Application.EnableEvents = False
ActiveSheet.DisplayPageBreaks = False
'...Code...
Application.ScreenUpdating = True
Application.Calculation = xlCalculationAutomatic
Application.EnableEvents = True
ActiveSheet.DisplayPageBreaks = True

'Declare Public Variables to use its values in
different macros
Public Variable As Variant

'Use StrSafe when declaring Functions to adapt
them from 32 to 64-bits
#If VBA7 Then
    Declare PtrSafe Function ...
#Else
    Declare Function ...
#End If

```

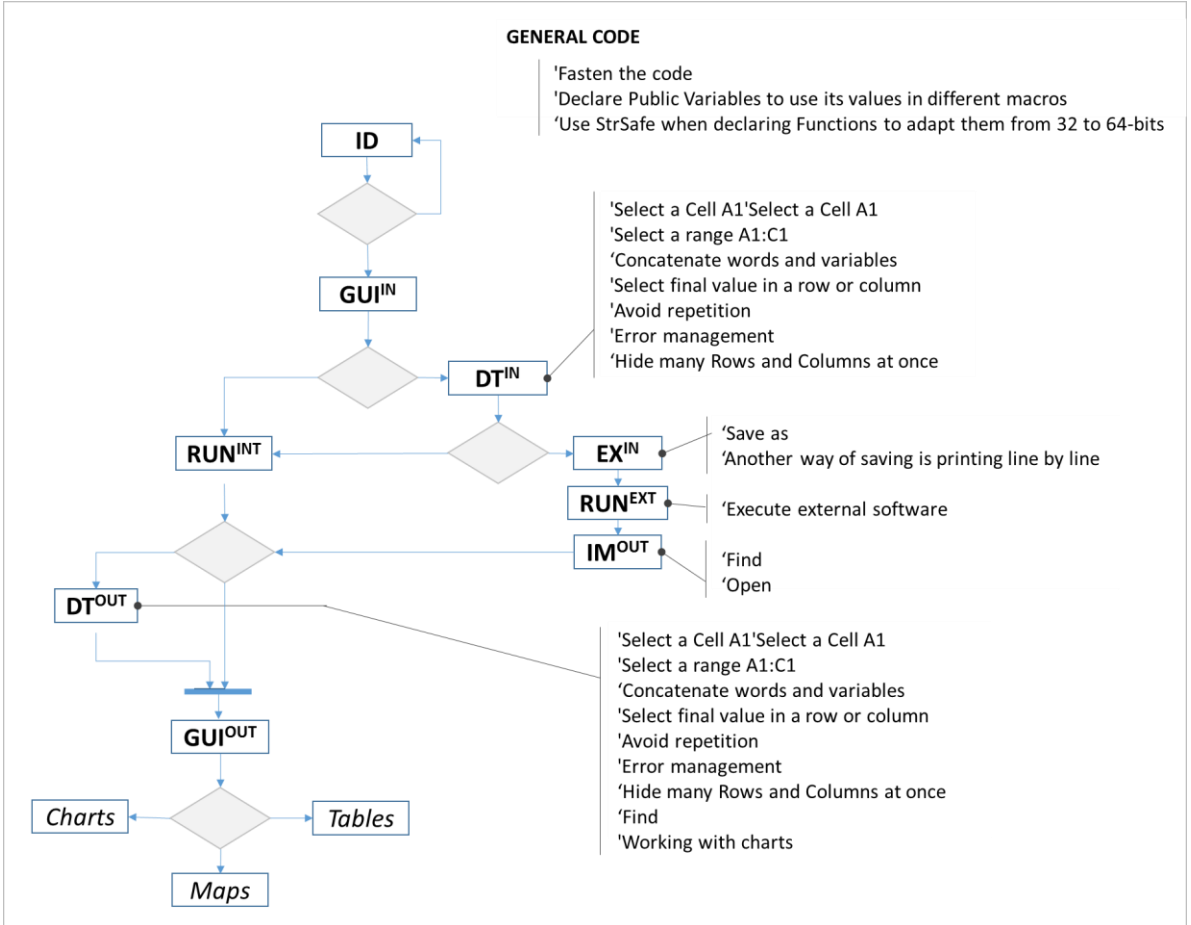


Figure 36. Decision Flow Diagram with some code comments related to the appendix.

6.2. Supplementary material Chapter 3

Two pumping tests (T1 and T2) were performed in the study site before to start the construction. T1 was performed in the South side of the study site while T2 was undertaken on the North side. One pumping well and four piezometers were drilled for each test (Figure 37). The pumping wells penetrated down to the base of the aquifer and were totally screened. The piezometers were screened at different depths to know the groundwater response at different layers. Tests taken 3 days (2 of pumping and 1 of recovering) and the average pumping rates were 1000 and 400 m³/d for T1 and T2, respectively.

The hydraulic parameters of the aquifer layers in the study site (Table 3) were automatically computed using the finite element code TRANSIN-IV (Medina and Carrera, 1996, 2003; Medina et al., 2000) by inverse problem (or back analysis). Fitting curves of the piezometers during the tests are shown on Figure 38. Additionally, the computed piezometric head in steady state (before to start the construction) was compared with that measured at 16 piezometers drilled around the study site. Differences between them were acceptable given the dimensions of the modelled area. Figure 38 also shows measured vs. computed piezometric heads. It is possible to observe that all points are highly correlated.

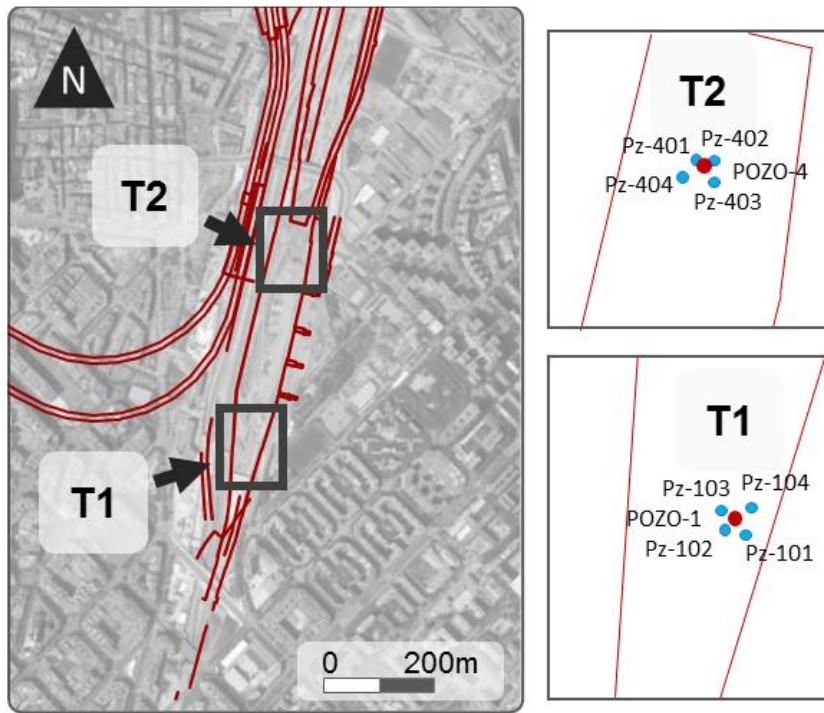


Figure 37. Pumping test wells and piezometers location.

Layer	Storage Coef.	Trans.(m ² /d)
c1	6.3E-05	5E-01
c2	1.1E-04	7E-02
c3	6.3E-05	2E+01
c4	1.1E-04	1E-01
c5	6.3E-05	2E+01
c6	1.1E-04	9E-02
c7	6.3E-05	6E-01
c8	1.1E-04	9E-02
c9	6.3E-05	2E+01
c10	1.1E-04	1E-02
c11	6.3E-05	3E+01
c12	1.1E-04	1E-02
c13	6.3E-05	1E+01
c14	1.1E-04	3E+00
c15	7.7E-05	2E+01
c16	1.1E-04	1E-02
c17-1	7.0E-05	7E+02
c17-2	1.0E-04	5E+00

Table 3. Hydraulic parameters of the aquifer layers in the study site.

Appendix

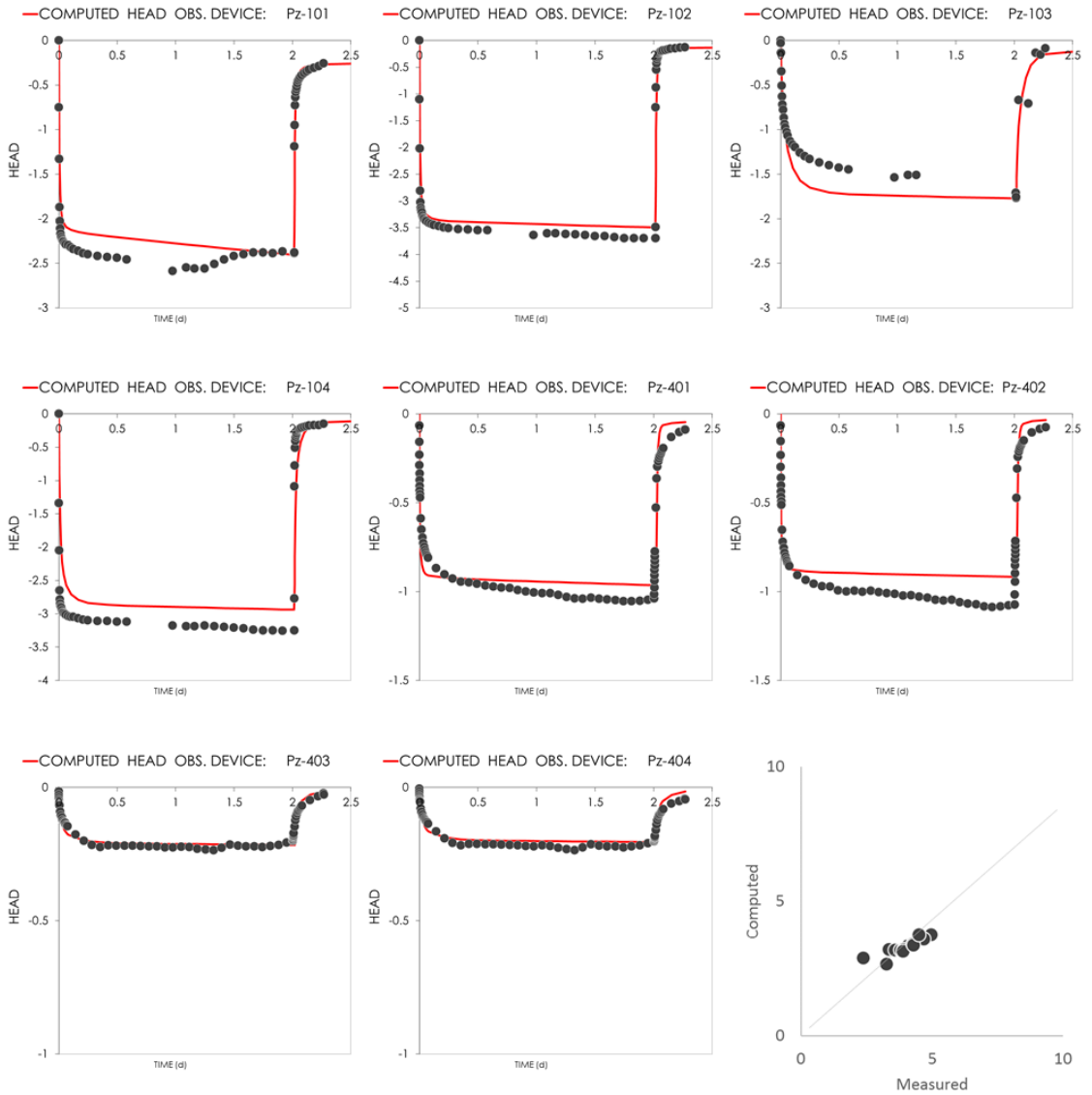


Figure 38. Fitting curves of the numerical model during the pumping test.

6.3. Supplementary material Chapter 4

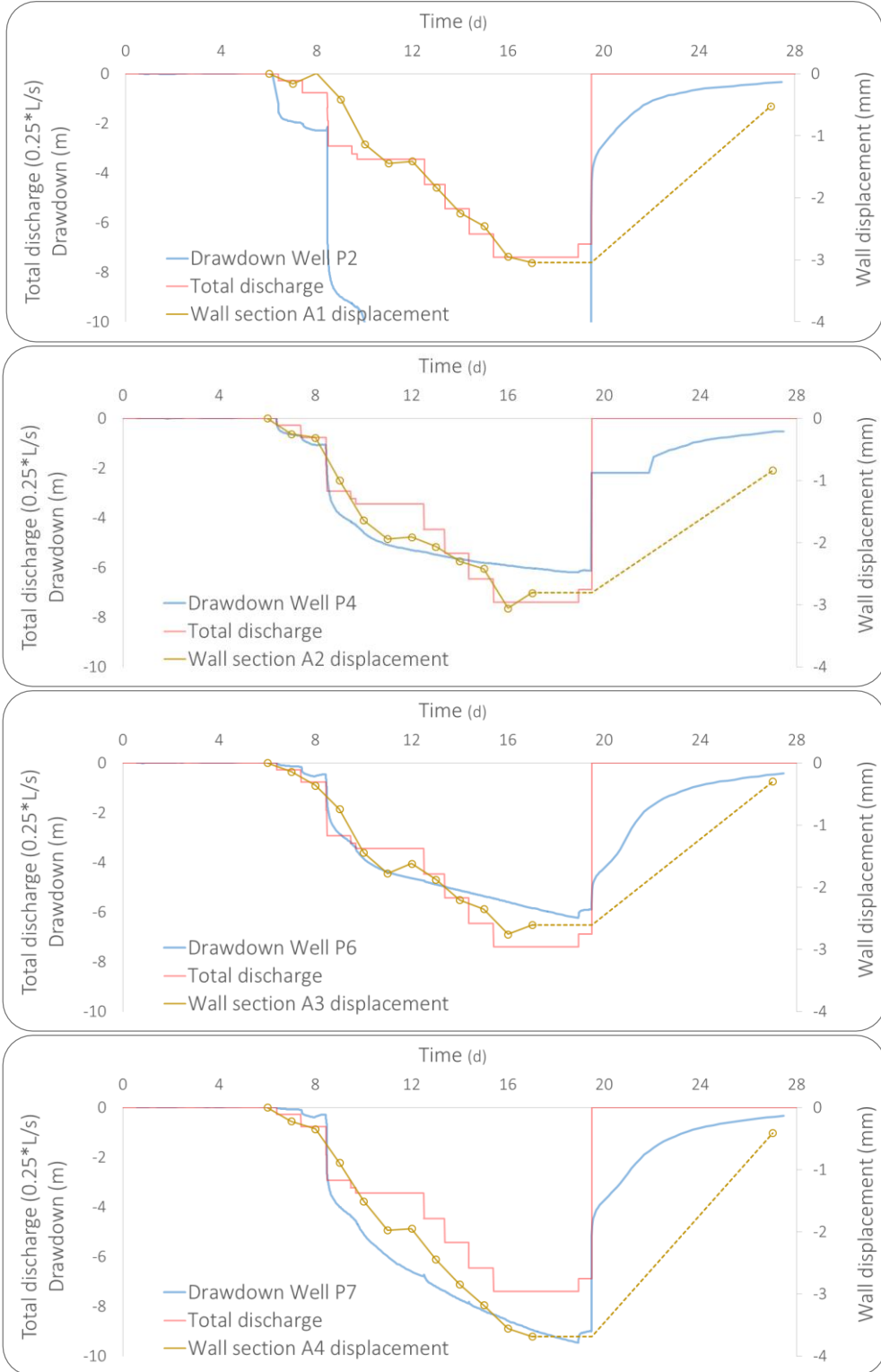


Figure 39. GB-SAR, traditional monitoring data and hydromechanical model results for all cross-sections.

Appendix

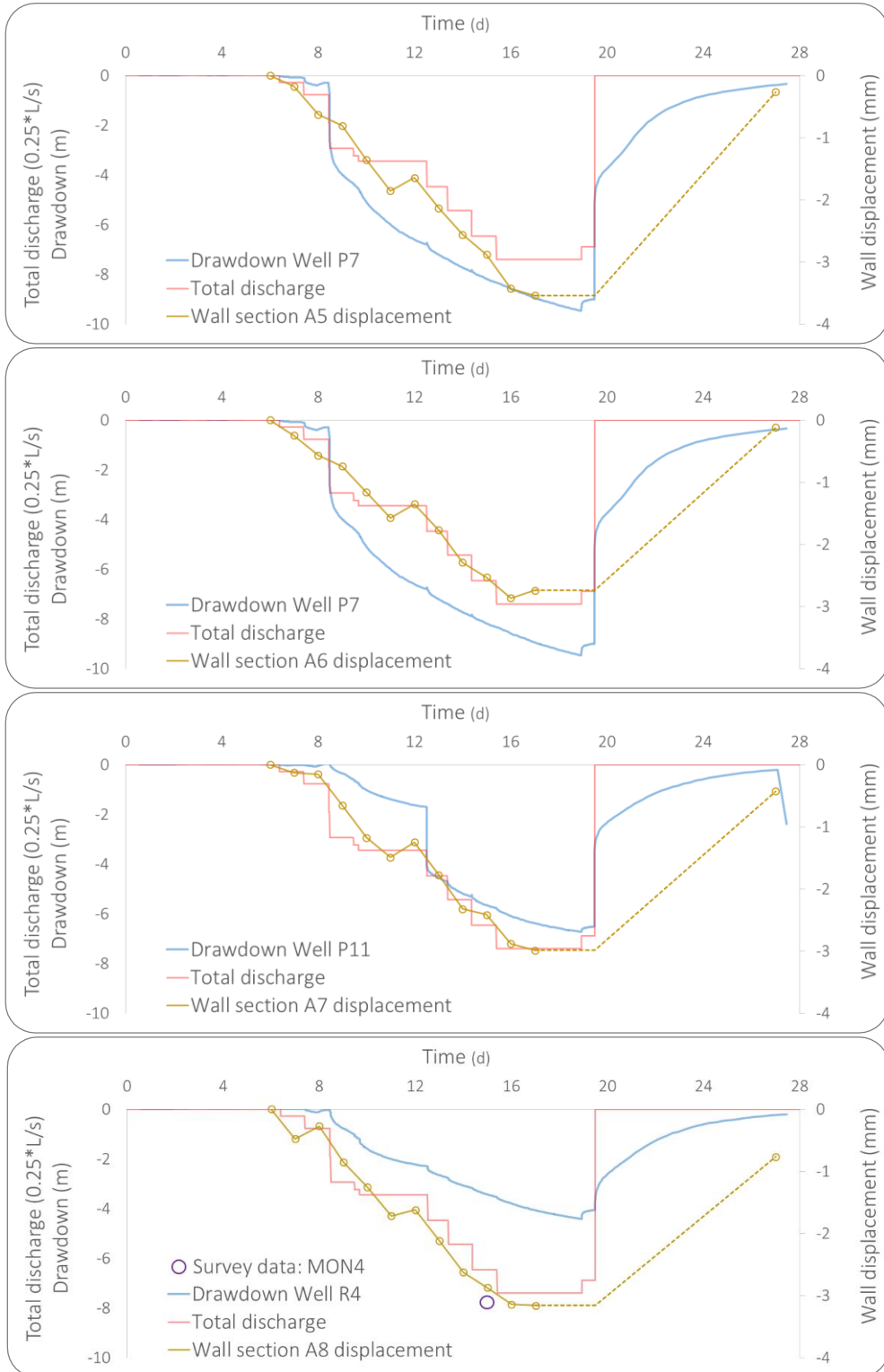


Figure 40. GB-SAR, traditional monitoring data and hydromechanical model results for all cross-sections.

References

References

- Aaron Marcus (1995). "Principles of effective visual communication for graphical user interface design". Human-computer interaction: toward the year 2000. San Francisco: Morgan Kaufmann Publishers Inc.. pp. 425–441. ISBN 1-55860-246-1.
- Administrador de Infraestructuras Ferroviarias (ADIF), 2015. Barcelona Sagrera Alta Velocitat. 2015.
- Agarwal, B. N. P., & Srivastava, S. (2008). FORTRAN codes to implement enhanced local wave number technique to determine the depth and location and shape of the causative source using magnetic anomaly. *Computers & Geosciences*, 34(12), 1843–1849. doi:10.1016/j.cageo.2007.10.012
- Agarwal, B. N. P., & Srivastava, S. (2010). A FORTRAN program to implement the method of finite elements to compute regional and residual anomalies from gravity data. *Computers & Geosciences*, 36(7), 848–852. doi:10.1016/j.cageo.2009.11.002
- Akagi, H., 2004. Geotechnical Aspects of Current Underground Construction in Japan. *Soils and Foundations*, 44(1), 1–24. doi:10.3208/sandf.44.1
- Akin, J. ., & Singh, M. (2002). Object-oriented Fortran 90 P-adaptive finite element method. *Advances in Engineering Software*, 33(7-10), 461–468. doi:10.1016/S0965-9978(02)00048-0
- Alberti, M. (2010). Analysis of kinematic correlations in faults and focal mechanisms with GIS and Fortran programs. *Computers & Geosciences*, 36(2), 186–194. doi:10.1016/j.cageo.2009.06.006
- Aliane, N. (2010). Data acquisition and real-time control using spreadsheets: interfacing Excel with external hardware. *ISA transactions*, 49(3), 264–9. doi:10.1016/j.isatra.2010.03.009
- Asuncion, H. U. (2013). Automated data provenance capture in spreadsheets, with case studies. *Future Generation Computer Systems*. doi:10.1016/j.future.2013.04.009
- Attard, G., Winiarski, T., Rossier, Y. and Eisenlohr, L., 2016. Review: Impact of underground structures on the flow of urban groundwater. *Hydrogeology Journal*, 24(1), pp.5-19.
- Ayala, M., Cabrerizo, M., Tito, M., Barreto, A., & Adjouadi, M. (2009). A spreadsheet application for processing long-term EEG recordings. *Computers in biology and medicine*, 39(9), 844–51. doi:10.1016/j.combiomed.2009.07.003
- Banda, E. and Santanach, P.: The Valencia trough (western Mediterranean): An overview, *Tectonophysics*, 208, 183-202, 1992.
- Bea, S. a., Carrera, J., Ayora, C., Batlle, F., & Saaltink, M. W. (2009). CHEPROO: A Fortran 90 object-oriented module to solve chemical processes in Earth Science models. *Computers & Geosciences*, 35(6), 1098–1112. doi:10.1016/j.cageo.2008.08.010
- Bear, J., Corapcioglu, M. Y., 1981a. Mathematical model for regional land subsidence due to pumping 2. Integrated aquifer subsidence equations for vertical and horizontal displacements. *Water Resources Research*, 17 (4), pp. 947-958.
- Bear, J., Corapcioglu, M. Y., 1981b. Mathematical model for regional land subsidence due to pumping 1. Integrated aquifer subsidence equations for vertical and horizontal displacements. *Water Resources Research*, 17 (4), pp. 947-958.
- Bell, J.W., Amelung, F., Ferretti, A., Bianchi, M., Novali, F., 2008. Permanent scatterer InSAR reveals seasonal and long-term aquifer-system response to groundwater pumping and artificial recharge. *Water Resour. Res.* 44 (2).
- Bernardini, G., Ricci, P., Coppi, F., 2007. A ground based microwave interferometer with imaging capabilities for remote measurements of displacements. In: Proc. GALAHAD Workshop Within the 7th Geomatic Week and the 3rd International Geotelematics Fair (GlobalGeo), Barcelona (Spain), 20–23 February.
- Bhanu Sridhar, M., Srinivas, Y., & Krishna Prasad, M. H. M. (2013). Software reuse in a paralysis dataset based on categorical clustering and the Pearson distribution. *Journal of King Saud University - Computer and Information Sciences*. doi:10.1016/j.jksuci.2013.12.003

References

- Bonduá, S., Berry, P., Bortolotti, V., & Cormio, C. (2012). TOUGH2Viewer: A post-processing tool for interactive 3D visualization of locally refined unstructured grids for TOUGH2. *Computers & Geosciences*, 46, 107–118. doi:10.1016/j.cageo.2012.04.008
- Bonomi, T., Bellini, R., 2003. The tunnel impact on the groundwater level in an urban area: a modelling approach to forecast it. *Materials and Geoenvironment*. 50, 45-48.
- BrineMIX (2013). Hydrogeological group (GHS), Institute of Environmental Assessment and Water Research (IDAEA- CSIC) and Department of Geotechnical Engineering and Geosciences, Universitat Politècnica de Catalunya (UPC). Available at www.h2ogeo.upc.es. Accessed 18/07/2013.
- Buccella, A., Cechich, A., Arias, M., Pol'la, M., Doldan, M. D. S., & Morsan, E. (2013). Towards systematic software reuse of GIS: Insights from a case study. *Computers & Geosciences*, 54, 9–20. doi:10.1016/j.cageo.2012.11.014
- Buregio, V.A.d.A., Almeida, E.S.d., Lucredio, D., Meira, S.R.d.L., (2007). Specification, design and implementation of a reuse repository. In: 31st IEEE Annual International Computer Software and Applications (COMPSAC) Conference – Short paper, Beijing, China.
- Câmara, G., Souza, R.C.M., Pedrosa, B.M., Vinhas, L., Monteiro, A.M.V., Paiva, J.A., Carvalho, M.T., Gattass, M., 2000. TerraLib: technology in support of GIS innovation. In: II Brazilian Symposium on Geoinformatics, GeoInfo2000. Sao Paulo.
- Carrera, J., Neuman, S., 1986. Estimation of aquifer parameters under transient and steady state conditions: 1. Maximum likelihood method incorporating prior information. *Water Resources Research*, 22 (2), 199-210.
- Carrera, J., Vázquez-Suñé, E., Castillo, O., & Sánchez-Vila, X. (2004). A methodology to compute mixing ratios with uncertain end-members. *Water Resources Research*, 40(12), n/a–n/a. doi:10.1029/2003WR002263
- Casagli, N., Catani, F., Del Ventisette, C., Luzi, G., 2010. Monitoring, prediction, and early warning using ground-based radar interferometry. *Landslides* 7 (3), 291–301.
- Cashman, P.M., Preene, M., 2001. *Groundwater lowering in construction – A practical guide*. Spon press, London.
- Choe, S., Kim, S., Choi, H., Choi, H., Chung, H., & Hwang, B. (2010). Automated toxicological screening reports of modified Agilent MSD Chemstation combined with Microsoft Visual Basic application programs. *Forensic science international*, 199(1-3), 50–7. doi:10.1016/j.forsciint.2010.03.003
- Costantini, M., 1998. A novel phase unwrapping method based on network programming. *IEEE Trans. Geosci. Remote Sens.* 36 (3), 813–821.
- Criollo, R., Velasco, V., Vázquez-Suñé, E., Serrano-Juan, A., Alcaraz, M. and García-Gil, A., 2016. An integrated GIS-based tool for aquifer test analysis. *Environmental Earth Sciences*, 75(5), pp.1-11.
- Crosetto, M., Monserrat, O., Luzi, G., Cuevas-González, M. and Devanthery, N., 2014. Discontinuous GBSAR deformation monitoring. *ISPRS Journal of Photogrammetry and Remote Sensing*, 93, pp.136-141.
- Crosetto, M., Monserrat, O., Cuevas-González, M., Devanthery, N., Luzi, G., Crippa, B., 2015. Measuring thermal expansion using X-band Persistent Scatterer Interferometry. *ISPRS Journal of Photogrammetry and Remote Sensing*, 100, pp. 84–91.
- Crosetto, M., Monserrat, O., Cuevas-González, M. Devanthery, N., Crippa, B., 2016. Persistent Scatterer Interferometry: a review. *ISPRS Journal of Photogrammetry and Remote Sensing*, 115, pp. 78-89.
- Culí, L., Pujades, E., Vázquez-Suñé, E. and Jurado, A., 2016. Modelling of the EPB TBM shield tunnelling advance as a tool for geological characterization. *Tunnelling and Underground Space Technology*, 56, pp.12-21.
- Cunha, J., Mendes, J., Saraiva, J., & Visser, J. (2014). Model-based programming environments for spreadsheets. *Science of Computer Programming*, 1, 1–22. doi:10.1016/j.scico.2014.02.002
- Custodio, E. and Carrera, J., 1989. Aspectos generales sobre la contaminación de las aguas subterráneas. *Revista OP*, (13), pp.96-109.

References

- De Dreuzy, J.-R., Bodin, J., Le Grand, H., Davy, P., Boulanger, D., Battais, A., Bour, O., et al. (2006). General database for ground water site information. *Ground water*, 44(5), 743–8. doi:10.1111/j.1745-6584.2006.00220.x
- Deursen, A.v., Klint, P., Visser, J., (2000). Domain-specific languages: an annotated bibliography. *ACM SIGPLAN Notices* 35 (6), 26–36.
- Deveughèle, M., Zokimila, P., & Cojean, R., 2010. Impact of an impervious shallow gallery on groundwater flow. *Bulletin of Engineering Geology and the Environment*, 69(1), 143–152. doi:10.1007/s10064-009-0226-x
- Devanathéry, N., Crosetto, M., Monserrat, O., Cuevas-González, M., Crippa, B., 2014. An approach to Persistent Scatterer Interferometry. *Remote Sensing*, 6, pp. 6662-6679.
- Dunnicliff, J., 1993. *Geotechnical instrumentation for monitoring field performance*. John Wiley & Sons.
- EASYBAL (2013) Hydrogeological group (GHS), Institute of Environmental Assessment and Water Research (IDAEA- CSIC) and Department of Geotechnical Engineering and Geosciences, Universitat Politècnica de Catalunya (UPC). Available at <http://www.h2ogeo.upc.es>. Accessed 18/07/2013.
- EASYQUIM (2013) Hydrogeological group (GHS) of Technical University of Catalonia (UPC) and Institute of Environmental Assessment and Water Research (IDAEA), CSIC, Barcelona, (Spain). Available at www.h2ogeo.upc.es. Accessed 03/06/2013.
- Elmore, A. (2007). "Applying a One-Dimensional Mass Transport Model Using Groundwater Concentration Data." *J. Environ. Eng.*, 133(4), 372–379.
- Endres, A., (1993). Lessons learned in an industrial software lab. *IEEE Software* 10 (05), 58–61.
- Ferretti, A., Novali, F., Bürgmann, R., Hilley, G., Prati, C., 2004. InSAR permanent scatterer analysis reveals ups and downs in San Francisco Bay area. *Eos, Trans. Am. Geophys. Union* 85 (34), 317–324.
- Ferris, J., Knowles, D., Brown, R., Stallman, R., 1962. *Theory of aquifer tests*. U.S. Geological Survey Water Supply Paper 1536-E.
- Font-Capo, J., Pujades, E., Vázquez-Suñé, E., Carrera, J., Velasco, V. and Montfort, D., 2015. Assessment of the barrier effect caused by underground constructions on porous aquifers with low hydraulic gradient: A case study of the metro construction in Barcelona, Spain. *Engineering Geology*, 196, pp.238-250.
- Forth, R.A., 2004. Groundwater and geotechnical aspects of deep excavations in Hong Kong. *Engineering Geology*. 72, 253–260.
- Fortuny, J., Sieber, A.J., 1994. Fast algorithm for a near field synthetic aperture radar processor. *IEEE Trans. Antennas Propagation* 41, 1458–1460.
- Frakes, W. B., Kang, K., (2005). Software reuse research: status and future. *IEEE Transactions on Software Engineering*, 31(7), 529–536. doi:10.1109/TSE.2005.85
- Gabriel, A.K., Goldstein, R.M., Zebker, H.A., 1989. Mapping small elevation changes over large areas: differential radar interferometry. *J. Geophys. Res.* 94 (B7), 9183–9191.
- Gómez, D., Simó, J.A., Lobo, F.J., Barnolas, A., Carrera, J., Vázquez-Suñé, E., 2009. Onshore-offshore correlation of the Llobregat deltaic system, Spain: Development of deltaic geometries under different relative sea-level and growth fault influences. *Sedimentary Geology*, 217, 65-84.
- Ghiglia, D.C., Pritt, M.D., 1998. *Two-dimensional phase unwrapping: theory, algorithms, and software*. Ed. Wiley, New York (USA).
- GHS (2013) estudios de mezcla de aguas y evolución de química durante la operación de los pozos. Instituto de Diagnóstico Ambiental y Estudios del Agua, CSIC. 458pp
- Sherif, K., Appan, R., Lin, Z., (2006). Resources and incentives for the adoption of systematic software reuse. *International Journal of Information Management* 26 (1), 70–80.

References

- Gordillo, S., Balaguer, F., Mostaccio, C., Das Neves, F., 1999. Developing GIS applications with objects: a design patterns approach. *Geoinformatica 3* (March (1)), 7–32. URL /<http://dx.doi.org/10.1023/A:10098095117705>
- Griss, M., (1995). Making software reuse work at Hewlett-Packard. *IEEE Software* 12 (01), 105–107.
- Gue, S.S., Tan, Y.C., 2004. Two case histories of basement excavation with influence on groundwater. Keynote Lecture, International Conference on Structural and Foundation Failures (ICSFF), Singapore, 2nd–4th August, 2004.
- Guo, J., Luqi, (2000). A survey of software reuse repositories. In: 7th IEEE International Conference and Workshop on the Engineering of Computer Based Systems. IEEE/CS Press, Edinburgh, Scotland, p. 92.
- Hamate, T . Sugimoto, T . Kozato, and Y . Hanaoka., 2003. Methods on observing groundwater flow and maintaining facilities for preserving natural groundwater flows. Proceedings of international symposium on groundwater problems related to geo-environment, Okayama, Japan, May 28–30.
- Hashimoto, T . , Arimoto, H . , Sugimura, T. and Ido, S., 2001. Case records on countermeasures against groundwater flow preservation. Case records in Kyoto and Kolbe, *The Foundation Engrg. and Equipment "Kisoko "*, 29(1 1), 4 1 -43
- Herrera, G., Tomás, R., Lopez-Sanchez, J.M., Delgado, J., Vicente, F., Mulas, J., Cooksley, G., Sanchez, M., Duro, J., Arnaud, A., Blanco, P., Duque, S., Mallorquí, J., De la Vega-Panizo, R., Monserrat, O., 2009. Validation and comparison of advanced differential interferometry techniques: Murcia metropolitan area case study. *ISPRS J. 64*, 501–512.
- Hopper, Grace. Its name is an acronym for COMmon Business-Oriented Language, 1959.
- Hsi, J., Small, J., 1992. Ground settlements and drawdown of the water table around an excavation. *Canadian. Geotechnical Journal*. 24, pp. 740–756.
- IBM, The IBM Mathematical Formula Translating System, San José, California, 1954.
- Ibrahim, D. (2009). Using the excel spreadsheet in teaching science subjects. *Procedia - Social and Behavioral Sciences*, 1(1), 309–312. doi:10.1016/j.sbspro.2009.01.058
- IDS. 2013. IBIS Guardian Software v. 02.00 – User Manual. IDS Ingegneria Dei Sistemi S.p.A., Pisa, Italy.
- Jacob, C. E., 1950. Flow of groundwater, in Rouseff, H. (Eds.), *Engineering Hydraulics*. John Wiley, New York, pp. 321–386.
- Jacobson, I., Booch, G. and Rumbaugh J. *The Unified Software Development Process* (ISBN 0-201-57169-2)
- JafarGandomi, A., & Takenaka, H. (2013). FDTD3C—A FORTRAN program to model multi-component seismic waves for vertically heterogeneous attenuative media. *Computers & Geosciences*, 51, 314–323. doi:10.1016/j.cageo.2012.07.022
- Jannach, D., Schmitz, T., Hofer, B., & Wotawa, F. (2014). Avoiding, Finding and Fixing Spreadsheet Errors - A Survey of Automated Approaches for Spreadsheet QA. *Journal of Systems and Software*. doi:10.1016/j.jss.2014.03.058
- Jones, W. R., Spence, M. J., Bowman, A. W., Evers, L., & Molinari, D. a. (2014). A software tool for the spatiotemporal analysis and reporting of groundwater monitoring data. *Environmental Modelling & Software*, 55, 242–249. doi:10.1016/j.envsoft.2014.01.020
- Joos, R., (1994). Software reuse at Motorola. *IEEE Software* 11 (05), 42–47. Kitchenham, B., Pleegeer, S., 2002. Principles of survey research. Part 2: Designing a survey. *ACM SIGSOFT Software Engineering Notes* 27 (1), 18–20.
- Kahmen, H.; Faig, W., 1988. *Surveying*; Walter de Gruyter: Berlin, Germany.
- Kay, R. (2002). *QuickStudy: System Development Life Cycle*. Computerworld, (http://www.computerworld.com/s/article/71151/System_Development_Life_Cycle)Kemeny, John G. and Kurtz, Thomas E., *Beginner's All-purpose Symbolic Instruction Code*, 1964

References

- Khan, H. A. (2006). SCEW: a Microsoft Excel add-in for easy creation of survival curves. *Computer methods and programs in biomedicine*, 83(1), 12–7. doi:10.1016/j.cmpb.2006.05.001
- Kim, J. M., Parizek, R. R., 1997. Numerical simulation of the Noordbergum effect resulting from groundwater pumping in a layered aquifer system. *Journal of Hydrology*, 202, pp. 231-243
- Kruchten, P. A brief history of the RUP's "hump chart". Technical report, University of British Columbia, 2003
- Krueger, C., (1992). Software reuse. *ACM Computing Surveys* 24 (02), 131– 183.
- Kusumoto, S., Omae, H., Sato, T., Watanabe, M., Kobayashi, N., & Nishida, K., 2003. Construction of preservation facilities on natural groundwater flows. *Proceedings of international symposium on groundwater problems related to geo-environment*, Okayama, Japan, May 28–30.
- Lan, H., Li, L., Liu, H. and Yang, Z., 2012. Complex urban infrastructure deformation monitoring using high resolution PSI. *Selected Topics in Applied Earth Observations and Remote Sensing*, IEEE Journal of, 5(2), pp.643-651.
- Lisboa Filho, J., Iochpe, C., Borges, K.A.V., 2002. Analysis patterns for GIS data schema reuse on urban management applications. *CLEI Electronic Journal* 5 (2)
- Liu, D., Sowter, A. and Niemeier, W., 2014. Process-related deformation monitoring by PSI using high resolution space-based SAR data: a case study in Düsseldorf, Germany. *Natural Hazards and Earth System Sciences Discussions*, 2(7), pp.4813-4830.
- Locock, A. J. (2008). An Excel spreadsheet to recast analyses of garnet into end-member components, and a synopsis of the crystal chemistry of natural silicate garnets. *Computers & Geosciences*, 34(12), 1769–1780. doi:10.1016/j.cageo.2007.12.013
- Locock, A. J. (2014). An Excel spreadsheet to classify chemical analyses of amphiboles following the IMA 2012 recommendations. *Computers & Geosciences*, 62, 1–11. doi:10.1016/j.cageo.2013.09.011
- López Espina, Ander, Carrera Ramírez, Jesús, 2009. Estudio analítico del efecto barrera: definición, tipología, soluciones y aplicación a caso real. Tesina de Máster. UPC.
- Lucredio, D., Almeida, E.S.d., Prado, A.F.d., (2004). A survey on software components search and retrieval. In: Steinmetz, R., Mauthe, A. (Eds.), 30th IEEE EUROMICRO Conference, Component-Based Software Engineering Track. IEEE/CS Press, Rennes – France, pp. 152–159.
- Lucrecio, D., dos Santos Brito, K., Alvaro, A., Garcia, V. C., de Almeida, E. S., de Mattos Fortes, R. P., & Meira, S. L. (2008). Software reuse: The Brazilian industry scenario. *Journal of Systems and Software*, 81(6), 996–1013. doi:10.1016/j.jss.2007.08.036
- Luzi, G., Pieraccini, M., Mecatti, D., Noferini, L., Macaluso, G., Tamburini, A., Atzeni, C., 2007. Monitoring of an alpine glacier by means of ground-based SAR interferometry. *IEEE Geosci. Remote Sens. Lett.* 4 (3), 495–499.
- MacLeamy, 2004. The "MacLeamy Curve". Introduced in the Construction Users Roundtable's "Collaboration, Integrated Information, and the Project Lifecycle in Building Design and Construction and Operation" (WP-1202, August, 2004)".
- Mahabadi, O. K., Grasselli, G., & Munjiza, a. (2010). Y-GUI: A graphical user interface and pre-processor for the combined finite-discrete element code, Y2D, incorporating material heterogeneity. *Computers & Geosciences*, 36(2), 241–252. doi:10.1016/j.cageo.2009.05.010
- Malavia M., Fernández Roure J., Valencia J., Amigó J., Borrell E., Herms I., Arnó G., 2008. Medida correctora frente al efecto barrera en el tramo de pantallas en la estación de I9 y I2 de parc logístic en el acuífero superficial del delta del llobregat. In: Carmen, M., Vallejos, A., Valverde, M., Lamban, L. (eds.), *el agua y las infraestructuras en el medio subterráneo*. Instituto geológico y minero de España, Madrid, pp. 459-464.
- Manager, S. (n.d.). DHI TECHNOLOGY.

References

- Marchamalo, M., Galán, D., Sánchez, J.A. and Martínez, R., 2011. La tecnología DGPS en la construcción: control de movimientos en grandes estructuras. *Informes de la Construcción*, 63(522), pp.93-102. doi:10.3989/ic.10.008
- Marinos, P., Kavvas, M., 1997. Rise of the groundwater table when flow is obstructed by shallow tunnels, in: Chilton, J. (Eds.), *Groundwater in the urban environment: Problems, processes and management*. Balkema, Rotterdam, pp. 49-54.
- MATLAB, The MathWorks, Inc., Natick, Massachusetts, United States, 1984.
- Mayborn, K. R., & Leshner, C. E. (2011). MagPath: An Excel-based Visual Basic program for forward modeling of mafic magma crystallization. *Computers & Geosciences*, 37(11), 1900–1903. doi:10.1016/j.cageo.2011.02.017
- Medina A, Carrera J, 1996. Coupled estimation of flow and solute transports parameters. *Water Resources Research*, 32 (10), 3063-3076.
- Medina A, Carrera J, 2003. Geostatistical inversion of coupled problems: dealing with computational burden and different types of data. *Journal of Hydrology*, 281 (4), 251-264.
- Medina, A., Alcolea, A., Carrera, J., Castro, L.F., 2000. Modelos de flujo y transporte en la geosfera: Código TRANSIN IV. [Flow and transport modelling in the geosphere: The code TRANSIN IV]. IV Jornadas de Investigación y Desarrollo Tecnológico de Gestión de Residuos Radioactivos de ENRESA. Technical publication 9/2000: 195-200.
- Merrick, N., Jewell, M., 2003. Modelling of the groundwater impact of a sunken urban motorway in Sydney, Australia. *Materials and Geoenvironment*. 50, 229-232.
- Microsoft, C++/CLI programming languages and integrated development environment (IDE), 1993.
- Microsoft, derived from BASIC in third-generation event-driven programming language and integrated development environment (IDE), 1991
- Mili, R., Mili, A., Mittermeir, R.T., (1997). Storing and retrieving software components: a refinement based system. *IEEE Transactions on Software Engineering* 23 (7), 445–460.
- Mili, A., Mili, R., Mittermeir, R.T., (1998). A survey of software reuse libraries. *Annals of Software Engineering Notes* 5, 349–414.
- MIX (2013). Hydrogeological group (GHS), Institute of Environmental Assessment and Water Research (IDAEA- CSIC) and Department of Geotechnical Engineering and Geosciences, Universitat Politècnica de Catalunya (UPC). Available at www.h2ogeo.upc.es. Accessed 18/07/2013.
- Molano, C. (2013, December). 2013 William A. McElhiney Distinguished Lecture Series in Water Well Technology—Groundwater Spreadsheets: Efficient and Practical Resource for Solving Simple and Complex Flow, Pollution, and Environmental Problems. In 2013 NGWA Groundwater Expo and Annual Meeting. Ngwa. Nath, S. K., Shahid, S., & Dewangan, P. (2000). SEISRES ð a Visual C ++ program for the sequential inversion of seismic refraction and geoelectric data p, 26.
- Montserrat, O., Crosetto, M. and Luzi, G., 2014. A review of ground-based SAR interferometry for deformation measurement. *ISPRS Journal of Photogrammetry and Remote Sensing*, 93, pp.40-48.
- Nishigaki, Makoto. "Geotechnical aspects of groundwater control." *Soils and foundations* 50, no. 6, 2010: 893-902.
- Odijk, D.; Kensing, F.; Hanssen, R. Integration of Leveling and INSAR Data for Land Subsidence Monitoring. In *Proceedings of the 11th FIG Symposium on Deformation Measurements*, Santorini, Greece, 25–28 May 2003.
- Ozcep, F. (2010). SoilEngineering: A Microsoft Excel® spreadsheet© program for geotechnical and geophysical analysis of soils. *Computers & Geosciences*, 36(10), 1355–1361. doi:10.1016/j.cageo.2010.01.015
- Palocsay, S. W., Markham, I. S., & Markham, S. E. (2010). Utilizing and teaching data tools in Excel for exploratory analysis. *Journal of Business Research*, 63(2), 191–206. doi:10.1016/j.jbusres.2009.03.008

References

- Paris, A., Teatini, P., Venturini, S., Gambolati, G., Bernstein, A.G., 2010. Hydrological effects of bounding the Venice (Italy) industrial harbour by a protection cut-off wall: a modeling study. *Journal of Hydrologic Engineering*. 15 (11), 882–891.
- Parkhurst, D.L., Appelo, C.A.J., 1999. User's guide to PHREEQC (Version 2)—A computer program for speciation, batch-reaction, one-dimensional transport, and inverse geochemical calculations. U.S. Geological Survey Water-Resources Investigations Report 99-4259, 312 pp.
- Pelzer, H., Niemeier, W., 1984. *Precise Leveling: Contributions to the Workshop on Precise Levelling Held at the University of Hannover, 16–18 March 1983*; Eds.; Ferd. Dümmlers Verlag: Bonn, Germany.
- Phong, V. V., Kumar, P., Drewry, D. T., & Quijano, J. C. (2012). A graphical user interface for numerical modeling of acclimation responses of vegetation to climate change. *Computers & Geosciences*, 49(null), 91–101. doi:10.1016/j.cageo.2012.07.007
- Pieraccini, M., Luzi, G., Mecatti, D., Fratini, M., Noferini, L., Carissimi, L., Franchioni, G., Atzeni, C., 2004. Remote sensing of building structural displacements using a microwave interferometer with imaging capability. *Non Destruct. Test. Eval.* 37 (7), 545–550.
- Prieto, G. a., Parker, R. L., & Vernon III, F. L. (2009). A Fortran 90 library for multitaper spectrum analysis. *Computers & Geosciences*, 35(8), 1701–1710. doi:10.1016/j.cageo.2008.06.007
- Pujades, E., López, A., Carrera, J., Vázquez-Suñé, E. and Jurado, A., 2012a. Barrier effect of underground structures on aquifers. *Engineering geology*, 145, pp.41-49. doi:10.1016/j.enggeo.2012.07.004
- Pujades, E., Carrera, J., Vázquez-Suñé, E., Jurado, A., Vilarrasa, V. and Mascañano-Salvador, E., 2012b. Hydraulic characterization of diaphragm walls for cut and cover tunnelling. *Engineering Geology*, 125, pp.1-10. doi:10.1016/j.enggeo.2011.10.012
- Pujades, E., Vázquez-Suñé, E., Carrera, J. and Jurado, A., 2014a. Dewatering of a deep excavation undertaken in a layered soil. *Engineering geology*, 178, pp.15-27. doi:10.1016/j.enggeo.2014.06.007
- Pujades, E., Vázquez-Suñé, E., Carrera, J., Vilarrasa, V., De Simone, S., Jurado, A., Ledesma, A., Ramos, G. and Lloret, A., 2014b. Deep enclosures versus pumping to reduce settlements during shaft excavations. *Engineering Geology*, 169, pp.100-111. doi:10.1016/j.enggeo.2013.11.017
- Pujades, E., Vázquez-Suñé, E., Culí, L., Carrera, J., Ledesma, A., Jurado, A. 2015. Hydrogeological impact assessment by tunnelling at sites of high sensitivity. *Engineering Geology*, 193, pp. 421-434.
- Pujades, E., Jurado, A., Carrera, J., Vázquez-Suñé, E., Dassargues, A., 2016. Hydrogeological assessment of non-linear underground enclosures. *Engineering Geology*, 207, pp. 91–102.
- Pulido-Bosch, A., Delgado, J., Sola, F., Vallejos, Á., Vicente, F., López-Sánchez, J.M. and Mallorquí, J.J., 2012. Identification of potential subsidence related to pumping in the Almería basin (SE Spain). *Hydrological Processes*, 26 (5), pp.731-740.
- Raucoules, D.; Bourguin, B.; de Michele, M.; le Cozanet, G.; Closset, L.; Bremmer, C.; Veldkamp, T.D.; Bateson, L.; Crosetto, M.; Agudo, M. *Persistent Scatterers Interferometry Independent Validation and Intercomparison of Results; Final Report, BRGM/RP-55649-FR; BRGM: Orléans, France, 2007*
- Ribera Urenda, Fidel, 2008. Las medidas preventivas y las medidas correctoras de las afecciones hidrogeológicas generadas por grandes infraestructuras. In: Carmen, M., Vallejos, A., Valverde, M., Lamban, L. (eds.), *el agua y las infraestructuras en el medio subterráneo*. Instituto geológico y minero de España, Madrid, pp. 259-272
- Ricci, G., Enrione, R., Eusebio, A., 2007. Numerical modelling of the interference between underground structures and aquifers in urban environment. The Turin subway – Line 1, in: Barták, Hrdine, Romancov and Zlámál (Eds.), *Underground Space*. Taylor and Francis Group, London, pp. 1323-1329.
- Robin, B. (1995). SUPPORTING GEOSCIENCE WITH INTERNET TOOLS FOR THE MACINTOSH, 21(6), 737–751.

References

- Roca, E. and Guimerà, J.: The Neogene structure of the eastern Iberian margin: structural constraints on the crustal evolution of the Valencia trough (western Mediterranean), *Tectonophysics*, 203, 203-218, 1992
- Roca, E. and Guimerà, J.: The Neogene structure of the eastern Iberian margin: structural constraints on the crustal evolution of the Valencia trough (western Mediterranean), *Tectonophysics*, 203, 203-218, 1992.
- Roy, D., Robinson, K.E., 2009. Surface settlements at a soft soil site due to bedrock dewatering. *Engineering Geology*. 107, pp. 109–117.
- Santamaría Arias, Carlos, León Buendía, Jaime, Gil Navas, Antonio, Díaz García, Jesús, 2008. Sistemas para dar continuidad a los acuíferos afectados por la interposición de muros pantalla. Descripción tipológica y selección de soluciones. In: Carmen, M., Vallejos, A., Valverde, M., Lamban, L. (eds.), *el agua y las infraestructuras en el medio subterráneo*. Instituto geológico y minero de España, Madrid, pp. 319-326
- Sanz, P. (1988) .El pla de Barcelona: Constitució i característiques físiques (Coneguem Catalunya) (Catalan Edition).
- Scheiber, L., Ayora, C., Vázquez-Suñé, E. (2013a). Informe de datación de las aguas subterráneas en el entorno minero de CLC. IDAEA-CSIC Barcelona. Internal technical report. 225pp.
- Scheiber, L., Ayora, C., Vázquez-Suñé, E. (2013b). Establecimiento de porcentajes de mezcla entre mioceno y paleozoico en las aguas del sdr de la explotación minera de clc. IDAEA-CSIC Barcelona. Internal technical report. 218pp.
- Scheiber, L., Barbieri, M., Ayora, C., Vázquez-Suñé, E. (2013c). CSIC (2013) Estudio Hidrogeológico e Hidrogeoquímico del área minera de Cobre Las Cruces y su influencia en el Acuífero Niebla-Posadas. Instituto de Diagnóstico Ambiental y Estudios del Agua, CSIC. Fundación Migres, Sevilla, 197pp.
- Scheiber, L., Ayora C., Vazquez-Suñe, E., Soler, A., Yesares, L. (2014a). Geogenical ammonium in the deeper np aquifer in the southern Spain. Manuscript in progress
- Scheiber, L., Ayora C., Vazquez-Suñe, E., Soler, A., Cendon, D. (2014b). The role of geochemistry and inter-aquifer mixing processes in dating groundwater from the niebla-posadas regional aquifer, southern Spain. Manuscript in progress
- Schmidt, D.A., Bürgmann, R., 2003. Time-dependent land uplift and subsidence in the Santa Clara valley, California, from a large interferometric synthetic aperture radar data set. *J. Geophys. Res.: Solid Earth* (1978–2012) 108 (B9).
- Schulz, W.H., Coe, J.A., Shurtleff, B.L., Panosky, J., Farina, P., Ricci, P.P., Barsacchi, G., 2012. Kinematics of the Slumgullion landslide revealed by ground-based InSAR surveys. In: *Proc. Landslides and Engineered Slopes: Protecting Society through Improved Understanding – the 11th International and 2nd North American Symposium on Landslides and Engineered Slopes*, Banff (Canada), 3–8 June, pp. 1273–1279.
- Seacord, R.C., (1999). Software engineering component repositories. In: *International Workshop on Component-Based Software Engineering*, Held in conjunction with the 21st International Conference on Software Engineering (ICSE), Los Angeles, CA, USA.
- Serrano-Juan, A., Vázquez-Suñé, E., Criollo, R., 2015. Estudio y seguimiento hidrogeológico de las obras de la línea de alta velocidad Madrid-Barcelona-Figueroles, correspondientes a la construcción de la estación de la Sagrera y sus accesos. Periodo septiembre/2011 – enero/2015. Technical Report. Barcelona, Universitat Politècnica de Catalunya (UPC), Departament d'Enginyeria del Terreny, Cartogràfica i Geofísica, 131pp.
- Serrano-Juan, A., Vázquez-Suñé, E., Monserrat, O., Crosetto, M., Hoffmann, C., Ledesma, A., Criollo, R., Pujades, E., Velasco, V., Garcia-Gil, A. and Alcaraz, M., 2016. Gb-SAR interferometry displacement measurements during dewatering in construction works. Case of La Sagrera railway station in Barcelona, Spain. *Engineering Geology*, 2015, pp.104-115.
- Sokos, E. N., & Zahradnik, J. (2008). ISOLA a Fortran code and a Matlab GUI to perform multiple-point source inversion of seismic data. *Computers & Geosciences*, 34(8), 967–977. doi:10.1016/j.cageo.2007.07.005

References

- Solé, J., Cosca, M., Sharp, Z., and Enrique, P.: 40 Ar/ 39 Ar Geochronology and stable isotope geochemistry of Late-Hercynian intrusions from north-eastern Iberia with implications for argon loss in K-feldspar, *International Journal of Earth Sciences*, 91, 865-881, 2002.
- Sousa, J.J., Bastos, L., 2013. Multi-temporal SAR interferometry reveals acceleration of bridge sinking before collapse. *Nat. Hazards Earth Syst. Sci.* 13 (3), 659–667.
- Spada, G., & Stocchi, P. (2007). SELEN: A Fortran 90 program for solving the “sea-level equation.” *Computers & Geosciences*, 33(4), 538–562. doi:10.1016/j.cageo.2006.08.006
- Spada, G. (2008). ALMA, a Fortran program for computing the viscoelastic Love numbers of a spherically symmetric planet. *Computers & Geosciences*, 34(6), 667–687. doi:10.1016/j.cageo.2007.12.001
- Spreadsheet applications in engineering education. *International Journal of Engineering Education* 2004;20(6): [special issue]
- Strassberg, G., Maidment, D. R., & Jones, N. L., 2007. A geographic data model for representing ground water systems. *Ground water*, 45(4), 515–8. doi:10.1111/j.1745-6584.2007.00324.x
- Suri, P. K., & Garg, N. (2009). Software Reuse Metrics: Measuring Component Independence and its applicability in Software Reuse, 9(5), 237–248. Tang, G., Mayes, M. a., Parker, J. C., & Jardine, P. M. (2010). CXTFIT/Excel—A modular adaptable code for parameter estimation, sensitivity analysis and uncertainty analysis for laboratory or field tracer experiments. *Computers & Geosciences*, 36(9), 1200–1209. doi:10.1016/j.cageo.2010.01.013
- Takahashi, K., Matsumoto, M., Sato, M., 2013. Continuous observation of natural disaster-affected areas using ground-based SAR interferometry. *IEEE J. Sel. Top. Appl. Earth Observations Remote Sens.* 6 (3), 1286–1294.
- Tambara, M., Nishigaki, M., Hashimoto, T., Shinshi, Y., Daito, K., 2003. Basic concept on preservation natural groundwater flows from intercepting by underground structure, in: Kono, Nishigaki and Komatsu (Eds.), *Groundwater Engineering*. Swets and Zeitlinger, Lisse, pp. 217-222.
- Tapete, D., Casagli, N., Luzi, G., Fanti, R., Gigli, G., Leva, D., 2013. Integrating radar and laser-based remote sensing techniques for monitoring structural deformation of archaeological monuments. *J. Archaeol. Sci.* 40 (1), 176–189.
- Tarchi, D., Ohlmer, E., Sieber, A.J., 1997. Monitoring of structural changes by radar interferometry. *J. Res. Nondestruct. Eval.* 9 (4), 213–225.
- Tarchi, D., Rudolf, H., Luzi, G., Chiarantini, L., Coppo, P., Sieber, A.J., 1999. SAR interferometry for structural changes detection: a demonstration test on a dam. In: *Proc. IGARSS 1999, Hamburg, Germany*, pp. 1522–1524.
- Tarchi, D., Casagli, N., Fanti, R., Leva, D., Luzi, G., Pasuto, A., Pieraccini, M., Silvano, S., 2003. Landslide monitoring by using ground-based SAR interferometry: an example of application. *Eng. Geol.* 68 (1–2), 15–30.
- Tarchi, D., Antonello, G., Casagli, N., Farina, P., Fortuny-Guasch, J., Guerri, L., Leva, D., 2005. On the use of ground-based SAR interferometry for slope failure early warning: the Cortenova rock slide (Italy). In: *Landslides: Risk Analysis and Sustainable Disaster Management*. Ed. Springer, Berlin Heidelberg, pp. 337–342.
- Terzaghi, K., 1943. *Theory of Consolidation* (pp. 265-296). John Wiley & Sons, Inc..
- Tomas, R.; Romero, R.; Mulas, J.; Marturi, J.J.; Mallorqu, J.J.; Lopez-Sanchez, J.M.; Herrera, G.; Gutierrez, F.; Gonzalez, P.J.; Fernandez, J.; et al. Radar interferometry techniques for the study of ground subsidence phenomena: A review of practical issues through cases in Spain. *Environ. Earth Sci.* 2013, doi: 10.1007/s12665-013-2422-z.
- Toyokuni, G., & Takenaka, H. (2009). ACE—A FORTRAN subroutine for analytical computation of effective grid parameters for finite-difference seismic waveform modeling with standard Earth models. *Computers & Geosciences*, 35(3), 635–643. doi:10.1016/j.cageo.2008.05.005

References

- Ueda, T., 1999. Measures of groundwater preservation in underground construction at Nerima site Gaikan Highway, Case Records Concerned with Underground Structures and Groundwater, Japanese Geotechnical Society, 4 1 -52.
- UPC (2003). Codigo Visual Transin 1.1 R65. Developed in the Department of Geotechnical Engineering and Geosciences (ETCG), UPC.
- Van Baars, S., 2011. Causes of major geotechnical disasters. In: Vogt, Schuppener, Straub and Braü (Eds.), ISGSR 2011. Bundesanstalt für Wasserbau, Germany
- Van der Boom, J., 2011. Tunelling in urbana reas: the use of lateral walls to Project ancient buildings. Minor thesis. Universitat Politècnica de Catalunya (UPC).
- Vázquez-Suñé, E., Sánchez-Vila, X., & Carrera, J., 2004. Introductory review of specific factors influencing urban groundwater, an emerging branch of hydrogeology, with reference to Barcelona, Spain. *Hydrogeology Journal*, 13(3), 522–533. doi:10.1007/s10040-004-0360-2
- Vázquez-Suñé, E., Sánchez-Vila, X., Carrera, J., 2005. Introductory review of specific factors influencing urban groundwater, an emerging branch of hydrogeology, with referente to Barcelona, Spain. *Hydrogeology Journal*. 13, 522-533.
- Vázquez-Suñé, E., Pujades, E., Escorcia, J., Jurado, A., 2011. Evaluación de efecto barrera, efecto dren y caudales de drenaje durante la excavación del recinto de la estación de Sagrera. Technical Report. Barcelona, Universitat Politècnica de Catalunya (UPC), Departament d'Enginyeria del Terreny, Cartogràfica i Geofísica, 83pp.
- Vázquez-Suñé, E., Marazuela, M. Á., Velasco, V., Diviu, M., Pérez-Estaún, A., and Alvarez-Marrón, J.: A geological model for the management of subsurface data in the urban environment of Barcelona city, *Solid Earth Discuss.*, doi:10.5194/se-2016-64, in review, 2016.
- Velasco, V., Cabello, P., Vázquez-Suñé, E., López-Blanco, M., Ramos, E., Tubau, I., 2012. A sequence stratigraphic based geological model for constraining hydrogeological modeling in the urbanized area of the Quaternary Besòs delta (NW Mediterranean coast , Spain). *Geologica acta*, 10, 373–394. doi:10.1344/105.000001757.
- Velasco, V., Gogu, R., Vázquez-Suñé, E., Garriga, A., Ramos, E., Riera, J., & Alcaraz, M. (2012). The use of GIS-based 3D geological tools to improve hydrogeological models of sedimentary media in an urban environment. *Environmental Earth Sciences*. doi:10.1007/s12665-012-1898-2
- Velasco, V., Tubau, I., Vázquez-Suñé, E., Gogu, R., Gaitanaru, D., Alcaraz, M., Serrano-Juan, A., Fernández-García, D., Garrido, T., Fraile, J., Sanchez-Vila, X. (2014). GIS-based hydrogeochemical analysis tools (QUIMET). *Computers & Geosciences*. Doi 10.1016/j.cageo.2014.04.013
- Verplank, W.L. (1985). "Graphics in Human-Computer Communication: Principles of Graphical User-Interface Design". in Peterson H.E. and Schneider W.. *Proceedings of the IFIP-IMIA Second Stockholm Conference on Communication in Health Care*, Stockholm, Sweden. pp. 113–130.
- Vilarrasa, V., Carrera, J., Jurado, A., Pujades, E. and Vázquez-Suné, E., 2011. A methodology for characterizing the hydraulic effectiveness of an annular low-permeability barrier. *Engineering Geology*, 120(1), pp.68-80. doi:10.1016/j.enggeo.2011.04.005
- Wang, J.-P., & Huang, D. (2012a). RosenPoint: A Microsoft Excel-based program for the Rosenblueth point estimate method and an application in slope stability analysis. *Computers & Geosciences*, 48, 239–243. doi:10.1016/j.cageo.2012.01.009
- Wang, J.-P., Huang, D., & Yang, Z. (2012b). Deterministic seismic hazard map for Taiwan developed using an in-house Excel-based program. *Computers & Geosciences*, 48, 111–116. doi:10.1016/j.cageo.2012.05.014
- Wang, J.-P., Huang, D., Cheng, C.-T., Shao, K.-S., Wu, Y.-C., & Chang, C.-W. (2013). Seismic hazard analyses for Taipei city including deaggregation, design spectra, and time history with excel applications. *Computers & Geosciences*, 52, 146–154. doi:10.1016/j.cageo.2012.09.021
- Wang, X., Ma, W., Gao, S., & Ke, L. (2008). GCDPlot: An extensible microsoft excel VBA program for geochemical discrimination diagrams. *Computers & Geosciences*, 34(12), 1964–1969. doi:10.1016/j.cageo.2007.10.014

References

- Wasowski J., Bovenga F., Refice A., Nitti D. and Nutricato R., 2015. Chapter 63: Landslide Processes High Resolution PSI for Mapping Ground Deformations and Infrastructure Instability. *Engineering Geology for Society and Territory – Volume 2*. © Springer International Publishing Switzerland 2015. DOI 10.1007/978-3-319-09057-3
- Wong, K. W. W., & Barford, J. P. (2010). Teaching Excel VBA as a problem solving tool for chemical engineering core courses. *Education for Chemical Engineers*, 5(4), e72–e77. doi:10.1016/j.ece.2010.07.002
- Xu, Y.S., Ma, L., Shen, S.L. and Sun, W.J., 2012. Evaluation of land subsidence by considering underground structures that penetrate the aquifers of Shanghai, China. *Hydrogeology Journal*, 20(8), pp.1623-1634.
- Zerbini, S., Richter, B., Rocca, F., van Dam, T., Matonti, F., 2007. A combination of space and terrestrial geodetic techniques to monitor land subsidence: case study, the Southeastern Po Plain, Italy. *J. Geophys. Res.: Solid Earth* 112 (B5).
- Zhou, Y.; Stein, A.; Molenaar, M. Integrating interferometric SAR data with leveling measurements of land subsidence using geostatistics. *Int. J. Remote Sens.* 2003, 24, 3547–3564.
- Zou, Y.-R., Wang, L., Shuai, Y., & Peng, P. (2005). EasyDelta: A spreadsheet for kinetic modeling of the stable carbon isotope composition of natural gases. *Computers & Geosciences*, 31(7), 811–819. doi:10.1016/j.cageo.2005.01.011

List of publications

6.4. Scientific articles

Serrano-Juan, A., Vázquez-Suñè, E., Alcaraz, M., Ayora, C., Velasco, V., Criollo, R. and Scheiber, L. Using spreadsheets and vba to reuse, customize and extend hydrogeological software. May 2016 - Hydrogeology Journal. *Under review.*

Over the last few decades the scientific community has been using computer-aided tools to solve different kinds of geoscience problems. The first programming languages appeared in the mid 1960s and by the 1990s they changed to visual languages that are more user friendly than their predecessors. Technologies evolve rapidly and new software must be dynamic, visual and interactive. This article presents a new approach for the easy updating of any hydrogeological software. VBA enables us to update any hydrogeological spreadsheet and other non-Excel-based software, giving us the possibility of adding new features and functionalities. An application is provided to demonstrate the modernization of an outdated hydrogeological program and to show the insights of the process. The combination of the methodology and VBA requires only a small number of operations to achieve outstanding results.

Serrano-Juan, A., Vázquez-Suñè, E., Pujades, E., Velasco, V., Criollo, R., Jurado, A. Integration of groundwater by-pass facilities in the bottom slab design for large underground structures. May 2016 - Tunnelling and Underground Space Technology. *Under review.*

The interaction of underground constructions with groundwater generates impacts. These impacts can usually be minimized by using mitigation measures. The most common impacts caused by underground constructions are the groundwater barrier effect (impact on the groundwater) and the groundwater pressure distribution and limitation under the bottom slab (impact in the underground construction). In the literature there are many examples and designs to mitigate both groundwater barrier effect and groundwater pressure distribution and limitation under the bottom slab. However, to the authors' knowledge, there is not any design that integrates both solutions. Since it is illogic to design a solution without considering all the factors involved in the problem, all mitigation measures depending on or affecting the groundwater head should consider the groundwater head variation caused by the affection of other mitigation measure. This paper presents an innovative groundwater by-pass design that enables the groundwater flow through the structure and provide a homogenous distribution of the water pressure under the bottom slab. The new grated design was applied to the largest underground infrastructure of Barcelona: La Sagrera railway station. A hydrogeological model was implemented to test the original and the integrated designs in three different scenarios. This new solution mitigates the groundwater barrier effect and optimizes the bottom slab, reducing considerably the costs and increasing safety during the construction phase.

Serrano-Juan, A., Pujades, E., Vázquez-Suñè, E., Crosetto, M. **Levelling vs. Insar in urban underground construction monitoring: pros and cons. case of La Sagrera railway station (Barcelona, Spain).** May 2016 - Engineering Geology. *Under review.*

Monitoring is required when dewatering underground constructions in order to anticipate unexpected events and preserve nearby existing structures and/or buildings. The most accurate and spread monitoring method to measure displacements is levelling, a point-like surveying technique that typically allows for tens of discrete in-situ sub-millimetric measures per squared kilometer. Another emerging technique for mapping soil deformation is the Interferometric Synthetic Aperture Radar (InSAR), which is based on SAR images acquired from orbiting satellites. This remote sensing technique can provide better spatial point density than levelling, more extensive spatial coverage and cheaper acquisitions. This paper analyses, compares and discusses levelling and InSAR measurements when they are used to measure the soil deformation induced by the dewatering associated to underground constructions in urban areas. To do so, an experiment was performed in the future railway station of La Sagrera, Barcelona (Spain), in which levelling and InSAR were used to accurately quantify ground deformation by dewatering. Results showed that soil displacements measured by levelling and InSAR were not always consistent. InSAR measurements were more accurate with respect to the soil deformation produced by the dewatering while levelling was really useful to determine the real impact of the construction on the nearby buildings.

Serrano-Juan, A., Vázquez-Suñè, E., Monserrat, O., Crosetto, M., Hoffmann, C., Ledesma, A., Criollo, R., Pujades, E., Velasco, V., Garcia-Gil, A., Garcia-Alcaraz, M. **GB-SAR interferometry displacement measurements during dewatering in construction works: the case of La Sagrera railway station in Barcelona, Spain.** February 2016 - Engineering Geology. DOI: 10.1016/j.enggeo.2016.02.014.

Construction processes require monitoring to ensure safety and to control the new and existing structures. Traditional monitoring is based on land surveys and geotechnical instruments and only allows for point-like measurements. Ground-based Synthetic Aperture Radar (GB-SAR) is a remote sensing radar installed in the ground that offers the possibility of acquiring measurements in 2D covering areas of up to a few square kilometers in a single acquisition. Because the GB-SAR technology measures phase shifts along the line-of-sight, it only allows for measurements in the longitudinal direction. Moreover, this technology requires coherence between subsequent acquisitions. These restrictions can be a limitation to the usage of GB-SAR for monitoring a construction process because in this context, the movements of soil and existing structures occur in any direction and at a very fast pace. This paper aims to test the GB-SAR suitability to measure movements during construction. To do so, an experiment was performed in the future railway station of La Sagrera, Barcelona (Spain), in which GB-SAR was used to accurately quantify wall displacements induced by dewatering and proved to be helpful to understand structural deformations and to identify vulnerable areas. The results were compared to traditional monitoring data and numerical models to confirm the reliability of the GB-SAR measurements.

R. Criollo, V. Velasco, E. Vázquez-Suñé, **A. Serrano-Juan**, M. Alcaraz, A. García-Gil. **An integrated GIS-based tool for Aquifer Test Analysis**. November 2015 - Environmental Earth Sciences. DOI: 10.1007/698_2015_368.

The quantification of the hydraulic parameters is important to support decision making in environmental impact assessment, water resources evaluation or groundwater contamination remediation, among others. These kind of parameters derived from aquifer tests usually encompasses a vast amount of data (spatial and non-spatial) for management and analysis. To achieve this in a clear and understandable manner, the GIS environment is a useful instrument. Development of innovative software to analyze pumping tests in a GIS platform environment to support the hydraulic parameterization of groundwater flow and transport models is presented in this paper. This new platform provides three interconnected modules to improve (a) pumping test interpretation code through a user-friendly interface, (b) pumping test data visualization supported by a set of tools that perform spatiotemporal queries in a GIS environment and (c) the storage and management of hydrogeological information. Additionally, within the GIS platform, it is possible to process the hydraulic parameters obtained from the pumping test and to create spatial distribution maps, perform geostatistical analysis and export the information to an external software platform. Finally, a real-world application in the area of Barcelona (Spain) has shown the usefulness of the tools developed in support of hydrogeological analysis

Alejandro García-Gil, Enric Vázquez-Suñé, Maria M. Alcaraz, **Alejandro Serrano Juan**, José Ángel Sánchez-Navarro, Marc Montlleó, Gustavo Rodríguez, José Lao. **GIS-supported mapping of low-temperature geothermal potential taking groundwater flow into account**. November 2014 - Renewable Energy. DOI:10.1016/j.renene.2014.11.096

To promote the utilization of ground-source heat pumps, a new methodology to calculate the low-temperature geothermal potential (LTGP) of a region is presented. The methodology is applicable worldwide, and it considers both closed- and open-loop systems. This new approximation for closed-loops calculates the admissible heat flux exchange with the ground according to an analytical solution of the heat transport equation in porous media. Open-loop systems are calculated as a function of a sustainable removable water flux and the temperature difference between groundwater and a referenced external body. The automated calculation in the setting of a GIS platform has allowed the performance of multilayered 3D mapping of the low-temperature geothermal potential for both types of exploitations considering all of the available information. An example of the application of the methodology in the Metropolitan Area of Barcelona (Spain) is also presented. Finally, a finite element analysis has been performed to quantify the accuracy of the method and the influence of heat advection processes in the LTGP.

V. Velasco, I. Tubau, E. Vázquez-Suñé, R. Gogu, D. Gaitanaru, M. Alcaraz, **A. Serrano-Juan**, D. Fernández-García, T. Garrido, J. Fraile, X. Sanchez-Vila. **GIS-based hydrogeochemical analysis tools (QUIMET)**. September 2014 - Computers & Geosciences. DOI:10.1016/j.cageo.2014.04.013.

A software platform (QUIMET) was developed to improve the sorting, analysis, calculations, visualizations, and interpretations of hydrogeochemical data in a GIS environment. QUIMET is composed of a geospatial database plus a set of tools specially designed for graphical and statistical analysis of hydrogeochemical data. The geospatial database has been designed to include organic and inorganic chemical records, as well as relevant physical parameters (temperature, Eh, electrical conductivity). The instruments for analysis cover a wide range of methodologies for querying, interpreting, and comparing groundwater quality data. They include, among others, chemical time-series analysis, ionic balance calculations, correlation of chemical parameters, and calculation of various common hydrogeochemical diagrams (Salinity, Schöeller–Berkaloff, Piper, and Stiff). The GIS platform allows the generation of maps of the spatial distribution of parameters and diagrams. Moreover, it allows performing a complete statistical analysis of the data including descriptive statistic univariate and bivariate analysis, the latter including generation of correlation matrices and graphics. Finally, QUIMET offers interoperability with other external platforms. The platform is illustrated with a geochemical data set from the city of Badalona, located on the Mediterranean coast in NE Spain

6.5. Book chapters

Violeta Velasco, Enric Vázquez-Suñé, Mar Alcaraz, **Alejandro Serrano-Juan**, Isabel Tubau, Xavier Sánchez-Vila, Daniel Fernández-García, Teresa Garrido, Josep Fraile. GIS-based software platform for managing hydrogeochemical data. **Experiences from Ground, Coastal and Transitional Water Quality Monitoring. The EU Water Framework Directive Implementation in the Catalan River Basin District (Vol. II. Chapter 4) The Handbook of Environmental Chemistry**, pp. 91 - 118. June 26, 2015 - Springer International Publishing Switzerland, 2015. DOI: 10.1007/698_2015_368. Print ISBN: 978-3-319-23903-3. Online ISBN: 978-3-319-23904-0.

Chapter "GIS-based software platform for managing hydrogeochemical data" in the book "Experiences from Ground, Coastal and Transitional Water Quality Monitoring. The EU Water Framework Directive Implementation in the Catalan River Basin District (Vol. II. Chapter 4) The Handbook of Environmental Chemistry", pp. 91 - 118.

6.6. Proceedings

Alejandro Serrano Juan, Enric Vázquez-Suñe, Estanislao Pujades, Violeta Velasco, Rotman Criollo, and Anna Jurado. Integración de Medidas correctoras: efecto barrera y subpresión integrados en un único diseño. Caso de La Sagrera (Barcelona, SPAIN). Centro **Internacional de Hidrología Subterránea (FCIHS)**. "Celebración 50 Aniversario CIHS 1966-2016" - "Jornada Hidrogeología emergente". Barcelona. May 2016.

Alejandro Serrano Juan, Enric Vázquez-Suñe, Estanislao Pujades, Violeta Velasco, Rotman Criollo and Anna Jurado. Infrastructure design integration to optimize structures and minimize groundwater impacts. Case of a bottom slab and groundwater by-pass integration in La Sagrera railway station, Spain. **European Geosciences Union, EGU General Assembly 2016**. European Geosciences Union. Vienna, Austria. April 2016.

Serrano-Juan, A., Vázquez-Suñe, E., Monserrat, O., Crosetto, M., Hoffmann, C., Ledesma, A., Criollo, R., Pujades, E., Velasco, V., Garcia-Gil, A., Garcia-Alcaraz, M. GB-SAR interferometry for structure monitoring during construction works. **American Geophysical Union. 2015 AGU Fall Meeting**. San Francisco. December 2015.

Alejandro Serrano-Juan. GB-SAR interferometry for structure monitoring during infrastructure projects. **1st Meeting of Young Researchers from IDAEA-CSIC**. Barcelona, 22nd October 2015. **Award for the Best Oral presentation.**



Velasco V, Vázquez-Suñe E), Criollo R ,Alcaraz M, **Serrano A**, García A. GIS-based tools for facilitating the development of hydrogeological models. **42nd IAH Congress**. The International Association of Hydrogeologists. Rome, Italy, September 2015.

Velasco, V., Alcaraz, M., Vázquez-Suñe, E., Criollo, R., **Serrano, A.**, García-Gil, A. GIS-Based tools for facilitating the application of the groundwater related directives. **GEOProcessing 2015**. February 22-27, 2015 - Lisbon, Portugal.

Violeta Velasco, Enric Vázquez, Rotman Criollo, Mar Alcaraz, **Alejandro Serrano**, Alejandro Garcia Gil. Desarrollo de herramientas de análisis de datos hidrogeológicos en un entorno SIG. **II Congreso Ibérico de las Aguas Subterráneas (CIAS 2014)**, Valencia, España septiembre 2014. ISBN: 978-84-9048-239-1. Volumen 1, 885.

Alejandro Serrano Juan, Estanislao Pujades Garnes, Enric Vázquez Suñe. Drenaje de la estación intermodal de La Sagrera. **II Congreso Ibérico de las Aguas Subterráneas (CIAS 2014)**, Valencia, España septiembre 2014. ISBN: 978-84-9048-239-1. Volumen 1, 43-44.

R. Criollo, E. Vázquez-Suñe, V. Velasco, **A. Serrano-Juan**, M. Alcaraz, A. García-Gil (2014). Herramientas de interpretación de ensayos hidráulicos en un entorno SIG (Presentación). **II Congreso Ibérico de las Aguas Subterráneas (CIAS 2014)**, Valencia, España septiembre 2014. ISBN: 978-84-9048-239-1. Volumen 1, 215.

Velasco, V., Vázquez-Suñè, E., Criollo, R., Alcaraz, M., **Serrano-Juan, A.**, García-Gil, A., Tubau, I., Gogu, R., Gaitanaru, D. GIS-based Hydrogeological Database and Analysis Tools. **INFOCOMP2013. The Third International Conference on Advanced Communications and Computation**. 17-22 Noviembre, Lisboa (Portugal). IARIA, 2013. ISBN: 978-1-61208-310-0. Vol1, 105-109.

V. Velasco, E. Vázquez-Suñè, R. Gogu, M. Alcaraz, D. Gaitanaru, **A. Serrano**, R. Criollo, A. García-Gil. GIS-based hydrogeological analysis tools (Poster). **The Fifth International Conference on Advanced Geographic Information Systems, Applications, and Services. GEOProcessing 2013**. February 24 - March 1, 2013 - Nice, France.

V. Velasco, I. Tubau, E. Vázquez-Suñè, D. Gaitanaru, R. Gogu, M. Alcaraz, **A. Serrano**, X. Sánchez, D. Fernandez, J. Fraile, T. Garrido (2012). GIS based Hydrochemical Analysis Tools (QUIMET). **7th EUREGEO 2012**, Bolonia, Italia, June, 12th - 15th. Volumen 1, 419-420.

6.7. Software registration

Software Registration: **EASYQUIM**

Alejandro Serrano Juan and Enric Vázquez Suñé. Spain CG3420743, Issued March 31, 2015. Software Registration by the Spanish National Research Council (CSIC).

First version of EasyQuim was designed by Enric Vázquez-Suñé in 1999 to graphically represent chemical data. This version computes some calculations such as unit conversion, balance errors or ionic relationships. It also plots Piper, Schöeller, SAR (Salinity) and Stiff diagrams of 24 samples and allows the user to select which to represent. Everything is set in spreadsheets with functions, except one small macro that activates the “No representation of samples” that can be only activated once. The new version provides three main advantages. (1) increase the number of samples (up to 200), (2) “Sample Selector” addition and (3) possibility of a space-time analysis. The updated EasyQuim can work as a Database and plot different sample combinations and it is connected to the GIS-based software QUIMET. Graphical User Interface (GUI). A UserForm is used as a menu which through its buttons the user can easily activate the different program options, for example changing from one plot to another. Some spreadsheets contain dynamic tables which should be filled with the input data. Another ones show the results. EasyQuim is an Excel-Based program that runs all actions through the functions set along the different spreadsheets. For this reason, non-export nor import data is necessary. Everything runs internally (IRUN). All results are basically presented in graphs (Piper, Schöeller, SAR and Stiff diagrams). The new version have been connected to the GIS-based software QUIMET (Velasco, 2014). On one side, it is possible to export some data and allow their spatial representation in GIS. On the other side, it is also possible a temporal and spatial input data selection in a GIS environment and import it to fill the input data tables to perform the analysis in EasyQuim.

Software Registration: **LAUNCH MIX**

Alejandro Serrano Juan and Enric Vázquez Suñé. Spain CG3420733, Issued March 31, 2015. Software Registration by the Spanish National Research Council (CSIC).

The first version of MIX was created by Carrera et al, -2004 to assess a methodology to compute mixing ratios with uncertain end-members. Given that the software was developed in FORTRAN, it requires one input file and generates two output ones, both files being very long. The input file contains information about the water samples (which can be split into “Sources” or “Wells”), their end-member concentration values and covariance. Additional information such as restrictions or initial conditions can also be set. Briefly, the Launch_MIX satisfies the need for GUI, proposing a GUI based on the MS Excel environment. This GUI prepares input templates based on the user’s needs to perform the analysis in external software. Part of the generated output is plotted and rearranged in GUI, enabling the user to check the entire output data files. Other advantages are its potential use as a Database (providing the opportunity to select different combinations of sources, wells and end-members for analysis) and its connection to a GIS environment.

Software Registration: **EASYBAL**

Alejandro Serrano Juan and Enric Vázquez Suñé. Spain CG3420724, Issued March 31, 2015. Software Registration by the Spanish National Research Council (CSIC).

The first version of EasyBal was designed in 1999 to evaluate water balance per unit of soil area as a function of precipitation, the ETP, Temp and irrigation. Outputs are the deficit and the recharge of the aquifer. It required up to six steps to introduce the input data into six different Excel sheets. All data analysis periods had to be between 01/1970 and 12/1997. Each month has 30 days instead of the real number of days. Main improvements: need to solve the current data period restriction and all functions should be reorganized to allow the autofill of the formula in a single line. Some extras have been also included in the new EasyBal version. On the one hand, the user can select the program language, English or Spanish. On the other hand, the ETP can be introduced as input data or can be automatically calculated (using the Hargreaves and Thornthwaite methods) and graphically compared with the input data, allowing the user to select the best option in the menu or graph. The most recent version bases its GUI on a Userform and spreadsheets. The Userform has all the buttons that allow the user to move along the different program pages and to activate actions and events, whereas the input and results are set along the different spreadsheets. Moreover, depending on the original data (daily or monthly), the program allows us to use all or just some options. EasyBal runs internally. All the output is presented in three tables and plotted in two graphs (rain vs. recharge). No data treatment is needed for the input or for the output. In this case, it is not necessary to export results to other software. Briefly, the main improvements to the new EasyBal are language selection, intuitive GUI, ETP plot selector, open input data range period analysis, formula rearrangement and structured output.

Software Registration: **BRINEMIX**

Alejandro Serrano Juan, Enric Vázquez Suñé and Carlos Ayora. Spain CG3420764. Issued March 31, 2015. Software Registration by the Spanish National Research Council (CSIC).

BrineMIX seeks to create a GUI that automatically generates the input and reads the output of PHREEQC for a specific water mixing analysis. In the input only the chemical water samples, the mixing percentage and the mineral selection are set, whereas the output shows the chemical composition of the final water and its chemical precipitates. The purpose of this new program is to simplify a specific PHREEQC analysis for the user who does not usually work with it. The GUI is a spreadsheet with locked cells, form controls, cell conditionals and some buttons to activate the macros. The input is restricted to 5 samples with 8 different chemical species, density and temperature. When the "RUN" button is activated, the input file is created and exported (ERUN), and PHREEQC is automatically opened with the generated input file already loaded. The macro remains in standby till the end of the PHREEQC analysis and subsequently the output file is imported and displayed to the user. The whole process takes less than 5 seconds. Briefly, BrineMIX is a PHREEQC adaption to allow a non-chemical user to perform rapid water mixing analyses.

Software Registration: **MJ-PUMPIT**

Rotman Criollo Manjarrez, **Alejandro Serrano Juan** and Enric Vázquez Suñé. Spain CG3420754, Issued March 31, 2015. Software Registration by the Spanish National Research Council (CSIC).

MJ-Pumpit is a GUI for MariaJ code which simplifies the data handle and the model selection needed to execute MJ code (Carbonell et al., 1997). MJ-Pumpit is the interconnection with the GIS-based tool HYYH which was designed to analyze and visualize different hydrogeological measurements and results of field tests stored in the HYDOR Database (Velasco, 2013) for a complete hydrogeological analysis

6.8. Projects developed and related with the thesis

6.8.1. Public Research Projects

Mezcla y dispersión en el transporte de energía y solutos. (MEDISTRAES)

Financial entity: CICYT

Reference: CGL2013-48869-C2-1-R

Duration: 2014 to 2016

Responsible: Jesus Carrera / E. Vázquez Suñé

FREE and open source software tools for WATer resource management. (FREEWAT)

Financial entity: Unión Europea

Reference: Grant agreement nº: 642224

Duration: 2015 to 2018

Responsible: Enric Vázquez Suñé

6.8.2. Private Research Projects

Estudio de la interacción entre las obras de la línea de alta velocidad Madrid-Barcelona-Figueras, correspondientes a la construcción de los accesos a la futura Estación de La Sagrera.

Financial entity: UTE ACCESOS-ADIF

Duration: January. 2011 - December. 2012

Responsible: E. Vázquez-Suñé

Estudio de la interacción entre las obras de la línea de alta velocidad Madrid-Barcelona-Figueras, correspondientes a la construcción de la Estación de La Sagrera.

Financial entity: UTE ESTRUCTURA-ADIF

Duration: January. 2011 - December. 2012

Responsible: E. Vázquez-Suñé

List of reports:

Authors: **Serrano, A.**, Criollo, R., Vázquez-Suñé, E, Pujades, E., Escorcía, J., Jurado, A.

- INFORME TÉCNICO: EVALUACIÓN DE EFECTO BARRERA, EFECTO DREN Y CAUDALES DE DRENAJE DURANTE LA EXCAVACIÓN DEL RECINTO DE LA ESTACIÓN DE SAGRERA.
- PROYECTO DE AGOTAMIENTO DE AGUAS FREÁTICAS DURANTE LAS OBRAS DE LA ESTACIÓN DE LA SAGRERA
- INFORME DE CALIDAD DE LAS AGUAS SUBTERRÁNEAS NOVIEMBRE DE 2011 Ref. UES-1411
- NOTA TÉCNICA: EVALUACIÓN DEL RIESGO DE INTRUSION MARINA DEBIDO AL DRENAJE DE AGUAS SUBTERRÁNEAS DURANTE LA EXCAVACIÓN DEL RECINTO DE LA ESTACIÓN DE SAGRERA
- Características de pozos para el drenaje en obra y definitivo del recinto de la Estación de la Sagrera.
- PROTOCOLO A SEGUIR EN LA FASE INICIAL DEL BOMBEO PARA EL AGOTAMIENTO DEL NIVEL FREÁTICO EN LA ESTRUCTURA DE LA ESTACIÓN DE LA SAGRERA
- NOTA TÉCNICA: PROTOCOLO PARA LA VIGILANCIA Y CONTROL DEL SISTEMA DE AGOTAMIENTO DE NIVEL FREÁTICO EN LA ESTRUCTURA DE LA ESTACIÓN DE LA SAGRERA

Drenaje para la excavación del Túnel del tramo Montcada - Mollet del AVE Madrid-Barcelona. FASE II

Financial entity: CONSTRUCTORA SAN JOSE.

Responsible: E. Vázquez-Suñé / J. Carrera

Duration: Julio 2011 - Oct 2011.

List of reports:

Authors: Escorcía, J., **Serrano, A.**, Pujades, E., Vázquez-Suñé, E. and Carrera, J.

- Propuestas de bombeo en el tramo del AVE Montcada – Mollet
- Cálculo de los caudales de drenaje para la excavación de los módulos 9 y 10 del túnel del tramo Montcada – Mollet. AVE Madrid-Barcelona.
- Drenaje para la excavación del túnel del tramo Montcada – Mollet. AVE Madrid-Barcelona.
- Nuevo dimensionado de los caudales de extracción en los pozos ubicados en las zonas de Tablestacas T' y T'' para el drenaje de la excavación del Túnel del tramo Montcada – Mollet. AVE Madrid-Barcelona.
- Control del Factor de Seguridad ante el riesgo de levantamiento del suelo entre PK 200+000 y PK 200+286. Montcada – Mollet. (AVE Barcelona-Frontera Francesa).

Trabajos de consultoría hidrogeológica relativos a la construcción de la estación del metro de York en Toronto.

Financial entity: BRIDGES TECHNOLOGIES, S.L.

Responsable: E. Vázquez-Suñé

Duration: Septiembre - December 2011

MODELACION DE LOS IMPACTOS HIDROGEOLOGICOS DEL METRO DE QUITO (ECUADOR)

Financial entity: EVREN y Metro Quito

Responsable: E. Vázquez-Suñé

Duration: Febrero – Abril, 2012

AVALUACIÓ I ACTUALITZACIÓ DEL BALANÇ DE MASSA DE LES AIGÜES SUBTERRÀNIES AL PLA DE BARCELONA. APLICACIÓ DEL MODEL HIDROGEOLOÒGIC DEL PLA DE BARCELONA I DELTA DEL BESÒS.

Financial entity: Ajuntament de Barcelona

Responsable: E. Vázquez-Suñé

Duration: April a June 2012

MODELACIÓN DEL ACUÍFERO DE CALAMA, SECTOR MEDIO DE LA CUENCA DEL RÍO LOA

Financial entity: Matraz, UPC

Responsable: Daniel Fernández, E. Vázquez-Suñé

Duration: Julio - December 2012

DISEÑO DEL BOMBEO DE LA ESTACIÓN DE YORK EN TORONTO

Financial entity: BRIDGES TECHNOLOGIES, S.L.

Responsable: E. Vázquez-Suñé

Duration: Septiembre 2012

AVALUACIÓ I ZONIFICACIÓ DE LES POSSIBILITATS D'APROFITAMENT TÈRMIC DEL SUBSÒL A L'ÀMBIT DE L'ÀREA METROPOLITANA DE BARCELONA.

Financial entity: Barcelona Regional

Responsible: E. Vázquez-Suñé

Duration: November 2012 - April 2013

ESTUDI I SEGUIMENT DE L'EVOLUCIÓ DEL DRENATGE I DELS NIVELLS FREÀTICS A L'ENTORN DE LA PLAÇA DE LA VILA DE SANT ADRIÀ DE BESÒS (2007-2012).

Financial entity: Ajuntament de Sant Adrià del Besòs

Responsible: E. Vázquez-Suñé

Duration: January – December 2012

EVALUACIÓN DE LOS EFECTOS DEL INCIDENTE DE LOS TANQUES DE ÁCIDO SULFÚRICO Y EVALUACIÓN DE OTRAS ZONAS CON RIESGOS SIMILARES EN LA EXPLOTACIÓN MINERA DE COBRE LAS CRUCES, SEVILLA.

Financial entity: Fundacion Migres

Duration: January 2013 – December 2013

Responsible: C. Ayora/E. Vázquez Suñé

MEZCLA DE SALMUERAS Y EVOLUCIÓN QUÍMICA DURANTE LA OPERACIÓN DE LOS POZOS (INTEGRACIÓN Y UPSCALING)

Financial entity: MATRAZ

Responsible: E. Vázquez-Suñé, C. Ayora

Duration: January – April 2013

ESTUDIOS DE MEZCLA DE SALMUERAS Y EVOLUCIÓN QUÍMICA DURANTE LA OPERACIÓN DE LOS POZOS

Financial entity: SQM

Responsible: E. Vázquez-Suñé, C. Ayora

Duration: January – December 2013

SEGUIMEINTO Y AMPLIACIÓN DE ESTUDIOS HIDROQUÍMICOS E HIDROGEOLÓGICOS EN LA EXPLOTACIÓN MINERA DE COBRE LAS CRUCES, SEVILLA.

Financial entity: Fundacion Migres

Duration: January 2014 – December 2014

Responsible: C. Ayora/E. Vázquez Suñé

AVALUACIÓ DE LES POSSIBILITATS D'APROFITAMENT DE L'ANOMALIA GEOTÈRMICA DETECTADA AL SECTOR DE FONDO DE SANTA COLOMA DE GRAMENET.

Financial entity: Consorci del Besòs

Responsible: E. Vázquez-Suñé

Duration: August 2014 – December 2014

ESTUDI I SEGUIMENT DE L'EVOLUCIÓ DEL DRENATGE I DELS NIVELLS FREÀTICS A L'ENTORN DE LA PLAÇA DE LA VILA DE SANT ADRIÀ DE BESÒS (2007-2013).

Financial entity: Ajuntament de Sant Adrià del Besòs

Responsible: E. Vázquez-Suñé

Duration: January – December 2014

ESTUDIO Y SEGUIMIENTO HIDROGEOLÓGICO DE LAS OBRAS DE LA LÍNEA DE ALTA VELOCIDAD MADRID – BARCELONA – FIGUERES, CORRESPONDIENTES A LA CONSTRUCCIÓN DE LA ESTACIÓN DE LA SAGRERA Y SUS ACCESOS.

Financial entity: UTE ESTRUCTURA-ADIF

Responsible: E. Vázquez-Suñé

Duration: Marzo 2014 – December 2014

List of reports:

Authors: **Serrano, A.**, Criollo, R., Vázquez-Suñé, E, Pujades, E., Escorcía, J., Jurado, A.

- NOTA TÉCNICA: Seguimiento de la construcción de pozos para el drenaje en obra y definitivo del recinto de la Estación de la Sagrera
- NOTA TÉCNICA: Seguimiento hidrogeológico de la Sagrera
- NOTA TÉCNICA: PROTOCOLO A SEGUIR EN LA PRUEBA DE ESTANQUEIDAD DE LAS PANTALLAS Y DETERMINACIÓN DEL ESTADO HIDROQUÍMICO INICIAL DE LAS AGUAS SUBTERRÁNEAS EN EL RECINTO DE LA ESTACIÓN DE LA SAGRERA.
- NOTA TÉCNICA: Dimensionamiento de la sección de aforo a la salida del recinto
- NOTA TÉCNICA: Caract. pozos para el drenaje de las salidas de emergencia - La Sagrera.
- NOTA TÉCNICA: NIVEL DEL FREÁTICO EN EL TRASDÓS DE LAS PANTALLAS DEL RECINTO DE LA ESTACIÓN DE LA SAGRERA.
- NOTA TÉCNICA: ESTUDIO SOBRE EL EFECTO BARRERA PRODUCIDO POR LA CONSTRUCCIÓN DE LA ESTACIÓN DE LA SAGRERA. PERIODO ABRIL/2011 – DICIEMBRE/2013
- NOTA TÉCNICA: ESTUDIO SOBRE LA POSICIÓN DEL NIVEL PIEZOMÉTRICO EN EL TRASDÓS DE LAS PANTALLAS DEL LADO MONTAÑA DE LA ESTACIÓN DE LA SAGRERA. DESPUÉS DE 85 DÍAS DE DRENAJE"
- INFORME TÉCNICO: ESTUDIO Y SEGUIMIENTO HIDROGEOLÓGICO DE LAS OBRAS DE LA LÍNEA DE ALTA VELOCIDAD MADRID-BARCELONA-FIGUERES, CORRESPONDIENTES A LA CONSTRUCCIÓN DE LA ESTACIÓN DE LA SAGRERA Y SUS ACCESOS. PERIODO SEPTIEMBRE/2011 – JUNIO/2014"
- NOTA TÉCNICA: ESTUDIO DE LA DISTRIBUCIÓN DE LAS PRESIONES HIDRÁULICAS SOBRE LA LOSA DE FONDO DE LA ESTACIÓN DE LA SAGRERA.
- ANEXO A LA NOTA TÉCNICA: ESTUDIO DE LA DISTRIBUCIÓN DE LAS PRESIONES HIDRÁULICAS SOBRE LA LOSA DE FONDO DE LA ESTACIÓN DE LA SAGRERA
- INFORME TÉCNICO: ESTUDIO Y SEGUIMIENTO HIDROGEOLÓGICO DE LAS OBRAS DE LA LÍNEA DE ALTA VELOCIDAD MADRID-BARCELONA-FIGUERES, CORRESPONDIENTES A LA CONSTRUCCIÓN DE LA ESTACIÓN DE LA SAGRERA Y SUS ACCESOS. PERIODO SEPTIEMBRE/2011 – ENERO/2015

MODELACION NUMERICA HIDROGEOLOGICA DEL PROYECTO MINERO IZCAYCRUZ, PERÚ.

Financial entity: Hydro-Geo (Perú)

Responsible: E. Vázquez-Suñé

Duration: June 2014 – December 2014

AVALUACIÓ DE LES POSSIBILITATS D'APROFITAMENT DE L'ANOMALIA GEOTÉRMICA DETECTADA AL SECTOR DE FONDO DE SANTA COLOMA DE GRAMENET.

Financial entity: Consorci del Besòs
Responsible: E. Vázquez-Suñé
Duration: October 2014 – March 2015

AVALUACIÓ DE LES POSSIBILITATS D'ESGOTAMENT DEL FREÀTIC DURANT LA CONSTRUCCIÓ DE LA NOVA PLAÇA DE GLÒRIES

Financial entity: Ajuntament de Barcelona / BIMSA
Responsible: E. Vázquez-Suñé
Duration: February 2015 – April 2015

GESTIÓN DE AGUAS SUBTERRÁNEAS EN LA ZONA MINERA DE COBRE LAS CRUCES, 2015

Financial entity: COBRE LAS CRUCES
Responsible: E. Vázquez-Suñé / C. Ayora
Duration: January 2015 – December 2015

AVALUACIÓ DE LES POSSIBILITATS D'ESGOTAMENT DEL FREÀTIC DURANT LA CONSTRUCCIÓ DE LA NOVA PLAÇA DE GLÒRIES

Financial entity: Ajuntament de Barcelona / BIMSA
Responsible: E. Vázquez-Suñé
Duration: February 2015 – April 2015

List of reports:

Authors: **Serrano, A.**, Criollo, R., Vázquez-Suñé.

- INFORME TÈCNIC: AVALUACIÓ DE LES POSSIBILITATS D'ESGOTAMENT DEL FREÀTIC DURANT LA CONSTRUCCIÓ DE LA NOVA PLAÇA DE GLÒRIES. Abril 2015

SEGUIMIENTO HIDROGEOLÓGICO DE LOS PROCESOS DE AGOTAMIENTO DEL FREÁTICO EN EL ÁMBITO DE LA EJECUCIÓN DEL TÚNEL DE LA PLAZA DE LAS GLORIAS

Financial entity: Ajuntament de Barcelona / BIMSA
Responsible: E. Vázquez-Suñé
Duration: September 2015 – September 2016

List of reports:

Authors: **Serrano, A.**, Criollo, R., Marazuela, M., Vázquez-Suñé.

- NOTA TÈCNICA: INTERPRETACIÓ DE L'ASSAIG HIDRÀULIC (AGOST-SETEMBRE DE 2015).
- NOTA TÈCNICA: Sobre l'ús d'interferometria com a eina d'auscultació a l'entorn de la plaça de Glòries de Barcelona. Abril 2016
- INFORME TÈCNIC: Informe de seguiment previ a l'esgotament del freàtic durant la construcció de la nova plaça de glòries. Abril 2016

"Keep it simple". This is the philosophy that powers and steers my career path.

About the author

Born on the 29th of April 1986 in Madrid. Early on my family moved to Sant Andreu de Llavaneras and later settled in La Garriga. I did my bachelor's degree in civil engineering, when I developed a water supply and sewage project in Ecuador. After that I specialized in hydroinformatics (Msc. EUROAQUAE) and lived and worked in Newcastle, UK, and Chennai, India. While in India I also worked briefly in the Vicenç Ferrer Foundation and later in Cetaqua (Agbar, Suez group). I began my Phd in the Institute of Environmental Sciences and Water Research, IDAEA (CSIC). The research aimed to understand how infrastructures that interact with groundwater were processed throughout the whole construction process cycle (project design, project construction and project exploitation) and to improve it.



During and concurrent with my PhD, I liked to explore different sources of data to find hidden relationships among the variables. Having collaborated with the CIC or the DIBA I was able to create useful analysis tools to provide knowledge about the social relationships among children and improving monitoring of endangered wildlife species. During this period, I also taught Advanced Data processing and VBA programming with Microsoft BI. All of this freelance experience allowed me to start in the data scientist world through Saptools S.L., where I am currently working.